ABSTRACT

HWANG, YOON JOONG : Characterization of Atmospheric Pressure Plasma Interactions with Textile/Polymer Substrates (Under the direction of Dr. Marian McCord and Dr. Jerome Cuomo)

The purpose of the research has been to understand plasma-substrate interactions and an application to adhesion enhancement of high performance fiber under capacitively-coupled atmospheric pressure plasma. Preliminarily, plasma-poly(ethylene terephthalate) (PET) film interactions with atmospheric pressure capacitively-coupled plasma were studied under closed-ventilation conditions with exposure times of 0-5 min., using He/Air and He/O_2 gases. The weight loss (%) increased initially and then decreased at further exposure times in both gas plasma treatments. Contact angle measurements showed that wettability increased rapidly up to 1 min. and was constant at further exposure times. Atomic Force Microscopy (AFM) was used to characterize the surface morphology change of the PET films. Surface functionalization and cross-linking were examined by X-ray Photoelectron Spectroscopy (XPS). Both plasma treatments induced functionalization after chain-scission, and generated etched particles, a potential source for re-deposition. Re-deposition effects on weight loss (%), roughness, carbon content and surface functionality increased with plasma exposure time. Cross-linking was dependent on plasma exposure time and also on helium content. Tensile strength and initial modulus of PET films increased after treatments in both gas plasmas. The contribution of helium was a major factor increasing cross-linking.

In order to investigate the effect of atmospheric pressure plasmas on adhesion between aramid fibers and epoxy, aramid fibers were treated with atmospheric pressure helium/air for 15, 30 and 60 seconds on a capacitively-coupled device at a frequency of 5.0 kHz and He outlet pressure of 3.43kPa. SEM analysis at 10,000 × magnification showed that

no significant surface morphological change resulted from the plasma treatments. XPS analysis showed a decrease in carbon content and an increase in oxygen content. Deconvolution analysis of C_{1s}, N_{1s} and O_{1s} peaks showed an increase in surface hydroxyl groups that can interact with epoxy resin. The microbond test showed that the plasma treatment for 60 seconds increased interfacial shear strength by 109% over that of the control (untreated). The atmospheric pressure plasma increased single fiber tensile strength by 16 – 26 %.

CHARACTERIZATION OF ATMOSPHERIC PRESSURE PLASMA INTERACTIONS WITH TEXTILE/POLYMER SUBSTRATES

by
YOON JOONG HWANG

A dissertation submitted to the Graduate Faculty of
North Carolina State University
in partial fulfillment of the requirements for the Degree of
Doctor of Philosophy

Fiber and Polymer Science

Raleigh

2003

APPROVED BY:



Co-chair of Advisory Committee

Co-chair of Advisory Committee

DEDICATION

I would like to dedicate this dissertation and all of the work involved in completing it to my parents (Hwan Sang Hwang and Jeong Soon Yoon), my lovely wife (Cottnip Bae) and son (Paul Seok-Joon Hwang).

BIOGRAPHY

Yoon Joong Hwang was born in July 25, 1969 in Chooncheon, Kangwon, Korea as a son of Hwan Sang Hwang and Jeong Soon Yoon. He was graduated from Chooncheon High School (Chooncheon) in February 1988 and received a B.S. degree in Textile Engineering at Inha University (Incheon) in February 1995 in Korea.

Pursuing his interests in textiles, he was enrolled in the Master Science program in Textile and Apparel Technology and Management (College of Textiles) at North Carolina State University in 1998. He worked for Nonwoven Cooperative Research Center and received a M.S. degree under the direction of Dr. Abdelfattah M. Seyam and Dr. William Oxenham

After graduated, he joined Baiksan Textile Co. Ltd. in Korea as a researcher, and developed medical textiles and artificial leather using hydroentanglement and plasma technologies for 2 years. In August 2000, he began his study in College of Textiles, Fiber and Polymer Science program at North Carolina State University, and completed his Ph. D work under the direction of Dr. Marian McCord and Dr. Jerome Cuomo in May 2003. Upon graduation, he will join Commonwealth Scientific & Industrial Organization in Australia as a research scientist.

ACKNOWLEDGEMENT

I would like to express the deepest appreciation to my advisors, Dr. Marian McCord and Dr. Jerome Cuomo, for their persistent support and advice through my study. I also thank my minor advisor, Dr. Mohamed Bourham, and other committee members, Dr. Yiping Qiu and Dr. Peter Hauser for help and advice. Their enthusiasm and encouragement helped me pursue deeper study of plasma.

I would like to expend my special appreciation to my parents (Hwan Sang Hwang and Jeong Soon Yoon), wife (Cottnip Bae) and son (Seok Joon Hwang) for endless support and love. And, I am grateful to my parents-in-law and brothers/sisters-in-law for their concerns and supports.

I wish to thank Brian Bures and Suzanne Matthews for their assistance and the National Textile Center for financial supports. I am very grateful to Dr. Shin Woong Park and Dr. Bok Chun Kang for their invaluable advice and guides.

Finally, I thank GOD for his love and peace in my family all the time, and extend my appreciation to all friends in Korea and Raleigh.

TABLES OF CONTENTS

Page

List of Figures…… x

List of Tables……. xiv

I. INTRODUCTION……1

II. PLASMA SYSTEMS AND APPLICATIONS TO TEXTILES……..4

1. Plasma Systems for Textiles……...4

1.1 Low-pressure Plasma Systems for Textile Applications……...4

1.1.1 Continuous Plasma Processing in Vacuum Chamber……. 4

1.1.2 Roll-to-Roll Batch Plasma Processing in Vacuum Chamber……..7

1.2 Atmospheric Pressure Plasma Systems for Textile Applications……..10

1.2.1 Corona Systems for Textile Applications……... 11

1.2.2 Atmospheric Pressure Glow Discharge (APGD)…… 13

1.2.3 APGD Systems for Textile Applications…… 15

2. Plasma Applications to Textile Processing…… 17

2.1 Wettability Enhancement…….. 17

2.2 Water Repellent Finishing……18

2.3 Anti-shrinkage Finishing……...20

2.4 Desizing……22

2.5 Flame Retardant Finishing…… 23

2.6 Adhesion Enhancement……24

2.7 Dyeability Enhancement……... 26

2.8 Sterilization……29

III. THE EFFECTS OF PLASMA ON SUBSTRATE PROPERTIES……32

1. Etching Effects of Plasma on Substrate Surface…….32

    1.1 Mechanism of Etching and Re-deposition…….33

    1.2 Surface Morphology and Roughness Change……... 34

    1.3 Selective Etching on Semi-crystalline Polymer in Plasma Treatment…….. 36

2. Radical Formation on Substrate Surface…… 37

    2.1 Radical Formation and Functionalization……. 38

    2.2 Radical Stability…… 39

3. Chain Scission of Surface Molecules on Polymer Substrate……..39

    3.1 Chain Scission by Chemical Interactions in Plasma Treatment…… 39

    3.2 Chain Scission by Ion Bombardment…… 40

4. Cross-linking Formation……43

    4.1 Cross-linking Mechanism on Polymer Substrate…….. 43

    4.2 The Depth of Cross-linking on Polymer Substrate……45

5. Functionalization on Polymer Surface by Gas Plasma Treatment……. 46

    5.1 Hydrophilic Functionalization…….. 46

    5.2 Hydrophobic Functionalization……48

    5.3 Depth Profile of Functionalization…… 49

    5.4 Ageing Effect…….51

6. Plasma Polymerization (Deposition)…….. 53

    6.1 Hydrocarbon Plasma Polymerization…… 54

    6.2 Fluorocarbon Plasma Polymerization……56

7. The Effects of Plasma Treatment on Physical Properties of Substrate…….. 57

7.1 Low-Pressure Plasma…… 58

7.2 Atmospheric Pressure Plasma……... 60

REFERENCES (CHAPTERS I-III)……... 63

IV. SURFACE MODIFICATION OF ORGANIC POLYMER FILMS TREATED IN ATMOSPHERIC PLASMAS…… 81

1. Abstract……...81

2. Introduction…….82

3. Experimental……...84

4. Results…..……... 86

4.1 Weight Loss (%)……86

4.2 Surface Morphology Change…….86

4.3 Wettability……. 88

4.4 Chemical Composition Change on PET Film Surface……..91

5. Discussion……...95

5.1 Etching and Re-deposition…… 95

5.2 Chain Scission and Funtionalization……97

5.3 Cross-linking……. 98

6. Conclusion…….. 103

7. References…….. 105

V. EFFECTS OF ATMOSPHERIC PRESSURE HELIUM/AIR PLASMA TREATMENT ON ADHESION AND MECHNICAL PROPERTIES OF ARAMID FIBERS……... 107

1. Abstract……...107

2. Introduction…….108

3. Experimental……...110

3.1. Plasma Treatment……110

3.2. Sample Preparation for Microbond Test…….. 110

3.3. Microscopic Examination……111

3.4. XPS Analysis……111

3.5. Interfacial Bond Strength Test and Single Fiber Tensile Test……. 111

3.6. Statistical Analysis……... 112

4. Results and Discussion……... 112

4.1. Microscopy Examination……. 112

4.2. XPS Analysis……112

4.3 Wettability of Fibers by Epoxy……. 119

4.4. Microbond Test…… 120

4.5. Single Fiber Tensile Strength……... 123

5. Conclusion…….. 125

6. References……...126

VI. STUDY OF PLASMA-POLYMERIC SUBSTRATE INTERACTION IN CAPACITIVELY-COUPLED ATMOSPHERIC PRESSURE PLASMA……...130

1. Introduction……130

2. Experimental……...131

3. Results……135

3.1 Weight Loss (%)……135

3.1.1 Weight Loss (%) after Plasma Treatment……... 135

3.1.2 Influence of Ageing on Weight Loss (%)……137

3.2 Surface Wettability (Contact Angle)……137

3.2.1 Wettability of Plasma Treated PET Film…… 137

3.2.2 Change of Wettability on Plasma Treated PET Film due to Ageing …. 140

3.3 Surface Chemical Analysis by X-ray Photoelectron Spectroscopy (XPS)….... 143

3.3.1 Surface Chemical Analysis and Depth Profile of PET Film……... 143

3.3.2 Surface Chemical Analysis of Silicon Wafer……..148

3.3.3 Surface Chemical Change by Ageing……. 148

3.4 Surface Morphology Analysis by Atomic Force Microscopy (AFM)…….. 150

3.4.1 Surface Morphology Change of PET Film……. 150

3.4.2 Surface Morphology Change of Silicon Wafer……...153

3.5 Tensile Properties of Plasma Treated PET Films……..155

4. Discussion……...156

4.1 Etching/Re-deposition Behavior……... 156

4.2 Functionalization by Chain Scission……. 158

4.3 Cross-linking……. 162

4.4 Ageing Behavior of Wettability…… 164

5. Conclusion…….. 164

6. References…….. 166

LIST OF FIGURES

Page

I. INTRODUCTION

II. PLASMA SYSTEMS AND APPLICATIONS TO TEXTILES

Figure 1. Proposed Continuous Grafting Plasma System by Bradley…… 5

Figure 2. Semi-Continuous Plasma System at Fraunhofer IGB, Stuttgart, Germany)... 6

Figure 3. Schematic Diagram of (a) UPCH-140 and (b) KPR-180…… 9

Figure 4. A Schematic Diagram of Continuous Corona Discharge System for Wool and Mohair…….. 12

Figure 5. Schematic Diagram of the Continuous Corona System for Polypropylene Fiber Tow Designed by Sherman Treaters Co. …… 13

Figure 6. Schematic Diagram of PALADIN……...15

III. THE EFFECTS OF PLASMA ON SUBSTRATE PROPERTIES

Figure 7. Mechanism of Plasma-Substrate Interaction…….33

Figure 8. Thickness Variation of the SiO_2 Aerogel Films before and after Various Gases Plasma Treatment (500W/50 min.)……..35

Figure 9. Etching Rate as a Function of Crystallinity of PE Film in a CF_4 Plasma…... 36

Figure 10. Schematic Illustration of the Side-Chain Scission in PMMA due to Low-Energy Ions…… 40

Figure 11. Degradation Mechanism of PET Film by He-O_2 Plasma; (a) Gas Species and Radicals Produced by Fragmentation Reaction, (b) CO and CO_2 Formation Mechanism and (c) H_2O Formation Mechanism…… 41

Figure 12. Degradation Mechanism of Poly(p-phenylene trerphthalamide) (PPTA) Films Treated by O_2 Plasma……... 42

Figure 13. Cross-linking by Recombination of Two Aryl Radicals Obtained by Hydrogen Abstraction From Benzene Ring in PET…….. 44

Figure 14. Possible Cross-linking Mechanism of Poly(p-phenylene terephthalamide) Film…… 44

Figure 15. The Scheme of Penetration into Substrate Surface by Plasma Particles…...45

Figure 16. Cross-Linking Reaction in Subsurface vs. Oxidation in Film Surface……. 46

Figure 17. Elemental Composition of Ar Plasma Treated PTFE as a Function of Depth, Determined using Angle-Resolved XPS…….51

Figure 18. Models of Molecular Mobility on Polymer Surface by Yasuda……... 53

Figure 19. Film Thickness vs. Deposition Time for Styrene, Acetylene, Butadiene and ethylene monomers in a Pulse Plasma Deposition Process, CW= Continuous Wave Mode…….56

Figure 20. Load-Unload Curves for Untreated, Helium and Nitrogen Treated PC Films……. 60

IV. SURFACE MODIFICATION OF ORGANIC POLYMER FILMS TREATED IN ATMOSPHERIC PLASMAS

Figure 1. Mechanism of Plasma-Substrate Interaction……...83

Figure 2. Atmospheric Pressure Plasma System Diagram (Closed Ventilation)……84

Figure 3. Weight Loss (%) of PET Film Treated by Atmospheric Pressure Plasma…..87

Figure 4. Scanning Electron Microscopy (SEM) Pictures of PET Films……... 87

Figure 5. AFM Images of Control and Atmospheric Pressure Plasma Treated PET Films……..88

Figure 6. Surface Roughness (RMS) of Plasma Treated PET Films by AFM: (a) 1 μm^2 Scanning and (b) 5 μm^2 Scanning…….. 89

Figure 7. AFM Pictures of Re-deposited Nano-Size Particles on Plasma Treated PET Films……... 90

Figure 8. Contact Angle Measurement of Plasma Treated PET Films……..90

Figure 9. C_{1s} Deconvolution Analysis of PET Films Treated by Atmospheric Pressure Plasma: (a) Control, (b) He/Air 1.0 min., and (c) He/O_2 2.0 min…… 93

Figure 10. Chain Scission Processes and Derivatives in PET Molecules by Helium Containing Plasma Treatment: (a) Position 1, (b) Position 2, (c) Position 3, and (d) Position 6……99

Figure 11. –COOH Group in C_{1s} Deconvolution Analysis of Plasma Treated PET Films……... 101

Figure 12. –C-OH Group in C_{1s} Deconvolution Analysis of Plasma Treated PET Films……... 101

Figure 13. Possible Cross-linking Positions in PET Molecules by He Containing Plasma: (a) Recombination between Benzene Rings and (b) Combination with other chains……102

Figure 14. –C-C Bond in C_{1s} Deconvolution Analysis of Plasma Treated PET Films……... 103

Figure 15. Mechanism of Re-deposition by Etched Species…….. 104

V. EFFECTS OF ATMOSPHERIC PRESSURE HELIUM/AIR PLASMA TREATMENT ON ADHESION AND MECHNICAL PROPERTIES OF ARAMID FIBERS

Figure 1. SEM Micrographs of Aramid Fiber Surfaces: (A) untreated, (B) He/Air-15 sec, (C) He/Air -30 sec (D) He/Air-60 sec……. 113

Figure 2. Possible Chemical Interactions of Epoxy Resin with the Plasma Treated Aramid Fiber Surface…… 114

Figure 3. Potential Reaction Sites (1-4) in Kevlar Molecular Structure…….118

Figure 4. Possible Reaction Mechanism for –OH Group Generation at Positions 1 and 3 in Kevlar Molecular Structure……118

Figure 5. Possible Chain Scission and Interactions at Position 2 in Kevlar Molecular Structures…… 119

Figure 6. Typical Load-Displacement Curves for the Control and 60-seconds He/Air Plasma Treated Samples in the Microbond Test…… 121

VI. STUDY OF PLASMA-POLYMERIC SUBSTRATE INTERACTION IN CAPACITIVELY-COUPLED ATMOSPHERIC PRESSURE PLASMA

Figure 1. Schematic Diagram of Capacitively-Coupled Atmospheric Pressure Plasma System…… 131

Figure 2. Weight Loss (%) of Plasma Treated PET Film with Gas Flow Conditions (F1: He=4 lpm and He/O_2=12/0.1 lpm, F2: He=8 lpm and He/O_2=12/0.2 lpm, F3: He =12 lpm and He/O_2=12/0.3 lpm)…… 135

Figure 3. Weight Loss (%) of Plasma Treated PET Film with Exposure Time (Flow Rate: He=12 lpm, He/O_2=12/0.3 lpm)……. 136

Figure 4. Ageing Behavior of Wettability on Plasma Treated PET Film Surface with Different Gas Flow Condition (F1: He=4 lpm and O_2=0.1 lpm, F2: He=8 lpm and O_2=0.2 lpm, F3: He=12 lpm and O_2=0.3 lpm)……139

Figure 5. Ageing Behavior of Wettability on Plasma Treated PET Film Surface with Different Exposure Time (He:12 lpm and O_2: He=12 lpm and O_2=0.3 lpm)……139

Figure 6. Contact Angle Change on He Plasma Treated PET Films with Different Gas Flow Rate: (a) Flow Rate and (b) Exposure Time (He Flow Rate = 12 lpm)…… 141

Figure 7. Contact Angle Change on He/O_2 Plasma Treated PET Films with Different Exposure Time (He Flow Rate = 12 lpm): (a) Flow Rate and (b) Exposure Time…… 142

Figure 8. AFM Pictures of PET Films:(a) Control, (b) He 5 min. and (c) He/O_2 5 min. (He Flow Rate=12 lpm and O_2 Flow Rate = 0.3 lpm)…… 152

Figure 9. AFM Pictures of Silicon Wafers: (a) Control, (b) He 3 min. and (c) He/O_2 3 min. (He Flow Rate=12 lpm and O_2 Flow Rate = 0.3 lpm)…… 154

Figure 10. (C_{1s}+Si_{2p3}) Composition of Plasma Treated PET Film (XPS Resolved Angle = 45º)…….. 158

Figure 11. Chain Radical Formation and Functionalization in PET Molecules by Helium Containing Plasma Treatment: (a) Position 1, (b) Position 2, (c) Position 3, (d) Position 4, (e) Position 5 and (f) Position 6…….. 160

Figure 12. C-C Bond Compositions (%) of He Plasma Treated PET Films along XPS Resolved Angle…….. 162

Figure 13. Possible Cross-linking Mechanism in Subsurface of PET Molecules by He Containing Plasma: (a) Recombination between Benzene Rings and (b) Combination with Other Carbon chains……163

LIST OF TABLES

Page

I. INTRODUCTION

II. PLASMA SYSTEMS AND APPLICATIONS TO TEXTILES

Table 1. Parameters of the Industrial Plasma Machine Manufactured by NIEKMI Institute for Textile Materials……8

Table 2. Comparison of Operating Parameters in Atmospheric Pressure Plasma……. 16

III. THE EFFECTS OF PLASMA ON SUBSTRATE PROPERTIES

Table 3. Relative Intensity Data of the Deconvoluted C_{1s} Core Level Spectra of PET Films Treated by Ar Plasma……... 47

Table 4. N_{1s}/C_{1s} Intensity Ratios as Determined by Angle Resolved XPS for Remote Nitrogen Plasma Treated Polyethylene Samples……51

IV. SURFACE MODIFICATION OF ORGANIC POLYMER FILMS TREATED IN ATMOSPHERIC PLASMAS

Table 1. Relative Chemical Composition and Atomic Ratio Determined by XPS for PET Film Treated by He/Air Atmospheric Pressure Plasma……91

Table 2. Relative Chemical Composition and Atomic Ratio Determined by XPS for PET Film Treated by He/O_2 Atmospheric Pressure Plasma……92

Table 3. Deconvolution of C_{1s} Spectra for PET Film Treated by He/Air Atmospheric Pressure Plasma…… 94

Table 4. Deconvolution of C_{1s} Spectra for PET Film Treated by He/O_2 Atmospheric Pressure Plasma…….94

Table 5. Bond Energies of Common Chemical Bonds in Polymers……...99

V. EFFECTS OF ATMOSPHERIC PRESSURE HELIUM/AIR PLASMA TREATMENT ON ADHESION AND MECHNICAL PROPERTIES OF ARAMID FIBERS

Table 1. Relative Chemical Composition and Atomic Ratios Determined by XPS for Aramid Fibers Untreated and Treated with Atmospheric Pressure Plasmas……114

Table 2. Results of Deconvolution of C_{1s} Peaks for Aramid Fibers Untreated and Treated with Atmospheric Pressure Plasmas……...116

Table 3. Results of Deconvolution of N_{1s} Peaks for Aramid Fibers Untreated and Treated with Atmospheric Pressure Plasmas……..116

Table 4. Results of Deconvolution of O_{1s} peaks for Aramid Fibers Untreated and Treated with Atmospheric Pressure Plasmas……..117

Table 5. Contact Angles between Epoxy Beads and Aramid Fibers……..120

Table 6. Interfacial Shear Strength Data……122

Table 7. Single Aramid Fiber Tensile Strength……..124

VI. STUDY OF PLASMA-POLYMERIC SUBSTRATE INTERACTION IN CAPACITIVELY-COUPLED ATMOSPHERIC PRESSURE PLASMA

Table 1. Experimental Design of PET Films and Silicon Wafer Treated by He and He/O_2 Atmospheric Pressure Plasma……... 132

Table 2. Weight Loss (%) of Plasma Treated PET Films with Different Storage Conditions (He/O_2: He flow rate = 12 lpm)……138

Table 3. Chemical Composition of Plasma Treated PET Films by XPS Angle Resolved Analysis (He plasma: He Flow Rate = 12 lpm, He/O_2 plasma: He Flow Rate=12 lpm and O_2 Flow Rate = 0.3 lpm): (a) 30 degree, (b) 45 degree and (c) 60 degree…… 144

Table 4. Deconvolution Analysis of Plasma Treated PET Films by XPS Angle Resolved Analysis (He plasma: He Flow Rate = 12 lpm, He/O_2 plasma: He Flow Rate=12 lpm and O_2 Flow Rate = 0.3 lpm): (a) 30 degree, (b) 45 degree and (c) 60 degree…… 145

Table 5. Chemical Composition of Silicon Wafer Treated by Atmospheric Plasma (He/O_2 plasma: He Flow Rate=12 lpm)……. 147

Table 6. Chemical Composition Change along Ageing Time of Plasma Treated PET Films by XPS Angle Resolved Analysis (He Flow Rate = 12 lpm)…….. 149

Table 7. Surface Roughness (RMS) and Increase of Surface Area (%) of Plasma Treated PET Film (He/O_2 plasma: He Flow Rate=12 lpm)……151

Table 8. Surface Roughness (RMS) of Silicon Wafer (He/O_2 plasma: He Flow Rate=12 lpm)……..153

Table 9. Tensile Strength of Plasma Treated PET Films (He/O_2 plasma: He Flow Rate=12 lpm)……..156

I. INTRODUCTION

Plasma is an ionized gas in a neutral state with an equal density of positive and negative charges (physical definition of plasma). Plasma was defined as the "4th state of matter" (solid → liquid → gas → plasma) by Crookes in 1879 [1]. The plasma state can be achieved in a wide range of temperatures and pressures. It consists of free electrons, radicals, ions, UV-radiation, and various highly excited neutral and charged species independent of the gases used. Plasma can be found easily in the universe. Solar coronas, lightening bolts and nuclear fusion are all examples of plasma. Plasmas also appear in man-made devices such as fluorescent lamps, neon tubes, welding arcs and gas lasers.

Plasmas play an essential role in many industrial areas, particularly in electronic parts such as semiconductor microchip manufacturing, and in automotive and aerospace industries. Recently, plasma techniques are utilized in lighting and large-screen televisions. In light of environmental regulations and concerns, the textile industry has become more interested in plasma applications as a novel finishing technology that significantly reduces toxic-chemical pollution. Plasma technology received enormous attention as a solution for environmental problems in textiles, and there has been rapid development and commercialization of plasma technology over the past decade. Plasma treatment is a dry process, i.e., it does not require water or wet chemicals. In addition, plasma is able to change substrate surface properties (such as micro-roughness and functionalization) without affecting bulk properties. Plasma surface modifications (such as desizing, wettability enhancement, water/soil-repellency, printability, dyeability, shrink-resistance, adhesion enhancement and sterilization etc.) can be achieved over large textile areas.

The various plasma applications are dependent upon the characteristics of the plasma, which consists of the mixture of ions, electrons, neutrals, excited molecules and photons. Plasma can be classified as hot-temperature or low-temperature plasma. Hot-temperature plasmas include solar coronas and nuclear fusion generated by thermonuclear reaction. Their temperature is about 100 million degrees (°C) when this reaction is sustained. However, in low-temperature plasmas (non-equilibrium and non-thermal), electron temperature is much higher than ion temperature. The high-energy electrons and low-energy molecular species can initiate reactions through electrical discharge without excessive heat causing substrate degradation. Low-temperature plasma has been used in a wide variety of engineering applications such as surface etching and material processing, including the textile processes. Low-temperature plasma is particularly suited to apply to textile processing because most textile materials are heat sensitive polymers. Low-temperature plasma treatments are conducted under low pressure or atmospheric pressure.

While most plasma treatments on polymeric materials including textile materials have been conducted using low-pressure plasma, the atmospheric pressure plasma treatments have recently emerged as a novel technique for textile applications. However, the results from low-pressure plasma applications can be used to predict, compare, or optimize atmospheric pressure plasma processes. In this thesis, Chapter II reviews plasma systems and plasma applications. In Chapter III, the effects of plasma on material surfaces are discussed in terms of plasma-surface interfacial interactions, which are physical and chemical alterations on the substrate surface. The most of research on the effects of plasmas was carried out under low-pressure plasma systems. However, these results may be useful to predict those of atmospheric pressure plasma treatments. Chapter IV is a report on a preliminary study of

plasma-substrate interaction under atmospheric pressure (Surface Analysis of Poly Ethylene Terephthalate (PET) Treated by He/Air and He/O_2 Atmospheric Pressure Plasma). Chapter VI illustrates a more definitive study of plasma-substrate interaction based on etching/re-deposition, cross-linking and ageing behavior of hydrophilicity. The application of atmospheric pressure plasma to high performance fibers is discussed in Chapter V (Effects of Atmospheric Pressure Helium/Air Plasma Treatment on Adhesion and Mechanical Properties of Aramid Fibers).

II. PLASMA SYSTEMS AND APPLICATIONS TO TEXTILES

1. Plasma Systems for Textiles

1.1 Low-pressure Plasma Systems for Textile Applications

Although low-temperature plasma has been used in various ways for industrial applications (surface modifications, etching, deposition, polymerization, wettability enhancement, hydrophobicity enhancement, adhesion enhancement and etc.), vacuum systems in low-pressure plasma (inductively-coupled and capacitively-coupled) not only impart additional cost to the system but also limit size and amount of products. However, initial plasma systems for the textile industry were designed to overcome these disadvantages even using vacuum system.

1.1.1 Continuous Plasma Processing in Vacuum Chamber

The first continuous plasma system in a vacuum chamber for textile treatment was proposed by Bradley [2] in 1971. This plasma system (Surface Activation Corporation, USA) was designed for continuous grafting of fabric, fiber bundle (tow) and tire cord as shown in Figure 1. This system was set up by combining the plasma excitation and monomer exposure chambers in sequence with other manufacturing and processing steps. The grafting applications with polyacrylic acid were very effective on wettability and moisture retention of polyester fabrics even after repeated washing. Also, these enhancements were obtained without alteration of bulk properties. Other synthetic fabrics treated by this process resulted in higher moisture regain and reduced static charge.

In early 1990's, Sando Iron Works Ltd. (Uzu, Wakayama, Japan) [3] developed continuous low-temperature plasma system for desizing and scouring of woven fabrics. This

plasma system can manage fabrics with maximum width, 1,500 mm and a speed range of 0-50 m/min under vacuum pressure, 0.1-2.0 Torr. No further information is available.

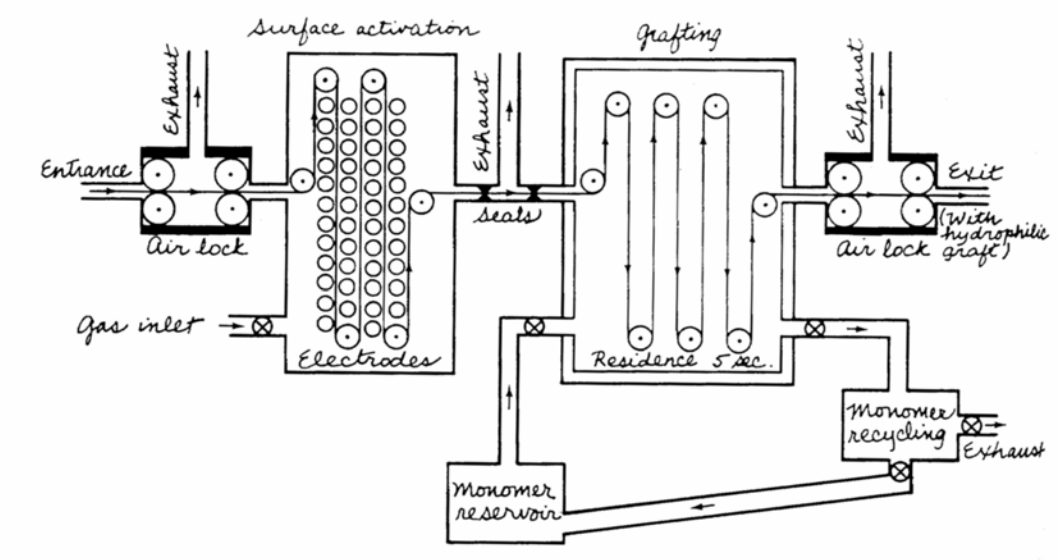

Figure 1. Proposed Continuous Grafting Plasma System by Bradley [2]

Rakowski [4,5] developed a continuous plasma system designed (Lódz Textile Institute at Poland) for wool anti-shrinkage and dyeing applications. This system has four step vacuum systems achieving plasma with the pressure of 50 Pa, and operates at 13.56 MHz with the energy density of 0.12 W/cm^3. The directional friction effects on wool fibers were remarkably enhanced after plasma treatment, resulting in the reduction of felting. Also, plasma treatment on wool resulted in higher interfiber cohesion involving in spinnability enhancement. Compared to a conventional printing process on wool fabrics, the plasma

surface treatment could not only reduce chemicals and water consumption, but also save energy consumption by 90 %. Moreover, the dyeing and mechanical properties were improved; less yellowing and graying, the enhancement of color fastness and better abrasion resistance and tensile strength. Anti-shrinkage finishing of plasma treated wool fabrics achieved higher felting resistance than the standard fabrics, even without using resins. Using this plasmas equipment, it made possible to save amount of chemicals, water and energy.

Vohrer [6,7] introduced a semi-continuous vacuum plasma system for textile (located at Fraunhorf IGB, Stuttgart, Germany), foils and membranes as shown in Figure 2. This system has four chambers designed for semi-continuous process operation at 13.56 MHz with the speed of 1-20 m/min. and a width of 18 cm. The working pressure ranges from 0.01 to 1 mbar, and the plasma power is between 10 and 10,000 W. The applications of this system include most textile wet-chemical finishing process.

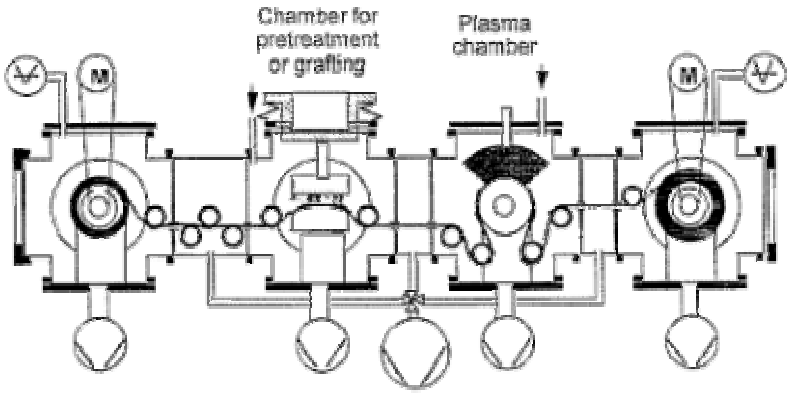

Figure 2. Semi-Continuous Plasma System at Fraunhofer IGB, Stuttgart, Germany) [7]

However, the commercialization of this was not successful. The vacuum systems maintaining low-pressure in the chamber were expensive to operate. In addition, this system required increased size when longer exposure times were necessary.

1.1.2 Roll-to-Roll Batch Plasma Processing in Vacuum Chamber

In 1986, the researchers at NIEKMI institute in Russia produced a semi-continuous plasma system (UPCH-140) for textile industry [5,8]. The LPCH-180SH and KPR-180 machines (Figure 3) were developed for wool fabric printing and are operating at Pavlovo Posad Shawl Manufactory Company in Russia. For plasma treatment of textile materials, polymer films, nonwovens and composites, new model KPR-270 was manufactured by, Tecnoplasma, S.A., a joint venture company between NIEKMI Institute and several European textile machine manufacturers. Table 1 shows the comparison between the plasma machines manufactured by NIEKMI Institute. Recently, H.T.P Unitex (Italy) took over the license and is manufacturing these systems. The roll-to-roll process is carried out inside a vacuum chamber, ranging from 20 to 200 Pa, and at speeds ranging from 5 to 50 m/min. [9]. While continuous vacuum plasma systems have two parallel electrodes, this system has a number of roll electrodes connected to a medium-frequency generator. A variety of fabrics, films and composite materials (50-320 cm width) can be treated by passage between the electrodes at chamber temperatures, less than 50 °C. Primary applications are enhancement of water-repellency, coating adhesion, wool anti-shrinkage, dyeing and printing.

Europlasma (Oudenaarde, Belgium) is manufacturing a roll-to-roll batch plasma systems for fabrics, films and nonwovens at widths up to 180 cm [10]. These plasma systems are designed for multiple applications including surface activation, surface cleaning, etching

and plasma polymerization under vacuum (10^{-2} – 10^{-3} mbar). At least 10 systems are currently installed and running. Polyplas (Emmerthal, Germany) also produces a roll-to-roll batch plasma system for surface activation and cleaning before dyeing, desizing and wet chemical processing [11]. 4th State (Belmont, California, USA) introduced a roll-to-roll batch plasma system for activation, cleaning, deposition and grafting applications to fibers and fabrics [12].

Table 1. Parameters of the Industrial Plasma Machine Manufactured by NIEKMI Institute for Textile Materials [8]

Parameter	**LPCH-180SH**	**KPR-180**	**KPR-270**
Working width, cm	180	180	270
Diameter of fabric roll, cm	<135	<110	<110
Treatment rate, m/min.	8-80	8-80	8-80
Power consumption, kW	180	75-110	75-110
Overall dimension, cm	1,350x780x400	780x520x420	1,240x520x420
Mass. kg	25,000	9,000	-

While the above mentioned vacuum plasma systems have been manufactured and used for variety industrial applications, these plasma systems have the following disadvantages:

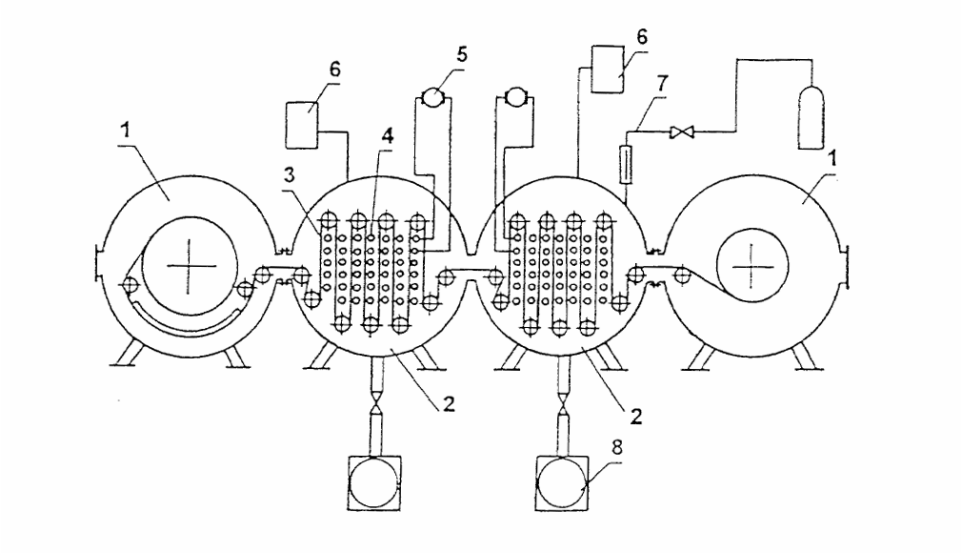

(a) Schematic Diagram of UPCH-140: 1-vacuum chamber, 2-plasmachemical reactor, 3-fabric, 4-electrodes, 5-power supply, 6-vacuum gauge, 7-gas supply system, and 8-gas supply system

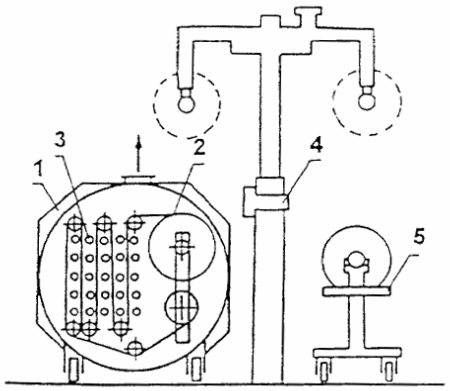

(b) Schematic Diagram of KPR-180: 1-plasma chemical reactor, 2-fabric, 3-electrodes, 4-roll loader and 5-transporting cart

Figure 3. Schematic Diagram of (a) UPCH-140 and (b) KPR-180 [5,8]

1) The various applications are easily limited in a vacuum plasma system.
    - The vacuum chamber and electrodes should be cleaned in order to prevent unfavorable contamination from a previous application.
    - It is preferable that each plasma system is specific to one application.
    - These plasma systems in vacuum chambers are not compatible with continuous production lines.
2) The batch process could lead to lower productivity for the textile manufacturing processes with mass production and high line speed.
3) Careful handling of fabrics after plasma treatment is necessary to avoid additional contamination before following processes.
4) Vacuum devices in the plasma system need higher energy consumption and system cost, leading to the limitation of a large-scale system construction.

1.2 Atmospheric Pressure Plasma Systems for Textile Applications

In light of the disadvantages of low-pressure plasma systems, there has been increasing interest in atmospheric pressure plasma systems and applications in the textile industry. The only available atmospheric pressure plasmas for textile industrial applications are glow discharge systems.

The three main glow discharges at atmospheric pressure are corona, dielectric barrier discharges (DBD) and atmospheric pressure glow discharge (APGD). As the effects of low-pressure plasmas are available at room temperature, the same effects can be obtained under atmospheric pressure if the plasma is given sufficient room and time for relaxation. By accelerating the electric field, the lighter particles (electrons) achieve more kinetic energy

than heavier ions and neutral gas particles. High-energy electrons induce collisions and release their kinetic energies to the surroundings, and then the plasma system reaches thermal equilibrium. In order to avoid thermal relaxation at atmospheric pressure, a largely inhomogeneous electric field is required [13]. When sufficient voltages are supplied to accelerate electrons in the inhomogeneous electric field on one of the electrodes, a sharp needlepoint, a localized plasma (corona discharge) can be generated. An alternative way to prevent thermal relaxation at atmospheric pressure is to introduce a changing current frequency into a discharge. At low and high frequency, a discharge is initiated each time between the parallel electrodes. This discharge, found in DBD, could be generated under atmospheric pressure but would not remain uniform on the whole electrode area. Very narrow filaments (Diameter= 100 μm and foot radius = 0.5 cm)[14] are seen between electrodes in DBD. However, Kanazawa et al. [15] showed initially that uniform, homogeneous and stable atmospheric pressure plasma was possible continuously by applying 3 kHz and radio frequency. In sequence, several researchers reported that stable atmospheric pressure plasma could offer more effective applications under highly uniform plasma processes [16-28].

1.2.1 Corona Systems for Textile Applications

Corona systems have been studied for availability in the textile industry because they can be operated in atmospheric pressure. Although many corona systems are utilized for continuous processing for mass production with high speed, some of examples are presented in this paper. One of the early studies discussed improvement of shrink resistance for wool and mohair top [29,30]. These results were obtained by using a continuous corona system,

which was able to pass through substrates between parallel Pyrex electrodes as shown in Figure 4. This pilot scale corona device was available to not only make high-speed production of wool and mohair top, but also improve shrink-resistance and spinnability [30].

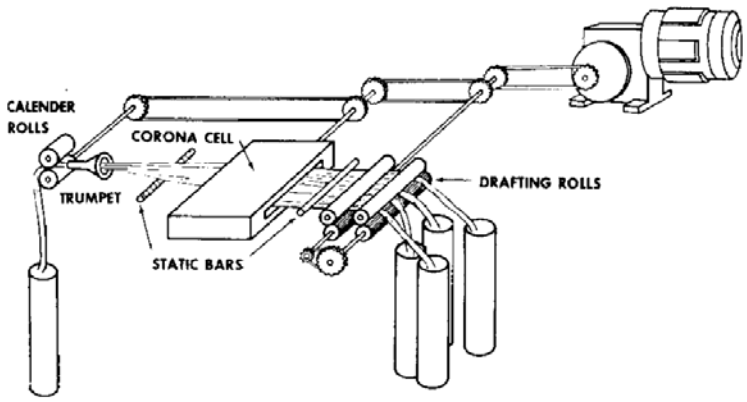

Figure 4. A Schematic Diagram of Continuous Corona Discharge System for Wool and Mohair [42]

For another example, Abbot [31,32] showed the enhancement of cotton sliver cohesiveness using the corona systems with a cotton sliver passing between the large and small corona rollers. Softal Electronic GmbH (Hamburg, Germany) [33,34] developed a continuous corona system for film surface modification. This system was designed for the roll-to-roll process, applying to adhesion, coating, printability and deposition. Sherman Treaters Co. (Oxon, UK) [35] designed a continuous corona system for surface modification of polypropylene tow following melting spinning process (Figure 5). These results showed improvement of antistatic, friction and wettability of the treated fibers, and could reduce the

quantity of spinning finish added resulting in cost-saving, environmental issues and fiber performance.

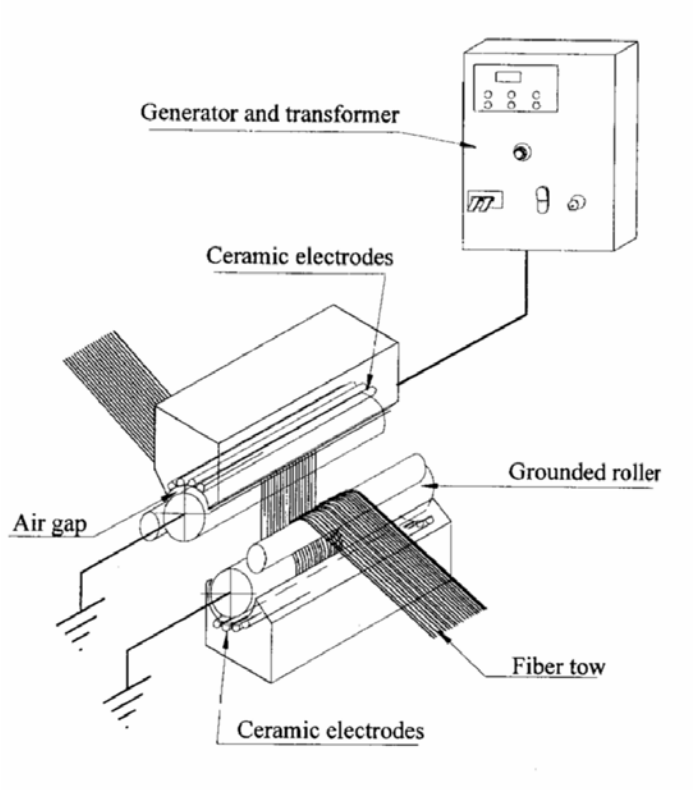

Figure 5. Schematic Diagram of the Continuous Corona System for Polypropylene Fiber Tow Designed by Sherman Treaters Co. [35]

1.2.2 Atmospheric Pressure Glow Discharge (APGD)

The foundation of a stable and homogeneous plasma under atmospheric pressure was reported in 1998 [15]. This stable and homogeneous discharge required as the following conditions:

1) Helium was used as dilute gas,
2) Heat resistance insulating plate was set on the lower electrode plate while upper electrode was a brush style, and
3) Power supply frequencies were 3,000 Hz and Radio-frequency (13.56 MHz).

However, this discharge could be transformed into thermal plasma such as arc discharge when strict plasma conditions were not applied. Fluorination of poly(ethylene terephthalate) (PET) film was successful compared to the results in vacuum plasma using optical emission spectroscopy. Consequently, Yokoyama et al. [16] improved an atmospheric pressure plasma device by placing a brush style upper electrode into a plane electrode. This APGD plasma treatment introduced same effects on organic films as low-pressure plasma treatment. Also, they discussed the mechanism of APGD plasma [17] and explained that stabilization of this system was related to the requirements of a stable APGD plasma (He gas, dielectric electrode plate and high frequency). Roth and co-workers developed the one-atmospheric glow discharge plasma reactor, called one atmosphere uniform glow discharge plasma (OAUGDP), and applied plasma treatment to textile materials [36] for surface modification and sterilization [37]. This reactor has two parallel electrodes covered by an insulating coating and can generate uniform plasma in helium according to Kanazawa's model [15]. Another independent development of APGD was carried out at North Carolina State University, the parallel plate atmospheric plasma device for industry (PALADIN), designed specifically for the industrial applications [38]. A schematic diagram of PALADIN

is shown in Figure 6. This capacitively-coupled device was designed for a RF power supply. Table 2 shows a comparison of operating parameters in atmospheric pressure plasma systems.

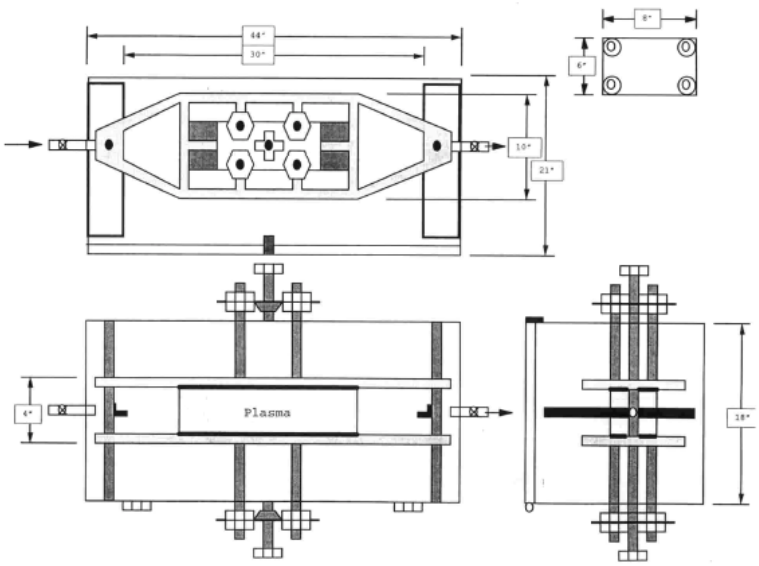

Figure 6. Schematic Diagram of PALADIN [38]

1.2.3 APGD Systems for Textile Applications

Atmospheric pressure plasma systems are suitable for textile industrial applications, which involve mass production at high speeds, because it is possible to carry out continuous processing without size limitation. Recently, even though atmospheric pressure plasma systems were developed in Japan and the United States, Dow Corning Plasma Solutions is the only available APGD machine manufacturer for textile applications in the world. A model of APGD, AP-100 (width 100 cm, but width of machine is variable depending on

textile process conditions.), is able to generate a stable and uniform glow discharge and leads to continuous processing at a maximum speed of 60 m/min [46].

Table 2. Comparison of Operating Parameters in Atmospheric Pressure Plasmas

Properties	**Corona /DBD**	**APGD**	**AP-100**	**OAUGDP**	**PALADIN**	**APNEP**	**APPJ**
Operating Gas	air, Ar. O_2, N_2	He+O_2, CF_4	He + O_2, air	He, Ar, N_2O, CO_2, air	He+Any Gas	Any Gas	He, O_2, Ar, air, N_2
Frequency	20-50 kHz	>3 kHz	50-350 kHz	0.5-40 kHz	1-12 kHz	2.45 GHz	13.56 MHz
Power, W	0.5-10/cm	16-50	0-3 kVA	10-2,000	1-250	1,000-3,000	250
Voltage, V	10-20 kV	<10 kV	0-25 kV	1.5-18 kV_{rms}	7.8 kV_{rms}	-	320 kV_{rms}
Plasma Volume, cm^3	-	-	-	30-2,800	774	-	-
Electrode Gap, cm	0.1-0.5	<1	<3.0	0.2-2.8	0.8-3.0	-	-
Gas Input, dm^3/min.	-	5	-	100-150	-	0-160	-
Reference	14	15,16	23	28	38,214	215	123

Dow Corning Plasma Solutions has supplied APGD plasma systems to several production lines in Europe [47]. One of them, installed at Institute of Fiber and Polymer Technology Research (IFP, Sweden), is applied to adhesion enhancement of polymer coatings (Almedahl AB, Sweden), surface modification of automobile textiles (Borgstena Textile Sweden AB, Sweden), increasing hydrophobicity of cellulose based materials, and improvement of adhesion of polymer materials (SCA Hygiene Products AB, Sweden). In

German, Kirchhoff GmbH & Co. has been applying APGD plasma system to anti-shrinkage finishing. The same APGD system at Polisilk S.A. in Spain is being used to improve binding properties of polypropylene-based coating. In addition, Plasma Ireland supplied another APGD system to Scapa Group in England for printing applications.

2. Plasma Applications to Textile Processing

2.1 Wettability Enhancement

The wettability enhancement of polymeric surfaces can be obtained easily by plasma treatment in oxygen containing gas. However, after exposure to air, the wettability is not durable due to the ageing process. For the textile applications of wettability enhancement, increased durability has been obtained using plasma graft polymerization techniques. The monomers used in plasma graft polymerization for wettability enhancement are acrylic acid [2,48], nitro compounds [49], 2-hydroxyethyl methacrylate (HEMA)[50], methyl methacrylate (MMA) [50], acrylamide (AAm) [51,52] and acrylonitrile [52].

In 1971, the first commercial application of plasma graft polymerization for wettability enhancement on fabrics was conducted by Bradley [2]. After surface functionalization by argon plasma for PET fabrics, the acrylic acid monomer was introduced into vacuum chamber leading to uniform grafting polymerization. This technique could render PET fabrics as wettable as cotton and improve moisture retention and washing durability. In addition, handle properties of fabrics were improved without alteration bulk properties. Cotton fabrics treated by this technique showed better hand properties obtained. Regardless of these superior results, this system has not been used since 1975 [53].

Inagaki et al. [49] reported that plasma graft polymerization of nitro compounds (nitro ethane and nitropropane) in the vapor phase could be used to improve wicking of PET fabrics using. Compared to oxygen plasma treatment, the PET fabrics deposited by nitro compounds showed no decay of contact angle. The washing durability after 10 times laundering showed that the wicking time of 1 min. treated PET fabric increased from 46 to 80 second. Regardless of reduction of washing durability, the wicking time was much shorter than untreated PET fabric. In addition, it was reported that plasma graft polymerization with acrylic amide monomer introduced a significant increase of hydrophilicity on the silk surface [51]. Bhat et al. [52] investigated the surface electrical resistance of cotton and PET fabrics treated by plasma grafting polymerization with acryl amide and acryl nitrile. The change of surface electrical resistance was due to the formation of hydrophilic groups and surface morphology change on the surface of fibers, leading to an increase of moisture content. Cotton and PET fabrics treated by plasma grafting polymerization showed a significant reduction of electrical resistance with only small amount of monomer.

Grancarz et al. [48] investigated the filtration efficiency of polysulfone membrane polymerized with acrylic acid in solution and vapor phase after plasma treatment. The membrane grafted in solution did not show improved filtration efficiency due to pore blocking by long polymer chains. This membrane was not recommended for ultra-filtration. However, the membranes modified by plasma graft polymerization in vapor showed higher hydrophilicity and improved filtration properties due to small changes in pore size and distribution.

2.2 Water Repellent Finishing

Fluorocarbon, hydrocarbon and mixtures of fluorocarbon and hydrocarbon gases have been used to increase hydrophobicity of polymer substrates in plasma. Compared to oxygen and air plasma treatment, fluorocarbon and mixtures of fluorocarbon and hydrocarbon gas plasma showed higher durability in air exposure [54,55]. Moreover, fluorocarbon plasma or plasma polymerization with fluorocarbon monomers can more easily and simply render a polymer surface hydrophobic than plasma graft polymerization techniques.

Iriyama et al. [56] studied the water-repellency of nylon fabrics treated in fluorocarbon plasmas (CF_4, C_2F_4, C_3F_6 and C_6F_{14}). The durability of water-repellency after 30 min. washing was better in fabrics treated with saturated fluorocarbon plasmas than unsaturated. The saturated fluorocarbon plasma introduced longer chains of polymer on fabric surface, leading to better hydrophobicity and durability. Wang et al. [57] found similar results from plasma treatment on PET film with mixtures of fluorocarbon and methane. McCord et al. [58] found that the fluorocarbon functional group, $-CF_3$, played an important role in increasing water-repellency. C_3F_6 plasma treatment on denim fabric could achieve better water-repellency than CF_4. Moreover, the fluorocarbon plasma is effective as an oil repellent finishing for textile materials [7]. Cotton-polyester fabrics treated C_3F_6 plasma achieved not only higher water-repellency but also oil-repellency.

Regardless of good results from previous research works, fluorocarbon plasma treatments have not been used commercially to improve water-repellency or oil-repellency of textile materials. First, fluorocarbon plasma can generate a Teflon-like film not only on the substrate surface, but also on the inside of the plasma chamber. The fluorocarbon coating on the chamber, which is hard to remove, can block gas nozzles and contaminate the inside of the plasma chamber. Thus, use of fluorocarbon plasmas for industrial scale low-pressure

plasma system is not recommended [59]. Secondly, the durability against washing was not examined for water-repellent finishing of textiles although most of plasma applications to textiles have not been available to satisfy commercial needs yet. In order to overcome these issues against fluorocarbon plasma applications, it is suggested that a new plasma system designed, plasma conditioning and pre-conditioning of fabrics should be considered to optimize durability of washing for textile industrial requirement.

2.3 Anti-shrinkage Finishing

Anti-shrinkage finishing using plasma treatment is the first successful commercialized technique for the textile industry. The first attempt at anti-shrinkage finishing was a corona treatment for wool fabrics [60]. Wool garments treated by corona showed better shrink resistance and stability than untreated. Thorsen et al. [30] suggested that corona treatment could be applied to mass production of wool fabric to improve shrink resistance. Compared to corona treatment, the efficiency of anti-shrinkage in plasma treatment shows better effect. Recently, low-pressure plasma and corona are available for anti-shrinkage finishing in textile industry. Plasma treatment is considered an environmentally friendly alternative to the conventional anti-shrinkage finishing, wool chlorination. Rakowski [4] showed the advantages of low-pressure plasma treatment for anti-shrinkage finishing of wool fabrics based on economical and environmental issues. Regardless, further studies are still needed to apply plasma treatment to industrial production for anti-shrinkage finishing as well as enzymatic treatment, which is another possible environmentally friendly method for anti-shrinkage finishing [61].

Oxygen was known as the most effective gas for shrink proofing of wool fabrics made from plasma-treated yarns [62]. Oxygen plasma was also effective for bleaching and controlling anti-shrinkage of wool fabrics without deteriorating tensile strength. The anti-shrinkage effect through plasma treatment of wool fibers can be explained by surface morphology and chemistry changes. The morphology change is a result of etching by the plasma of the wool fiber surface, leading to friction coefficient changes in the direction (u_1) with and against scales (u_2) [63]. The plasma treatment reduces the difference u_2-u_1 value in dry state while u_2-u_1 value in wet state increases greatly over untreated wool fiber. The surface chemistry changes contribute to the anti-shrinkage effect on wool fibers [64,65]. The hydrophilic groups on the surface of wool fibers could build up a thin water layer during washing, and separate the wool fibers from each other, reducing the differential frictional coefficient and shrinkage. In addition, sulphonate and carboxylic functional groups can generate a shrink-proofing effect. The increase in concentration of anionic groups in the cuticle generates electrical double layers on the wool fiber surface, inducing an electrostatic separation of the fibers. The oxidation of protein chains in the cuticle increases the number of molecules in the cell, resulting in expanded osmotic pressure and an advanced swelling of cuticle cells. These behaviors could lead to the reduction of fiber-to-fiber friction, which is responsible for the increase of anti-shrinkage. Also, anti-shrinkage of wool fabrics can be improved by post-plasma treatment and subsequent graft polymerization in vapor [66]. It is believed that an increase in hydrophilicity plays an important role in increasing shrink-resistance due to higher spreading and adhesion of hydrophilic monomers on plasma-treated wool.

It has been reported that atmospheric pressure plasma can induce same effects on wool fibers as low-pressure plasma: etching and surface functionalization [67,68]. Higher shrink-resistance can be introduced into wool fabrics treated by atmospheric pressure plasma using mixtures of helium/argon and acetone/argon [69].

2.4 Desizing

The application of size to warp yarns before weaving plays an important role in enhancement of weaving efficiency due to an increase of yarn strength and reduction of yarn hairiness. Also, it is important to remove size after weaving for further processes, dyeing and finishing. The conventional desizing process is conducted by washing in hot water bath. Regardless of high temperature, complete removal of size on fabrics is impossible due to re-deposited sizes on yarns during the desizing process, resulting in poor bleaching, dyeing and printing. Moreover, the desizing waste is a major concern of pollution world-wide, even though a recycling technique is available.

Plasma desizing was performed as a novel technique to solve the environmental problem of desizing [70]. The plasma desizing process consisted of two steps: gas plasma treatment on the sized fabric and washing in solution. Compared to hydrogen peroxide desizing, plasma treatment plus cold-water washing showed better size removal on cotton fabrics. With only oxygen plasma treatment for sized yarns, up to 70% PVA (polyvinyl alcohol) size was converted into gas, and only 4 % of fiber loss was obtained even under severe plasma conditions without significant tensile strength loss. Oxygen plasma was more effective in desizing than either air or nitrogen. Two possible plasma effects are involved in the plasma desizing. First one is gas vaporization of sizes by the etching effect of plasma.

The second one is hydrophilic functionalization of size molecules, possible in conjunction with either chain scission or cross-linking. The increase in hydrophilic groups may lead to higher solubility in wash solution. Kuo [71] found similar results of plasma desizing on PET and PET/cotton blended fabrics. Plasma treatment for 20 min. removed about 70 % of size while 90% of size was removed by pre-washing and subsequent 5 min. plasma treatment.

Sando Iron Works Co. Ltd [72,73] is manufacturing commercial plasma systems for desizing and scouring applications. Also, Tomasino et al. [74] suggested continuous roll-to-roll low-pressure plasma system for desizing application. However, these plasma systems are designed as vacuum plasma systems, leading to higher manufacturing cost and batch processing. Cai et al. [75] reported that atmospheric pressure plasma could overcome these drawbacks. Helium atmospheric pressure plasma resulted in desizing of PVA without alteration of tensile strength of cotton fabrics. With cold water washing, up to 97% of size could be removed from cotton fabric pre-treated by helium atmospheric pressure plasma.

2.5 Flame Retardant Finishing

Flame retardant finishing of textiles has been accomplished via plasma treatment. As one of initial studies for flame retardant finishing on textiles, Simionescu et al. [76,77] studied flame retardant finishing on natural and synthetic fabrics. The fabrics pre-absorbed with phosphorus and halogen containing monomers were exposed to nitrogen low-pressure plasma, leading to graft polymerization on fabric surface. The graft polymerization by plasma with phosphorus and halogen containing monomers improved the flame retardant properties of fabrics. In addition, it was proposed that plasma application of flame retardant finishing could have economical and environmental advantages compared to conventional

wet-chemical finishing processes. For flame retardant finishing for cotton fabrics [78], cotton fabrics treated by argon plasma with THPOH/NH_3 and H_2O_2 washing were durable to 50 launderings and launderings with chlorine bleaching.

Akovali et al. [79] explained that cross-linking by plasma have a negative effect on flame retardancy. The cross-links on the surface of fibers could hold the burned and non-burned parts together, leading to keeping most of the heat in the pre-flame layer of burning during combustion and inhibiting dripping of the burning materials. Thus, flammability can increase from fiber surface to inside without spending much heat. Flame retardancy decreases when the chain scission of macromolecule chain by plasma generates low molecular-weight molecules [80]. However, grafted polymerization with flame retardant monomers can overcome the negative effect of cross-linking and chain scission. With an increase in grafting, the ignition time was extended the limited oxygen index (LOI) increased [81]. Moreover, an increase in grafting rate resulted in an increase of char, indicating that a grafted layer of acrylic acid can not only be charred, but also promote charring of the polymer substrate.

2.6 Adhesion Enhancement

Most of composite materials, including UHMPE (ultrahigh modulus polyethylene), PPTA (poly(p-phenylene terephthalate) and carbon fibers, have excellent mechanical properties. However, chemical inertness and smoothness of their surfaces can be a serious problem to apply to resin matrix for composite applications. Compared to conventional wet-chemical surface modification, plasma techniques can overcome the disadvantages of high

performance fibers easily and improve adhesion to resin matrix without altering physical properties.

Ultrahigh-modulus polyethylene (UHMPE) fibers such as Spectra® fibers do not form strong bonds with most commercially available matrix materials due to their inert chemical structure. Low-pressure plasma treatments have been shown to greatly enhance the bonding between UHMPE fiber and resin matrices such as epoxy and vinyl ester resins [82]. The plasma treatment created not only micro-roughness on the surface of UHMPE fibers, resulting in a better mechanical interlocking of the fiber surface to resin matrix, but also functional groups, leading to chemical interfacial bonding between the fiber and matrix. Kevlar® (poly *p*-phenylene terephthalamide) fibers have high stiffness, strength and thermal resistance with low density. These outstanding properties are applicable to spacecraft, aircraft, automobiles, military and sport products. However, Kevlar® fiber has restrictions on its uses due to the inert chemical structure and smooth surface resulting from high crystallinity. These limitations lead to poor out-of-plane (off-axial) strength composites because of weak chemical and mechanical adhesion to most commercially available matrix. Great enhancement of the interfacial strength between Kevlar® and epoxy resin was shown by low-pressure plasma treatments using various gases (NH_3, H_2O, O_2, Air and Ar) [83,84]. These gases can not only generate possible reactive chemical groups (–COOH, -OH, and -NH_2) with epoxy resin but also create surface roughness. Carbon fibers have various advantages for composite materials such as high strength and stiffness, lightweight, high fatigue and corrosion resistance, low thermal expansion, and high thermal and electrical conductivity. However, the non-polarity of carbon fiber surface results in poor chemical bonding with a resin matrix, and the smooth surface leads to a reduction of mechanical

interlocking. Gas plasma treatments (NH_3, H_2O, O_2, Air and Ar/NH_3) [47,48], can overcome these drawbacks of carbon fibers by introducing micro-roughness and chemical functional groups, resulting in significant adhesion enhancement. Also, atmospheric pressure plasma is capable of treating high performance fibers for composite applications continuously [85-88].

The major effects of plasma treatment adhesion enhancement of the fiber-resin matrix are the following:

1) Surface cleaning – plasma can remove organic contamination from fiber surface, which can interfere with bonding between fiber and resin.
2) Etching/ablation – the etching effect of plasma can reduce weak boundary layers and increase the surface area, but the diameter of fibers is not reduced and its tensile strength is not deteriorated.
3) Cross-linking on surface – plasma can induce higher cohesive strength by formation of a thin cross-linking layer, which can mechanically stabilize the surface against the diffusion of low molecular weight species to the interface.
4) Functionalization on surface – the formation of chemical functional groups can lead to acid-base interactions and covalent linkages with resin, resulting in enhancement of adhesion between fiber and resin.

2.7 Dyeability Enhancement

Dyeing in textile industry requires the development of environmentally friendly and economic processes due to pollution and economic limitations. Plasma techniques have been studied to replace or aid the conventional wet dyeing process. The initial approach of plasma

was corona treatment. Previous studies [40,89] showed that corona assisted dyeing was ecologically and economically favorable as compared to conventional dyeing processes. Low-pressure plasmas also have been used to enhance dyeability of textile materials using various approaches: non-polymerizable gas plasma treatment before dyeing [55,63,90-102], plasma-induced graft polymerization before dyeing [103-109], etching/sputtering on dyed fabrics [110-112], and anti-reflective coating on dyed fabrics [113,114]. Atmospheric pressure plasma showed feasibility for dyeing applications [115].

However, some studies showed that plasma treatment did not increase dyeability of cotton. Kubota et al. [90] found that dyeability of reactive and direct dyes on cotton decreased after argon plasma treatment. The reduction of dyeability resulted from the increase of crystalline regions by etching away of dyeable amorphous regions, although water absorption of the cotton fiber increased after plasma treatment because of the capillary effect and hydrophilic group formation on the fiber surface. In addition, cross-linking could play important roles in deteriorating dyeability of cotton fabric [91]. Enzyme treatment and enzyme plus plasma treatment has been shown to increase dyeability of cotton fabrics at higher dyeing rate [91,92]. For wool fabric dyeing, plasma treatment enhanced dyeability of wool fabrics with acid dye [63,93-95]. Plasma treated wool fabrics showed a higher degree of dye fixation than untreated with faster dye-uptake and higher dyeing evenness. The degradation of the cuticle layer, a barrier to the diffusion of dyes, and more hydrophilic fiber surface could lead to significant increase of affinity of the fibers for dye [93]. In addition, plasma treatment, chlorination, plasma deposition, and their combination increased dyeability of wool fabrics as well as anti-shrinkage [95]. Enhancement of dyeability for PET fibers by air plasma treatment could be derived from a modification of microstructure on the fiber

surface resulting in a disintegration of the diffusion barrier [96]. Oxygen and tetrafluoromethane plasmas increase dyeability of PET film [55]. Water uptake and dyeability were enhanced by oxygen plasma treatment whereas tetrafluoromethane plasma induced water-repellency on PET fabric surface and improvement of dyeability. However, Okuno et al. [97] observed that an increase in crystallinity of PET fiber resulted in the reduction of dyeability. Etching of plasma treatment was dominant in amorphous region, a dyeable domain, and led to an increase of crystallinity of PET fiber. Wakida's group [99-101] extensively investigated the effect of plasma treatment on dyeing properties of nylon 6 fibers. Compared to acid dyes, oxygen plasma treatment enhanced the dye uptake, dyeing rate and dye exhaustion for nylon fibers dyed with basic dyes. Oxygen plasma treatment incorporated –OH and –COOH functional groups on the nylon fiber surface, leading to electronegativity on the fiber surface. Thus, the adsorption of basic dye can be higher than that of acid dye for oxygen plasma treated nylon fibers.

Byrne et al. [103] showed that plasma-induced graft polymerization with acrylic acid improved dyeability of PET fabric using basic dye, as well as anti-soiling and soil-release. Rayon, polyamide and polyester fibers grafted with benzidine achieved higher dyeability with sufficient wash fastness [104]. Park et al. [106] explained that generation of carboxylic acid groups (-COOH) on the PET surface could result in dyeability enhancement. When acrylic acid was grafted on PET fabric in plasma, the higher wettability resulted form the generation hydrophilic functional groups, and the carboxylic acid groups can help to interact with basic dye, resulting in enhancement of dyeability. Öktem et al. [107] also suggested that the carboxylic acid groups played an important role in dyeability improvement when PET fabrics grafted with acrylic acid were dyed with basic dye. Seto et al. [108] and Park et al.

[109] confirmed that the concentration of carboxylic acid generated by acrylic acid grafting had a significant relationship to an increase of dyeability when basic dye was used, resulting in the acid-base intermolecular interaction between acidic functional groups and basic dyes.

Sputtering technology was used to improve the depth of shade comparing to plasma treatment [110-112]. Dyed fabrics etched by sputtering showed higher color depth than untreated and low-pressure plasma treated fabrics. It was believed that the increase of color depth resulted from the generation of micro-craters by etching effect of sputtering, leading to the reduction of reflection of incident light. In addition, it was shown that anti-reflective coating by plasma polymerization was significantly effective on improvement of deep coloring on dyed fabrics [113,114].

Wakida et al. [115] showed the possibilities of atmospheric pressure plasma for wool fabric dyeing applications. The atmospheric pressure plasma treatment with a mixture of helium and argon was very effective on the reduction of half-dyeing time and an increase of dye exhaustion with acid dyes.

2.8 Sterilization

Sterilization processes are designed to destroy viable microorganisms before biomaterial contact with living organisms. In general, either a physical or chemical process or both are carried out sterilization. The conventional sterilization methods including heat, radiation, and chemical treatment can terminate the microorganisms [116]. Heat treatment is an easy method but bacteria with a pore could survive at high temperature and under some conditions. Additionally, heat treatment is not acceptable to low-melting polymer materials and it needs a relatively long period treat time. Ethylene oxide (ETO) is used as a chemical

treatment to sterilize many polymeric medical products. However, ETO is not only a highly toxic gas causing cancer but easily absorbed in plastic materials. Gamma radiation and X-ray can exterminate bacteria or viruses by breaking bonds inside the bacteria cells and virus capsides. However, some of microorganisms resist radiation, and radiation causes undesirable changes of substrate [117].

Considered disadvantages of conventional sterilization methods, the low-pressure plasma for sterilization is a promising alternative method to heat sensitive materials or plastic materials. The costs of low temperature gas plasma were nearly the same as steam sterilization and lower than formaldehyde and ETO sterilization [118]. Furthermore, gas plasma sterilization not only terminates bacteria and viruses but also eliminates dead bodies of bacteria and viruses from the biomaterial surface [116]. Compared to gamma radiation sterilization, gas plasma could induce less degradation and morphology alteration of biomaterials [120]. Gogolewski et al. [119] showed that gas plasma treatment (Ar, N_2, O_2, and CO_2) did not affect tensile properties and melting points of polylactide, nevertheless their molecular weights increased slightly and surface became smoother after plasma sterilization.

Low pressure plasma sterilization has restrictions, which are high cost of vacuum system and batch processing. However, atmospheric plasma system can solve these restrictions. Because the power density of atmospheric plasma is not high, it does not alter the bulk properties of substrates where bacteria and viruses live. Also, the successful design of a remote exposure reactor can eliminate many constraints of workpiece size and shape. Recently, the atmospheric pressure plasma has been investigated as novel sterilization technique [37,45,121-123]. One of successful designs is one atmosphere uniform glow discharge plasma (OAUGDP, University of Tennessee, Knoxville (UTK)).

Generally, the mechanisms of plasma sterilization processes are still unknown. Possible physicochemical mechanisms under low-pressure (vacuum) plasma were suggested [116,124-126] that the activated gas species (O_2) initially interacted with hydrocarbon bonds in bacteria cell walls, and then weakened bacteria cell walls. The plasma removes the outer bacteria layer with repetitions of this reaction (physical sputtering of the outer cell walls). Then the bacterial cells will be ruptured out by osmotic pressure, or the activated oxygen species and the UV light will destroy its internal structure (chemical degradation by reactive species and/or UV radiation from plasma). Koulik et al. [127,128] proposed the mechanism of sterilization under atmospheric pressure plasma as following;

(1) Plasmochemical reaction – oxidation and etching,

(2) Electron bombardment,

(3) UV radiation,

(4) Surface ablation and

(5) Chemical reaction after plasma treatment.

III. THE EFFECTS OF PLASMA ON SUBSTRATE PROPERTIES

In plasma bulk, the reactive species (positive and negative ions, neutral species, atoms, metastables and free radicals) are generated by ionization, fragmentation and excitation. And, they lead to chemical and physical interactions between plasma and substrate surface, depending on plasma conditions such as gas, power, pressure, frequency and exposure time. Non-polymerizable gas plasmas (Ar, He, O_2, N_2, CO_2, etc.) usually change surface morphology and induce the surface roughness of polymer films. Ions and neutral species in plasma collide with the molecules on the substrate surface, and then etch away physically: that is, etching effect. Consequently, the long molecular chains would be broken into short ones: chain scission. Also, the reactive species lead to chemical interaction with surface molecules, generating new functional groups (functionalization) and radicals. Radicals induce cross-linking generatation on the uppermost few mono-layers of polymer. Hydrocarbon and fluorocarbon gases can be been used to achieve deposition, and plasma polymerization can be obtained by using monomer gas. In this chapter, the effects of plasma on material surface are discussed based on the phenomena of plasma-surface interaction in the plasma bulk as shown in Figure 7.

1. Etching Effects of Plasma on Substrate Surface

Etching in plasma is a physical removing process of material on the surface of substrate. It is known recently that the etching effect plays an important role to sterilize medical materials [124]. Etching in plasma treatment has no unfavorable effect on the physical properties of substrate because only few hundred Å layers are etched away [129]. Surface morphology and micro-roughness are achieved by etching process, preferring to

removing amorphous region: that is, selective etching. However, the particles etched would be re-deposited on substrate surface again, and provide undesirable results on etching processing. Solid particles can be generated in the plasma when the concentration of particles coming off substrate surface is dense enough to interact with molecules on substrate surface or wall of reactor of plasma system [130].

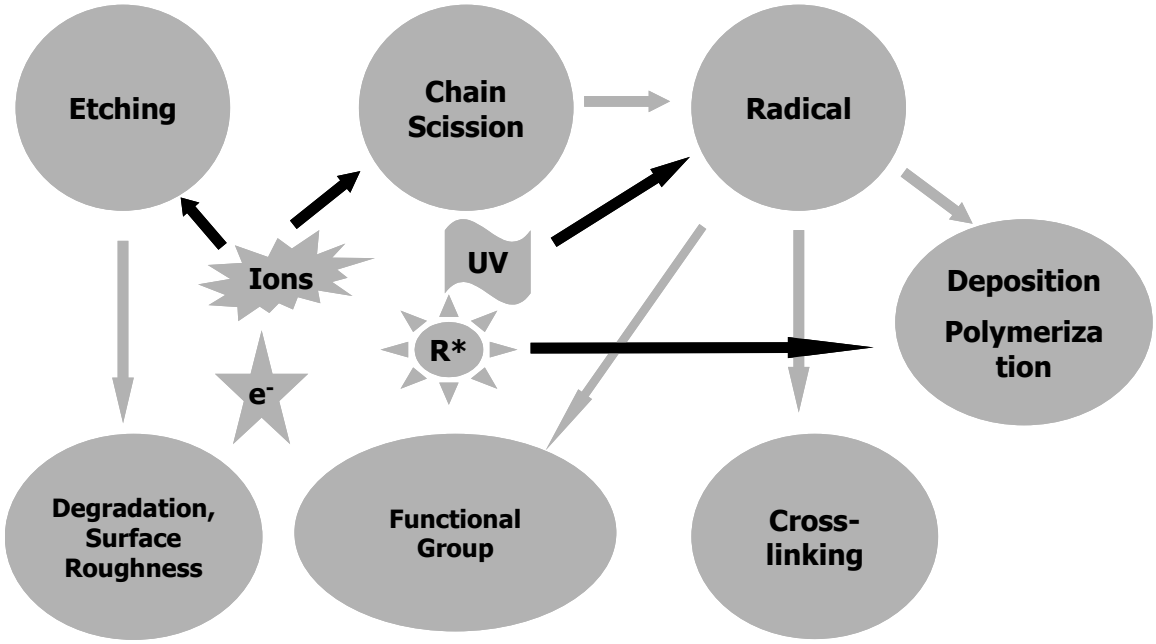

Figure 7. Mechanism of Plasma-Substrate Interaction

1.1 Mechanism of Etching and Re-deposition

It is known that both etching and re-deposition occurred simultaneously in the plasma process [131]. Etching and deposition rates are strongly related to the ion energy flux and

etching and deposition species, that is, the reactive species collide with the molecules on substrate surface, and the etching species could be re-deposited by interaction with the active particles on the substrate surface [132]. Roth [28] summarized the steps in an etching reaction as follows:

1) Removal or penetration of adsorbed mono-layers by energetic ions and etching species
2) Adsorption of etching species on the surface of the layer to be etched
3) Dissociation of the molecules of the etching species
4) Formation of a reaction product on the surface
5) Desorption of the product molecule

The etched species would be dissociated or ionized, and then deposited on the substrate surface. Consequently, the deposited species would generate new polymer layers or tiny particles. The new polymer layers would be etched by the ions in plasma, and deposited again. The etching and deposition processes are repeatedly conducted.

1.2 Surface Morphology and Roughness Change

The etching effect derives not only surface morphology change but also surface roughness change of the substrate surface [132], examined by Scanning Electron Microscopy (SEM) and Atomic Forces Microscopy (AFM). Most of non-polymerizable gases (Ar, He, O_2, N_2, CF_4, CO_2, etc.) are apparently effective on etching [129,132-135]. While surface of untreated PET film is quite smooth, plasma treatment increase roughness of substrate surface

under various plasma conditions. Oxygen and carbon dioxide plasma treatments caused similar change of surface roughness and higher etching effect than nitrogen and air plasma [135]. This can be explained that oxygen atoms play an important role to etch the substrate surface. The similar results were obtained from plasma treated SiO_2 aerogel film [133]. The reduction of film thickness after plasma treatment was in order of $O_2 > N_2 > Ar > He \cong H_2$ as shown in Figure 8. Riekerink et al. [129] explained that the etching effect was dependent on the film surface properties. The lamellar surface structure of low-density poly(ethylene) (LDPE) film was changed into a nanoporous-like structure with uniform pores while high-density poly(ethylene) (HDPE) did not show significant the surface structure change by CF_4 plasma treatment.

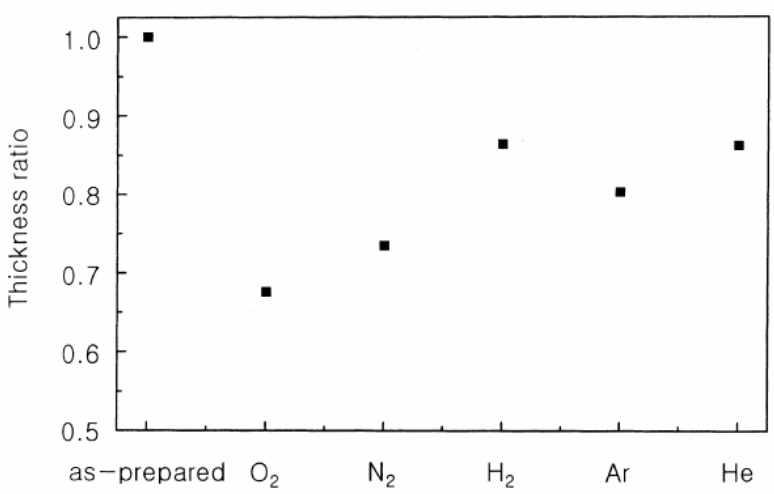

Figure 8. Thickness Variation of the SiO2 Aerogel Films before and after Various Gases Plasma Treatment (500W/50 min.)[133]

1.3 Selective Etching on Semi-crystalline Polymer in Plasma Treatment

Most of polymer materials are consisted of amorphous and crystalline region, that is, a semi-crystalline polymer. Padhye et al. [28] studied the effect of etching on PET filaments and nylon 66 films in RF gas discharge. They expected that the etching effect would be stronger at the amorphous region than crystalline because of the loose molecular structure; thus, the weight loss of PET film treated by plasma would be lower in the films with higher crystallinity ratio. However, they did not find significant change of the crystallinity while the surface morphology change was significant. The similar results were observed for the silk fibers [137].

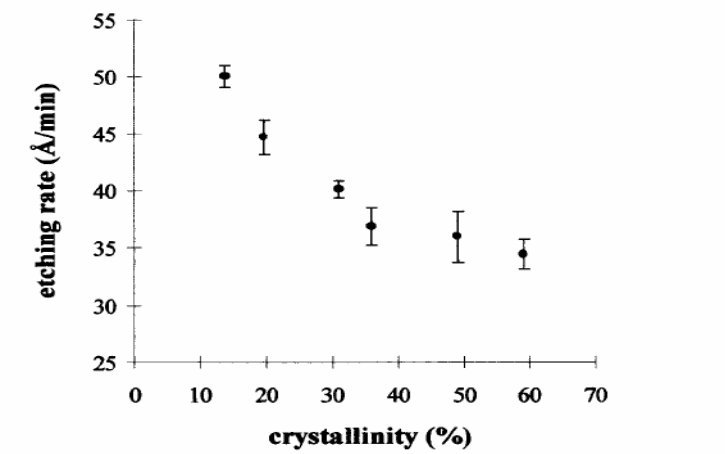

Figure 9. Etching Rate as a Function of Crystallinity of PE Film in a CF_4 Plasma [21]

Regardless, Friedrich et al. [138] explained that the selectivity of plasma etching on amorphous region of film was based on inhomogeneous polymer structure. Also, the appropriate plasma treatment could control the degree of selective etching on polymer surface. The crystallinity of polymer materials was strongly related to plasma etching in

terms of weight loss and plasma susceptibility (weight loss in a given exposure time) after plasma treatment [97]. The weight loss of fibers after air plasma treatment increased with decreasing crystallinity, and the dyeability decreased with increasing crystallinity of fibers. Riekerink et al. [129] showed that the etching rate was linearly dependent upon the crystallinity (Figure 9), and that the amorphous region was more susceptible to chemical or physical changes.

2. Radical Formation on Substrate Surface

When the substrate is exposed on gas plasma, the plasma species (ions, electrons, radicals, UV-radiation, neutrons, etc.) interact with substrate chemically and physically. Initially, the gas molecules are dissociated into active species such as ions, electrons, and radicals in the plasma chamber. The active species would collide with the molecules on substrate surface. UV-radiation and the collisions lead to the radical formation by chain scission of molecules and abstraction (taking-off of atoms on molecular chain) [139]. Free radicals generated in the plasma treatment on polymeric materials play an important role in surface modification. Radical species on plasma would interact with the radicals on substrate molecules, and then new functional groups are generated. Moreover, the chain cross-linking is induced by re-combination between radicals [140]. After plasma treatment on the substrate, unstable free radicals would recombine rapidly with other active species while stable free radicals remain as living radicals [141]. These phenomena would make graft polymerization on substrate surface by inducing monomer gas in vacuum chamber without generating plasma [142-146].

2.1 Radical Formation and Functionalization

The radical formation on polymer surface is essential to initiate functionalization on polymer surface. Clark et al. [147] studied the defluorination of PTFE (poly (tetrafluoroethylene)) film surface by hydrogen plasma, and suggested the reaction mechanism between PTFE molecules and hydrogen plasma. The hydrogen atoms in plasma initiate abstraction of a fluorine atom from the polymer chain, and then radicals are generated on polymer chain. The radicals on the polymer chain recombine with hydrogen atom, or the saturate polymer chain is obtained by eliminating HF. Inagaki et al. [139] suggested the radical formation processes based on abstraction and chain scission in hydrogen plasma on PTFE film. The radical formation processes are summarized as follows:

Process 1. – Radical formation by abstraction of atoms

1) Elimination of atoms on the backbone of molecules of polymer surface by radicals generated from gas molecules in the plasma,
2) Generation of carbon radicals on polymer surface
3) Chemical combination of carbon radicals with other radicals in the plasma
4) Functionalization - Formation of functional groups on the polymer surface

Process 2. – Radical formation by chain scission

1) Electron and ion bombardments on polymer chains
2) Chain scission of polymer chain and formation of radicals at the end of polymer chains
3) Degradation products generated leading to the reduction of molecular weight on the polymer surface

4) Chemical combination of carbon radicals with other radicals in the plasma

5) Functionalization - Formation of functional groups on the polymer surface

2.2 Radical Stability

While some of unstable radicals, generated by plasma treatment, tend to interact with other active species rapidly, the stable radicals remain in polymer as living radicals. Ward et al. [148] found that decay of free radicals in cotton treated by nitrogen plasma was faster than ammonia plasma with exposure time in argon gas. The free radical intensity of plasma treated fibers is related to plasma parameters (gas, pressure, and exposure time), fiber structures and chemical composition of fibers [149,150]. The intensity of free radical increased in the following order: cotton>wool>silk>nylon 6 = PET. And, among cellulose fibers, the cotton and line had higher intensity of free radical (cotton>linen>mercerized cotton>polynosic fibers = viscose rayon). Also, CF_4 gas had the highest free radical intensity (CF_4>CO>H_2>Ar>CH_4>N_2 = O_2). However, the reason was not explained clearly. Chen [141,151] represented the same results of radical intensity as those of Wakida's [150].

3. Chain Scission of Surface Molecules on Polymer Substrate

3.1 Chain Scission by Chemical Interactions in Plasma Treatment

Inagaki et al. [139] described that the chain scission on PTFE film is related to degradation process on PTFE molecules by ion and electron bombardments. However, the chain scission could be generated by not only ion bombardment but also chemical interaction after radical formation in the plasma treatment, so called a slow chain scission. Lub et al. [152] showed that hydrogen atoms played an important role in chain scission on the polymer

chains. Gröning et al. [153] supported Lub's results by suggesting the two-step degradation mechanisms of PMMA surface by ions in Ar plasma. As shown in Figure 10, the ions in the plasma interact with the partially negatively charged carbonyl oxygen, and then form an unstable intermediate state. If an electron is transferred from the main chain groups (C-C chain), the whole side chain is removed from the polymer. Idage et al. [154] suggested the chain scission by chemical interaction on polystyrene films with N_2 plasma, based on XPS (X-ray photoelectron Spectroscopy) results. The chain scission by chemical interaction was attributed to carbonate linkage resulting from the polymer chain scission and new hydrophilic functional groups.

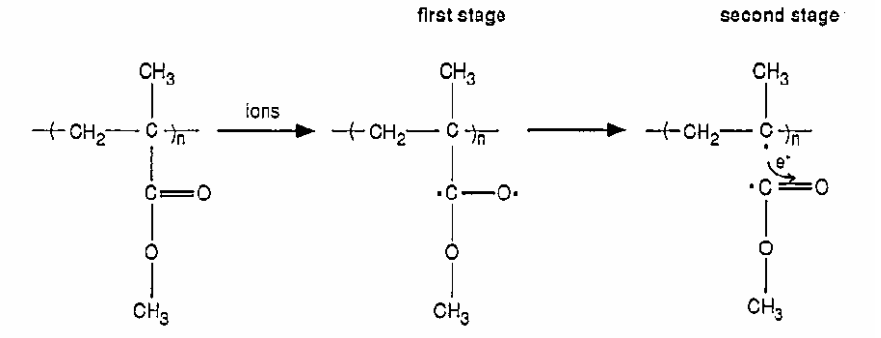

Figure 10. Schematic Illustration of the Side-Chain Scission in PMMA due to Low-Energy Ions [153]

3.2 Chain Scission by Ion Bombardment

Ion bombardment is main reason to break off molecular chains on substrate surface, resulting in functionalization. In addition, chain scission is strongly related to etching effects on polymer surface, leading to weight loss and reduction of molecular weight.

(a)

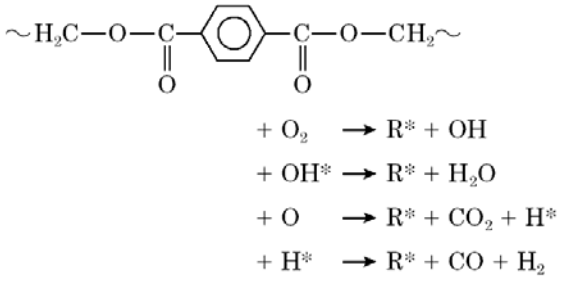

(b)

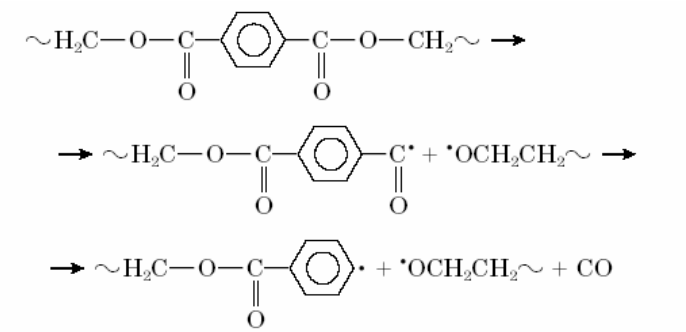

(c)

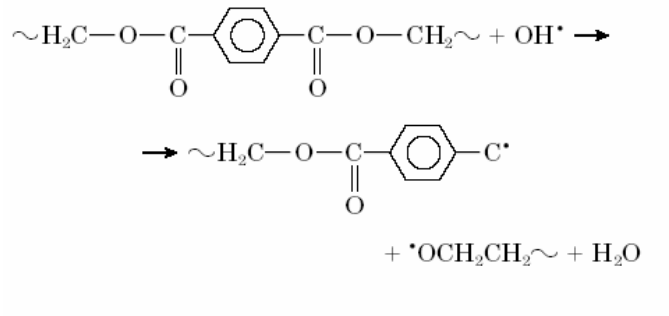

Figure 11. Degradation Mechanism of PET Film by He-O_2 Plasma; (a) Gas Species and Radicals Produced by Fragmentation Reaction, (b) CO and CO_2 Formation Mechanism and (c) H_2O Formation Mechanism [156]

Ward et al. [155] suggested the mechanisms of cellulose chain breakage by RF plasma treatment, based on radical formation process. Mainly, the chain breakages of cellulose molecules are carried out at glycosidic bond oxygen. Another possibility of chain scission would be ring opening. The degradation mechanisms of PET films treated by He-O_2

plasma are illustrated in Figure 11 [156]. The formation of CO and CO_2 gases is due to the chain breakage in the ester group of PET.

Inagaki et al. [157] suggested the chain scission mechanism of poly(*p*-phenylene trerphthalamide) (PPTA) film treated by oxygen plasma as shown in Figure 12. The XPS results showed the increase of carboxyl group due to chain breakage and chemical reactions on PPTA molecules. Wu et al. [158] suggested the same mechanism of chain scission for PPTA membrane treated by oxygen plasma.

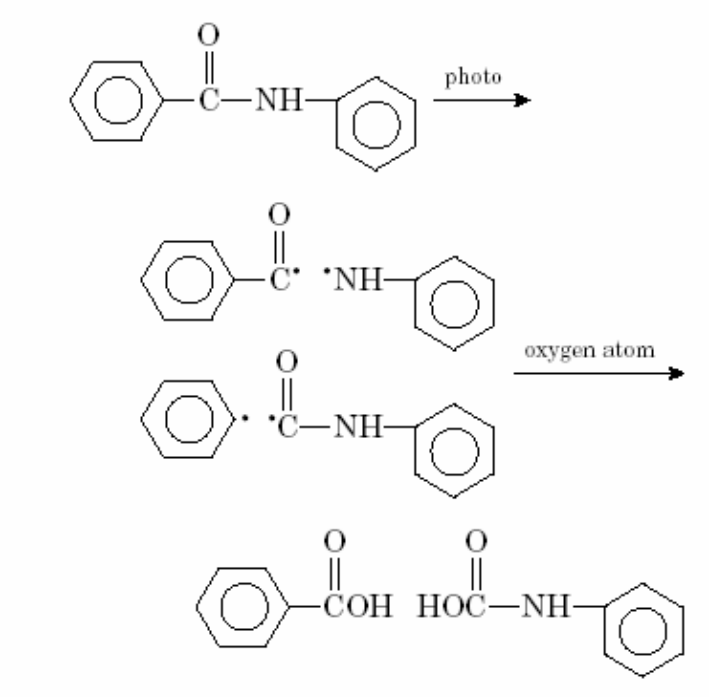

Figure 12. Degradation Mechanism of Poly(p-phenylene trerphthalamide) (PPTA) Films Treated by O_2 Plasma [157,158]

4. Cross-linking Formation

It is well known that the radical formation is strongly related to ion bombardment and UV-radiation. Cross-linking can be obtained by recombination of molecular radicals, leading to the increase of higher molecular weight molecules, while chain scission reduces molecular weight. In addition, chain scission occurs at the surface [159] while cross-linking is dominated in the subsurface [160]. Ion bombardment produces the radicals introducing mainly surface functionalization, while UV photons have sufficient energy to penetrate much deeper into the polymer substrate, and then create radicals [160].

4.1 Cross-linking Mechanism on Polymer Substrate

In PET film treated by oxygen plasma, the cross-linking reactions are expected from the destruction of benzene ring and ester groups, the combination of ethylene units and benzene ring, and the formation of peroxide [161]. As shown in Figure 13, the cross-linking of PET resulted from the recombination of two benzene ring radicals obtained by hydrogen abstraction from the benzene ring [156,162]. This mechanism was derived from an increase of intensity of C-C bonds with an increase of flow rate and concentration of helium gas. Also, it was mentioned that the cross-linking formation was strongly related to helium gas, which is the most efficient of the inert gases for cross-linking of a polymer [156].

Wu et al. [158] suggested the possible cross-linking mechanism of poly(*p*-phenylene terephthalamide) film treated by oxygen plasma as shown in Figure 14. It was shown that the binding energy of N_{1s} increased based on XPS spectra of nitrogen and spectra of N-substituted polyamide on ATR-FTIR, resulting from possible substitution of H atom in –CONH- by other atom or groups.

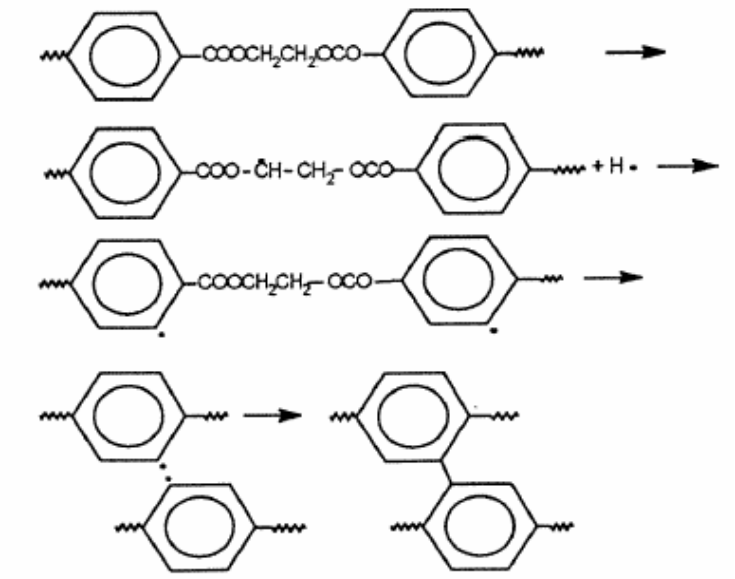

Figure 13. Cross-linking by Recombination of Two Aryl Radicals Obtained by Hydrogen Abstraction From Benzene Ring in PET [156,162]

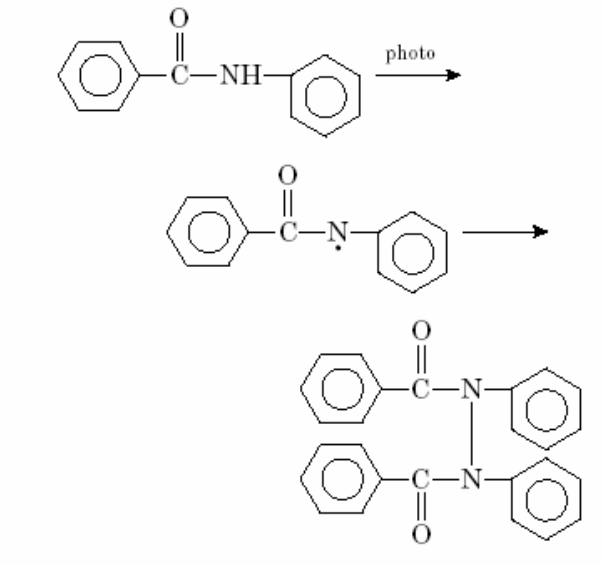

Figure 14. Possible Cross-linking Mechanism of Poly(p-phenylene terephthalamide) Film [158]

4.2 The Depth of Cross-linking on Polymer Substrate

The chain scission and cross-linking formation are competitive on the surface of substrate during gas plasma treatment. Yasuda et al. [163] explained that the cross-linking generated on the surface was propagated into thickness direction for butadiene containing copolymers treated by plasma. However, Holländer et al. [161] mentioned that cross-linking was generated dominantly by photochemical reaction, not in the outer surface. The UV-radiation in plasma can penetrate much deeper into the substrate, and the photons can generate the radicals inside of the substrate, where the active particles (ions and radicals) in plasma cannot penetrate as shown in Figure 15. In this region, so called subsurface, only photo-initiated reactions can be carried out without any chemical reactions by active species in plasma.

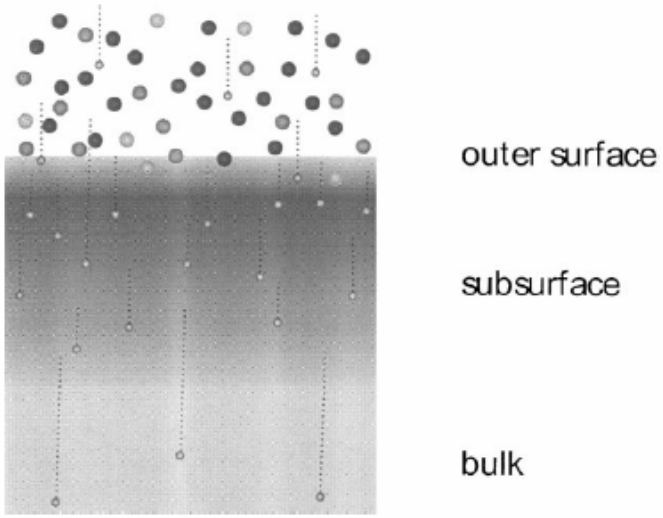

Figure 15. The Scheme of Penetration into Substrate Surface by Plasma Particles [161]

Tamai et al. [164] reconfirmed this behavior. The oxidation (carboxylic groups generated), obtained by reaction with the radicals and oxygen, takes place at the poly (4-trimethylsilylmethylstyrene) film surface while cross-linking formation is derived by recombination of the radicals inside the film (Figure 16). Thus, the chain scission and functionalization are dominated on the surface while cross-linking is generated in the subsurface of substrate.

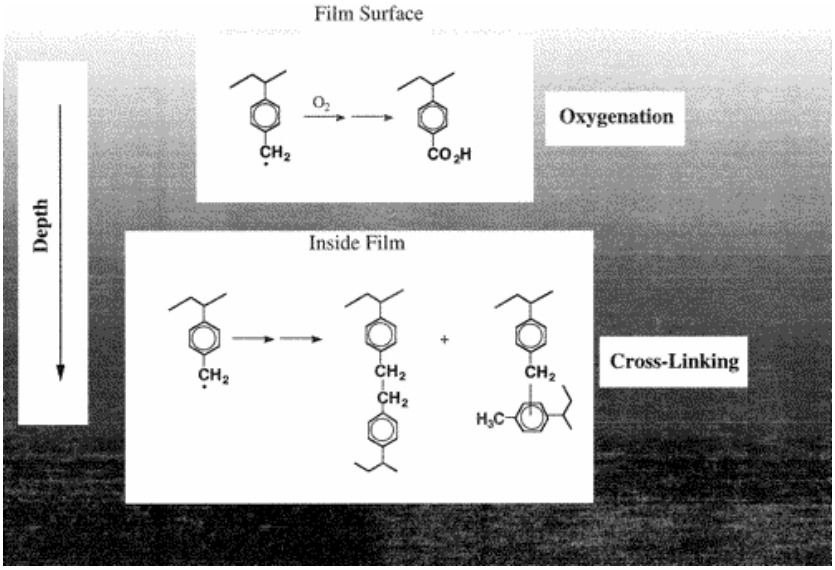

Figure 16. Cross-Linking Reaction in Subsurface vs. Oxidation in Film Surface [164]

5. Functionalization on Polymer Surface by Gas Plasma Treatment

5.1 Hydrophilic Functionalization

The inert gases used in plasma treatment are hydrogen, helium, neon and argon. Physical modification is a main effect on the surface by inert gas plasma treatment. Regardless, oxygen-related functional groups (-COH, -C=O and –COOH) were introduced

by inert gas plasma treatment [165-167] as shown in Table 3. In oxygen plasma, the various active particles of oxygen molecules can be obtained by dissociation and combination reactions in oxygen plasma, while the inert gas plasma has ions and electrons. However, the radicals generated by plasma can interact with oxygen and H_2O in air after plasma exposure, and then hydrophilic functional groups can be introduced on substrate surface.

Table 3. Relative Intensity Data of the Deconvoluted C_{1s} Core Level Spectra of PET Films Treated by Ar Plasma [165]

	Atomic Ratio (%)				
Exposure time (s)	—C—C— ~ 284.60[a]	—C—O— ~ 286.10[a]	—C—OH ~ 286.70[a]	—C═O ~ 288.10[a]	O═C—O ~ 288.75[a]
Untreated	62.06	20.66	—	—	17.28
20	53.04	15.4	7.62	3.78	20.15
40	51.8	16.08	8.47	3.36	20.33
60	51.9	16.35	8.70	3.72	19.37
100	52.2	13.75	11.59	3.8	18.65

Treatment conditions: plasma power, 80 W; Ar pressure, 0.4 mbar; Ar flow rate, 50 sccm; O_2 contact 1 h.
[a] Binding energy in eV.

In general, oxygen plasma treatment introduces various oxygen functional groups such as –CO-, -C=O, -COOH, -C-O-O-, O-COO- on the polymer surface [157,158,168-170], resulting in wettability enhancement. Water (H_2O) and H_2O_2 plasmas could introduce hydrophilic properties on the substrate surface, inducing alcohol and carboxylic acid groups [171-173]. In water plasma, H_2O molecules are dissipated into oxygen atoms and hydroxyl radicals, generating high density of alcohols directly by reaction with hydroxyl radicals with surface molecules. Compared to oxygen and argon plasma treatments, water and H_2O_2 plasmas showed better surface wettability, resulting from higher –C-OH bond generation.

Also, carbon dioxide plasma can lead to surface oxidation by forming oxygen containing hydrophilic groups [174-177].

Nitrogen plasma introduces nitrogen-containing functional groups such as amine, imine and amide groups on polymer surface [178,179]. Idage et al. [154] found that polystyrene surface treated by nitrogen plasma was highly reactive with oxygen after exposure to air. Ammonia plasma is also used to generate nitrogen-containing functional groups, improving wettability, printability, and adhesion.

5.2 Hydrophobic Functionalization

In fluorine-containing gas plasmas, etching, polymerization and functionalization are carried out simultaneously. In this section, the effects of non-double bonded gases, that is, only saturated gases (CF_4, SF_6, and CHF_3) on surface functionalization are introduced. The deposition by plasma polymerization will be discussed in the later chapter.

In the tetrafluoromethane gas (CF_4) plasma, the functionalization on the surface can be obtained by competition by etching and deposition. Etching can increase crystallinity rate and roughness on the polymer surface, while deposition can lead to functionalization, resulting in hydrophobicity on the polymer surface. The wettability polymer surface decreased after CF_4 plasma treatment as well as fluorine atom intensity increased [180]. The relative chemical composition of C_{1s} spectra showed incorporation of non-polar groups (–CHF, -CF_2- and -CF_3) on polymer surface, providing hydrophobicity on the surface [181,182]. At longer exposure time, the contents of non-polar groups also increased. CF_4 gas in plasma is decomposed into fluorine atoms, having higher concentration, and CF• and CF_2• radicals with relative low concentration [146]. The fluorine atom can be deposited directly

and the radicals can be grafted easily on polymer surface. Trifluoromethane (CHF_3) plasma also provides fluorine deposition on the substrate surface [183]. Compared to CH_2F_3 and $C_2H_2F_4$ gas plasmas, CHF_3 plasma yielded higher F/C ration and $–CF_2$ group. Poly(ethylene terephthalate) and cotton fibers treated by sulfur hexafluoride (SF_6) plasma showed higher hydrophobicity under various plasma conditions without altering the bulk properties [184]. The water-repellency and F/C ratio of both fibers increased with increases of exposure time and power. Compared to CF_4 plasma treatment for biomaterial application, fluorine contents were similar, but the degradation rate was much higher in SF_6 plasma [185]. This result is due to lower reactivity of CF_4 than SF_6. The bonding strength of C-F (552 kJ/mol) is higher than S-F (343 kJ/mol), thus, the fluorination of SF_6 is much higher than CF_4.

5.3 Depth Profile of Functionalization

X-ray photoelectron spectroscopy (XPS or ESCA) is one of useful techniques for polymer surface analysis. XPS can determine the degree of functionalization on polymer surface by providing quantitative information of the chemical composition (except hydrogen and helium) and chemical structure of polymer surface. Furthermore, the depth profile of chemical composition can be obtained by angle-resolved XPS technique. The depth of profile increases with a decrease of emission angle of XPS. The chemical composition of non-modified polymer surface would be same as inside polymer. However, the chemical compositions are variable through depth of polymer surface after plasma treatment. In general, the depth of surface modification is around several hundred Å for plasma treated polymers. The plasma parameters, such as power level and exposure time, have great influence on the depth of surface modification.

After argon plasma treatment on PTEF film, fluorine content increased with depth while oxygen and carbon content decreased as shown Figure 17 [186]. Fluorine atom is preferentially removed from surface molecules, and oxygen incorporation is dominated in outmost surface. Fluorine and carbon atomic concentrations become the original values with depth. Paynter [187] showed that oxygen content decreased with depth in polystyrene film treated by O_2/Ar plasma. In carbon dioxide plasma treatment for PET film, the similar results were obtained [175]. Foerch et al. [179] explained that functionalization at deeper layer of the film would be strongly related to the diffusion of gas atom into the polymer (Table 4). In the nitrogen plasma treatments for polyethylene, the depth profile of nitrogen content increased with an increase of exposure time, and then the maximum nitrogen content was obtained after 20 sec. exposure time and kept constant. In this steady state, the rate of diffusion of nitrogen might be equal to the amount of nitrogen absorption, and then the constant nitrogen content was achieved. In fluorine (F_2) gas plasma treatment for low-density polyethylene film [188] and PET fiber [189], the depth of fluorination increased with an increase of pressure and flow rate, and the fluorine content was lower in inner layer. At higher pressure and flow rate, the increase of active species concentration may lead to higher functionalization, related to higher diffusion rate into polymer inside. However, the depth of fluorination was limited to exposure time. This behavior might be related to etching and deposition mechanism.

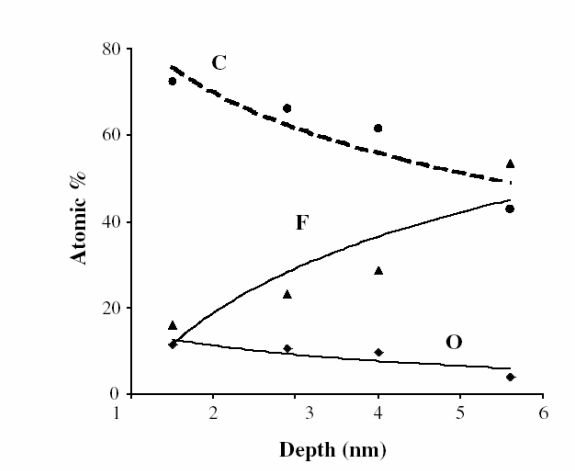

Figure 17. Elemental Composition of Ar Plasma Treated PTFE as a Function of Depth, Determined using Angle-Resolved XPS [188]

Table 4. N_{1s}/C_{1s} Intensity Ratios as Determined by Angle Resolved XPS for Remote Nitrogen Plasma Treated Polyethylene Samples [179]

1 s N_2 plasma exposure		15 s N_2 plasma exposure		1 min N_2 plasma exposure	
Angle [a] (deg)	N_{1s}/C_{1s}	Angle [a] (deg)	N_{1s}/C_{1s}	Angle [a] (deg)	N_{1s}/C_{1s}
75	0.007	65	0.069	65	0.073
25	0.009	45	0.049	45	0.071
0	0.005	25	0.053	25	0.066
			0.034	0	0.067

[a] Angle of emission is defined as the angle between the surface normal and the direction of emitted photoelectrons.

5.4 Ageing Effect

The functional groups generated on the polymer surface by plasma treatment are not stable and have higher mobility than in polymer bulk. In order to become stable after plasma treatment, the surface is likely to be reoriented by the migration of short chain oxidized

molecules and the diffusion of oxidized functional groups into polymer bulk [190,191]. The ageing of functional groups on plasma treated polymer surface can be reduced at low storage temperature [165,192] and in oxygen atmosphere [193]. The higher crystallinity and lower storage temperature could lead to slower ageing by reduction of the polymer chain mobility [194]. The rate of ageing can be much slower for highly cross-linked polymers, resulting in limiting the mobility of polymer chain [195].

The ageing behavior of nitrogen functional groups on polypropylene surface by nitrogen plasma treatment showed apparent reduction of nitrogen content and increase of oxygen content [179]. This result can be explained by replacement of nitrogen with oxygen. Gerenser [196] confirmed this mechanism with XPS study for nitrogen plasma treated polystyrene film. N_{1s} spectra for 15 sec. nitrogen plasma treated polystyrene showed the reduction of –C=N and increase of –C-N intensity after 10 min air exposure. In addition, PTFF film treated by ammonia plasma showed the same mechanism of ageing process as following [197];

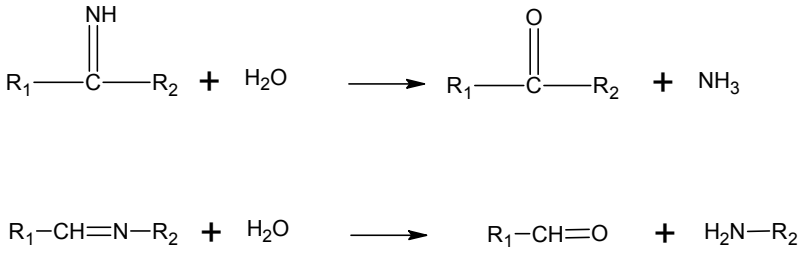

Yasuda et al. [195] found that the decay of wettability was dependent of degree of cross-linking on polymer treated by oxygen plasma. The suggested ageing mechanisms of plasma treated polymers depending on molecular structure of the polymer are shown in

Figure 18. In Model A (the main molecular chain with hydrophilic groups), the hydrophilic groups are rotated into polymer inside along the axis of the macromolecule. Model B illustrates the macromolecule with rigid backbone containing hydrophilic groups. There is no free rotation of hydrophilic groups into polymer bulk. Model C represents a cross-linked macromolecule with hydrophilic groups on polymer surface. Free rotation along the axis of polymer chain is limited due to cross-linking. Model D is for the cross-linked network of polymer having hydrophilic groups on polymer surface. No rotation of hydrophilic groups is in this model.

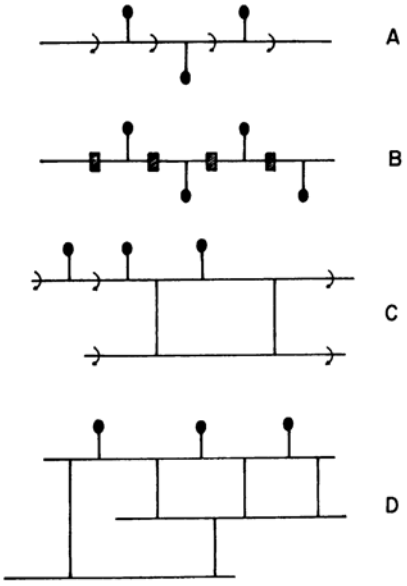

Figure 18. Models of Molecular Mobility on Polymer Surface by Yasuda [195]

6. Plasma Polymerization (Deposition)

Plasma polymerization is a distinctive technique to deposit a thin film on the substrate surface with advantages as following [198];

1) Ultra-thin thickness (< 1 μm) film can be obtained easily.
2) Thin film is highly cross-linked without pinhole.
3) Any kind of substrate is possibly used (polymer, ceramic, and metal), and good adhesion between substrate and deposited film can be easily achieved.

Plasma-deposited films result from polymerization with fed monomer gases into the plasma state such as hydrocarbon, fluorocarbon, nitrogen-containing and organosilicon monomers. The deposit process of plasma polymerization is not well understood due to complicate mechanism, and depends on power, monomer flow rate, temperature, monomer structure and exposure time. Plasma polymerization is carried out by interaction between active species of monomers in plasma whereas plasma-aid graft polymerizations are initiated by interactions between radicals and vapor, liquid or solid monomers. In addition, even saturated hydrocarbon and fluorocarbon gases can be used to generate deposited film while cannot be polymerized in conventional polymerization methods [144].

6.1 Hydrocarbon Plasma Polymerization

Sahre et al. [199] studied the hydrocarbon film deposition on polyethylene film using plasma polymerization with acetylene and ethylene. XPS and FTIR results showed that the deposited hydrocarbon films were consisted of amorphous, short-chain, C_xH_y functional structure with aryl units. When the hydrocarbon deposited films were exposed into air, polar groups were generated due to the reaction between radicals on surface and oxygen or water in air.

Retzko et al. [200] explained that plasma polymerization process resulted from chain reactions by radicals generated in pulse RF plasma. The polymerization mechanisms of

hydrocarbon monomer gases (styrene, acetylene, ethylene and butadiene) show in following reactions: (1) polystyrene and (2) poly(acetylene, ethylene and butadiene).

(1)

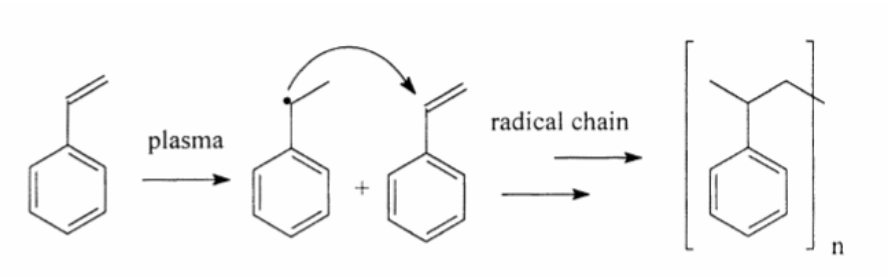

(2)

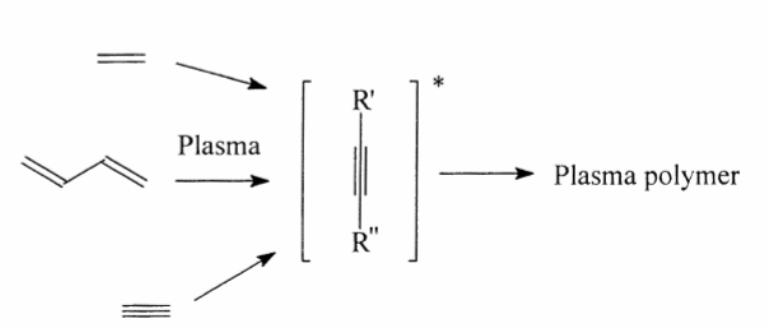

The deposition rate of styrene was higher than non-aromatic monomers, and acetylene has higher deposition rate among non-aromatic monomers as shown in Figure 19. The same results were observed by Yasuda [201] and Kobayashi et al. [202]. For styrene, the radicals generated in plasma are more stable due to benzene ring having sufficient electrons than non-aromatic monomers. The higher deposition rate of butadiene than ethylene is because butadiene has more double bonds, leading to more active polymerization.

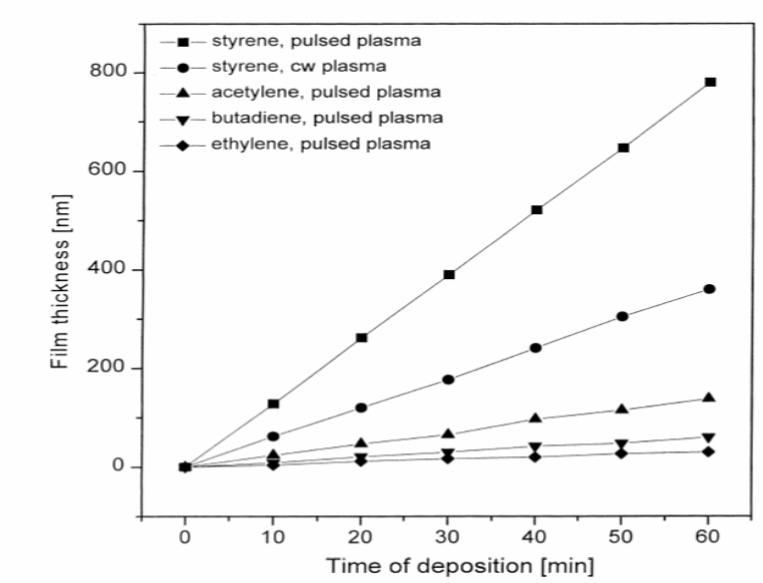

Figure 19. Film Thickness vs. Deposition Time for Styrene, Acetylene, Butadiene and ethylene monomers in a Pulse Plasma Deposition Process, CW= Continuous Wave Mode [200]

6.2 Fluorocarbon Plasma Polymerization

Fluorocarbon gases in plasma can form hydrophobic deposited films on substrate surface. Haque et al. [203] found that C_3F_8 and C_3F_6 gases in plasma generated fluorocarbon films with at least 100 Å, while C_2F_6 led to more etching and much thinner film deposition. XPS analysis for C_2F_6 showed lower fluorine content and fluorocarbon functions (-CF, -CF_2 and –CF_3) than C_3F_8 and C_3F_6.

Iriyama et al. [56] compared the durability after washing of deposited films on nylon 6 fabrics using saturated fluorocarbons (CF_4 and C_2F_6) and unsaturated fluorocarbons (C_2F_6 and C_3F_6). The deposited film with saturated fluorocarbon gases showed better durability

than unsaturated fluorocarbon gases, even though unsaturated fluorocarbon gases could generate deposited film more easily. Among saturated fluorocarbon gases, the longer chain gas (C_2F_6) deposited film had higher durability than that of shorter chain gas (CF_4). The drying condition after washing was found as an important factor influencing durability. At higher drying temperature, the hydrophobic groups seemed to rotate back into surface whereas remained inside of substrate at lower temperature.

Wang et al. [57] showed that the deposition rates of all fluorocarbon gases increased with an increase of CH_4 addition, but the further addition of CH_4 reduced the deposition rate again. For the same mixture rate of fluorocarbon/CH_4, the deposition rate was dependent of properties of fluorocarbon gases in the plasma with following order: C_3F_6>C_4F_8>C_2F_6>CF_4. CF_4 gas plasma has higher possibility of etching because CF_4 has higher concentration of F atoms, playing a main role in etching, and lower concentration of CF_x radicals, mainly leading to polymerization. The addition of CH_4 to fluorocarbon gases in plasma showed a considerable increase of deposition rate because hydrogen atoms, dissipated from CH_4, scavenge F atoms.

7. The Effects of Plasma Treatment on Physical Properties of Substrate

Functionalization can introduce chemical functional properties on the polymer surface while cross-linking, chain scission and etching are strongly related to physical property changes of the polymer substrate such as morphology, tensile properties and friction force. In general, it is known that plasma treatment does not alter bulk properties of the substrate. However, in the extreme conditions of plasma, the bulk properties can be

deteriorated. In order to overcome the defects of plasma, the optimum conditions should be considered to achieve advantages of plasma treatment.

7.1 Low-Pressure Plasma

Yasuda et al. [204] studied the effect of plasma treatment on fiber and fabrics using non-polymerizable gases (helium, air, nitrogen and tetrafluoromethane). For most of fibers treated by air plasma, it was found that weight loss increased with an increase of exposure time. Regardless, the deterioration of tensile strength for air plasma treated fibers was indistinctly. Also, compared to chemical treatment (30% NaOH aqueous solution), the PET fiber treated by air plasma had lower weight loss with 30 min. exposure time [205]. However, Wong et al. [206] found that fabric strength of plasma treated linen fabric treated with oxygen and argon decreased at longer exposure time, and linearly depended on weight loss. The fabric strength increased slightly at 10 min. exposure time because of the increase of interfacial friction, resulting from roughness of fibers by etching effect. However, after 20 min. plasma exposure time at higher discharge power, the apparent reduction of tensile strength was achieved. It is seemed that the severe plasma conditions could deteriorate bulk molecular structures due to more severe surface etching by bombardment of ions and excited particles. PET fibers treated by microwave plasma with oxygen and a mixture of oxygen and tetrafluoromethane showed the reduction of tensile strength even at short exposure time (<200 sec.) [207]. With comparison of oxygen to oxygen/tetrafluoromethane, oxygen plasma treatment was more effective to strength reduction. Even though there was no evidence of morphology change on the fiber surface, it was suggested that the reduction of fiber strength

might result from the embitterment of the surface related to different physical-chemical properties between the modified layer and the unmodified deeper layer.

In addition, during the plasma treatment, there is a competition between factors influencing tensile properties such as cross-linking, etching and chain scission on the substrate. When cross-linking dominates over etching or chain scission, the tensile strength increases and elongation decreases. Dahl et al. [208] showed that the formation of cross-linking layer enhanced Young's modulus and surface hardness of polycarbonate film treated by helium and nitrogen microwave plasmas as shown Figure 20.

Negulescu et al. [209] studied the physical property change of PET fabrics treated by $SiCl_4$ plasma. Kwabata Evaluation System (KES) measurement showed that the surface roughness of treated fabrics increased significantly in both filling and warp directions, resulting in a change of the handle properties of PET fabric after plasma treatment. While tensile, bending and compression properties were not changed, shear properties increased significantly because of higher friction and roughness. Yip et al. [210] found the similar result in nylon 6 fabrics treated by oxygen, argon and tetrafluoromethane plasmas, introducing higher surface roughness and shear properties. Tensile properties (tensile energy and extensibility) decreased at shorter exposure time, but increased at higher exposure time. Bending and shear properties showed same behavior. At short exposure time, the slight reduction of all properties might be related to smoothing effect. The considerable enhancement of all properties resulted from higher etching effects of oxygen and argon plasma at higher exposure time, resulting in higher fiber-to-fiber and yarn-to-yarn frictions. However, the further increase of exposure time showed no enhancement of tensile, bending and shearing properties because etching was dominated over cross-linking. Also,

compression resiliencies, representing fabric recovery, decreased at longer exposure time due to an increasing roughness.

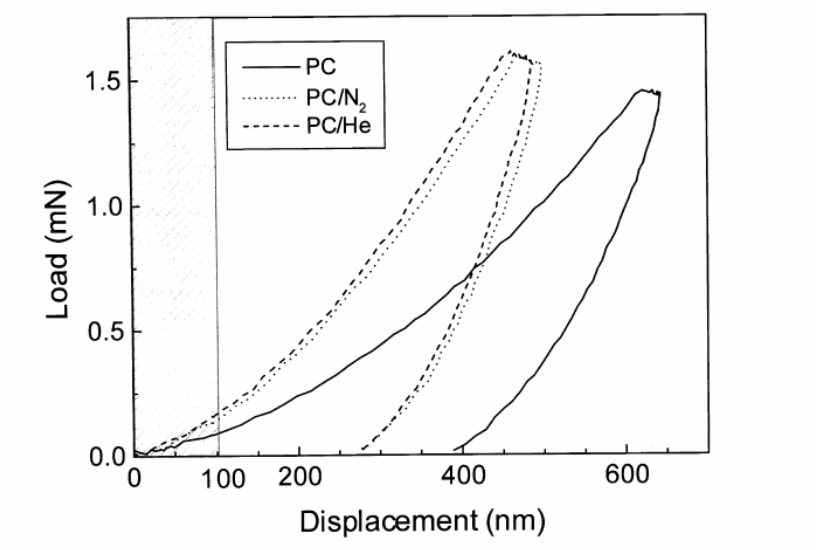

Figure 20. Load-Unload Curves for Untreated, Helium and Nitrogen Treated PC Films [208]

7.2 Atmospheric Pressure Plasma

Early study of gas plasma treatment for cotton yarns found a significant increase of breaking strength with an increase of exposure time [211]. Cotton yarns with lower twist factor had larger increase of breaking strength while the elongation of cotton yarn was lower after plasma treatment. However, the reason was not explained clearly. Using corona system designed for continuous processing, the cohesion of twistless slivers was enhanced with an increase of power and number of treat time with air, carbon dioxide, nitrogen and argon [31]. For cotton yarns treated by corona, the yarn tenacity increased with an increase of repeat treat

time, at lower yarn twist and coarser count [32,212]. However, spinnability of yarn was lower at lower yarn twist than untreated cotton due to higher end-break. In addition, corona treatment deteriorated softness of knitted fabrics. Thorsen [213] also found that corona treatment increased harshness of knitted fabrics, spinnability and strength of yarn and fabric. The reason was not explained clearly. The etching effect of corona on fiber and fabric surface increases roughness, leading to increase of harshness and tensile strength. Moreover, cross-linking would be another reason resulting in an increase of tensile strength. Unless the competition between cross-linking and etching is considered, it is not clear which effect is a major factor influencing on physical properties.

In atmospheric pressure plasma, there has been few study of handle and physical properties of fabric treated. McCord et al. [214] found that the tensile strength of nylon 66 fabrics treated by helium and helium/oxygen atmospheric plasma increased at some conditions with no surface morphology change. It is expected that the cross-linking would be related to the increase of tensile strength not due to frictions fiber-to-fiber or yarn-to-yarn. For Spectra® (HMWPE) and Kevlar® (PPTA) filaments treated by helium and helium/oxygen atmospheric plasmas, the apparent increase of tensile strength was achieved [85-88]. Spectra® filaments treated showed the significant surface morphology change, resulting from etching effect. However, the tensile strength of filament increased after atmospheric pressure plasma treatment. This phenomenon is conflicted because an increase of etching effect should lead to a lower tensile strength. Regardless, Kevlar® filament treated by atmospheric pressure plasma showed an increase of tensile strength whereas the surface morphology was not changed much. The potential cross-linking on the filament would be responsible for the increase of tensile strength. Another reason might be helium gas used in atmospheric

pressure plasma because helium is the most efficient of the inert gases for cross-linking of a polymer [152].

REFERENCES (CHAPTERS I-III)

(1) J.R. Roth. Industrial Plasma Engineering, Principles, Vol. 1, (Bristol: Institute of Physics Publishing), Philadelphia, 1995, ISBN 0-7503-0318-2

(2) A. Bradley and J. Fales J. Prospects for Industrial Applications of Electrical Discharge. *Chemical Technology*, 1(4): 232-237, 1971

(3) Sando Iron Works Ltd., USX Low Temperature Plasma Treatment Machine, http://www.sando.co.jp

(4) W. Rakowski. Plasma Modification of Wool under Industrial Conditions. *Melliand Textilberichte*, 70(10): 780-785 (E334-337), 1989

(5) W. Rakowski. Plasma Treatment of Wool Today: Part 1- Fibre Properties, Spinning and Shrinkproofing. *Journal of the Society of Dyers and Colourist*, 113 (9): 250-255, 1997

(6) U. Vohrer. Glow-Discharge Treatments for the Modification of Technical Textiles - An Innovative Technology with Increasing Market Potential. *Techtextil-Symposiums*, Frankfurt, 1997

(7) U. Vohrer, M. Műller and C. Oehr. Glow-discharge Treatment for the Modification of Textiles. *Surface and Coatings Technology*, 98: 1128-1131, 1998

(8) V. Rybkin, A. Maximov, B. Gorberg, V. Titov. Plasma Technology and Equipment for the Modification of Textiles and Polymer Films. *Textile Symposium for Technical Textiles and Textile Reinforced Materials*, Frankfurt on Mine, 14 May, 10-17, 1997

(9) H.T.P. Unitex, Plasma Division, Brochure, http://www.htpunitx.com

(10) Europlasma, Brochure, http://www.europlasma.be

(11) Polyplas GmbH, http://www.polyplas.de

(12) 4th State Inc., http://www.4thstate.com

(13) B. Mohamed. NE591 Principle Industrial Plasma and Plasma Chemistry, North Carolina State University, Class Note and Lecture, Fall 2001

(14) K. Pochner, W. Neff and R. Lebert. Atmospheric Pressure Gas Discharge for Surface Treatment. *Surface and Coatings Technology*, 74-75: 394-398, 1995

(15) S. Kanazawa, M. Kogoma, T. Moriwaki and S. Okazaki. Stable Glow Plasma at Atmospheric Pressure. *Journal of Physics D-Applied Physics*, 21: 838-840, 1988

(16) T. Yokoyama, M. Kogoma, S. Kanazawa, T. Moriwaki and S. Okazaki. The Improvement of the Atmospheric-Pressure Glow Plasma Method and the Deposition of Organic Films. *Journal of Physics D-Applied Physics*, 23: 374-377, 1990

(17) T. Yokoyama, M. Kogoma, T. Moriwaki and S. Okazaki. The Mechanism of the Stabilisation of Glow Plasma at Atmospheric Pressure. *Journal of Physics D-Applied Physics*, 23: 1125-1128, 1990

(18) S. Okazaki, M. Kogoma, M. Uehara and Y. Kimura. Appearance of Stable Glow Discharge in Air, Argon, Oxygen and Nitrogen at Atmospheric Pressure Using a 50 Hz Source. *Journal of Physics D-Applied Physics*, 26: 889-892, 1993

(19) M. Kogoma and S. Okazaki. Raising of Ozone Formation Efficiency in Homogeneous Glow Discharge Plasma at Atmospheric Pressure. *Journal of Physics D-Applied Physics*, 27: 1985-1987, 1994

(20) Y. Sawada, S. Ogawa and M. Kogoma. Synthesis of Plasma-Polymerized Tetraethoxysilane and Hexamethyldisiloxane Films Prepared by Atmospheric Pressure Glow Discharge. *Journal of Physics D-Applied Physics*, 28: 1661-1669, 1995

(21) F. Massines and G. Gouda. A Comparison of Polypropylene-Surface Treatment by Filamentary, Homogeneous and Glow Discharges in Helium at Atmospheric Pressure, *Journal of Physics D-Applied Physics*, 31: 3411-3420, 1998

(22) R. Gadri. One Atmosphere Glow Discharge Structure Revealed by Computer Modeling. *IEEE Transactions on Plasma Science*, 27: 36-37, 1999

(23) P. Herbert and E. Bourdin. New Generation Atmospheric Pressure Plasma Technology for Industrial On-line Processing. *Journal of Coated Fabrics*, 28: 170-182, 1999

(24) J. Roth. Method and Apparatus for Covering Bodies with a Uniform Glow Discharge Plasma and Applications thereof. *US Patent*, 5,669,583, 1997

(25) J. Roth. Method and Apparatus for Cleaning Surfaces with a Glow Discharge Plasma at One Atmosphere of Pressure. *US Patent*, 5,938,854, 1999

(26) J. Roth, P. Tsai and C. Liu. Steady-State, Glow Discharge Plasma. *US Patent*, 5,387,842, 1995

(27) J. Roth, P. Tsai, C. Liu, M. Laroussi and P. Spence. One Atmosphere, Uniform Glow Discharge Plasma. *US Patent*, 5,414,324, 1995

(28) J. Roth. Industrial Plasma Engineering, Volume II, Applications to Nonthermal Plasma Processing, (Bristol: Institute of Physics Publishing), Philadelphia, ISBN 0-7503-0545-2, 2001

(29) W. Thorsen. A Corona Discharge Method of Producing Shrink-Resistant Wool and Mohair, Part II: Effects of Temperature, Chlorine Gas and Moisture. *Textile Research Journal*, 38(6): 644-650, 1968

(30) W. Thorsen and R. Landwehr. A Corona Discharge Method of Producing Shrink-Resistant Wool and Mohair, Part III: A Pilot-Scale Top Treatment Reactor. *Textile Research Journal*, 40(8): 688-695, 1970

(31) G. Abbott. The Corona Treatment of Cotton, Part I: Sliver Cohesion. *Textile Research Journal*, 47(2): 141-144, 1977

(32) G. Abbott and G. Robinson. The Corona Treatment of Cotton, Part II: Yarn and Fabric Properties. *Textile Research Journal*, 47(2): 199-202, 1977

(33) J. Salge. Plasma-assisted Deposition at Atmospheric Pressure. *Surface and Coatings Technolgy* , 80: 1-7, 1996

(34) S. Meiners, J. Salge, E. Prinz and F. Förster. Surface Modification of Polymer Materials by Transient Gas Discharges at Atmospheric Pressure. *Surface and Coatings Technolgy*, 98, 1121-1127, 1998

(35) J. Hautojärvi and S. Laaksonen. On-Line Surface Modification of Polypropylene Fibers by Corona Treatment During Melt-Spinning. *Textile Research Journal*, 70(5): 391-396, 2000

(36) P. Tsai, L. Wadsworth and J. Roth. Surface Modification of Fabrics Using a One-Atmosphere Glow Discharge Plasma to Improve Fabric Wettability. *Textile Research Journal*, 67(5): 359-369, 1997

(37) T. Montie, K. Kelly-Wintenberg and J. Roth. An Overview of Research Using the One Atmosphere Uniform Glow Discharge Plasma (OAUGDP) for Sterilization of Surfaces and Materials. *IEEE Transactions on Plasma Science*, 28(1): 41-50, 2000

(38) H. Ngo, S. Vojta, J, Rohner, O. Hankins and M. Bourham. Design and Parameters Measurements of an Atmospheric Pressure Plasma, 25th IEEE-ICOPS, Paper 3B03, IEEE Cat. #98CH36221, 178, 1998

(39) M. Lieberman and A. Lichtenberg. Principles of Plasma Discharges and Materials Processing, (New York: John Wiley & Sons, INC.), New York, ISBN 0-471-00577-0, 1994

(40) N. Carneiro, A. Souto, E. Silva, A. Marimba, B. Tena, H. Ferreira and V. Magalhaes. Dyeability of Corona-treated Fabrics. *Coloration Technology*, 117(5): 298-302, 2001

(41) C. Chu, T. Ahn, J. Kim, S. Jeong and J. Moon. Effects of Fluorocarbon Polymer Deposition on the Selective Etching of SiO_2/Photoresist in High Density Plasma. *Journal of Vacuum Science and Technology B*, 18(6): 2763-2768, 2000

(42) J. Youngblood and T. McCarthy. Plasma Polymerization Using Solid Phase Polymer Reactants (Non-classical Sputtering of Polymers). *Thin Solid Films*, 382: 95-100, 2001

(43) H. Snyder and G. Anderson. Effect of Air and Oxygen Content on the Dielectric Barrier Discharge Decomposition of Chlorobenzene. *IEEE Transactions on Plasma Science*, 26(6): 1695-1699, 1998

(44) Y. Babukutty, R. Prat, K. Endo, M. Kogoma, S. Okazaki and M. Kodama. Poly(vinyl chloride) Surface Modification Using Tetrafluoroethylene in Atmospheric Pressure Glow Discharge. *Langmuir*, 15: 7055-7062, 1999

(45) M. Laroussi, Sterilization of Contaminated Matter with an Atmospheric Pressure Plasma. *IEEE Transactions on Plasma Science*, 24(3): 1188-1191, 1996

(46) Plasma Ireland Ltd., AP-100 Atmospheric Pressure Plasma Processing System, Brochure

(47) R. Shishoo and T. Herbert. Plasma Conquering the Textile Industry. *RTD info*, 24: 22-23, November 1999

(48) I. Gancarz, G. Pozniak, M. Bryjak and A. Frankiewicz. Modification of Polysulfone Membranes. 2. Plasma Grafting and Plasma Polymerization of Acrylic Acid. *Acta Polymerica*, 50: 317-326, 1999

(49) N. Inagaki and Y. Yasukawa. Improvement of Wicking Property of PET Fabrics by Plasma Polymerization of Nitro Compounds. *Sen'i Gakkaishi*, 44: 333-338, 1988

(50) J. Lai, C. Shih and S. Tsai. Plasma Deposition Modified Nylon 6 Membranes for Hemodialysis. *Journal of Applied Polymer Science*, 43: 1431-1440, 1991

(51) J. Zhang. The Surface Characterization of Mulberry Silk Grafted with Acrylamide by Plasma Copolymerization. *Journal of Applied Polymer Science*, 64: 1713-1717, 1997

(52) N. Bhat and Y. Benjamin. Surface Resistivity Behavior of Plasma Treated and Plasma Grafted Cotton and Polyester Fabrics. *Textile Research Journal*, 69: 38-42, 1999

(53) W. Rakowski, M. Okoniewski, K. Bartos and J. Zawadzki. Plasma Treatment of Textiles-Potential Applications and Future Prospects. *Melliand Textilberichte*, 63: 307-313, 1982

(54) N. Inagaki, S. Tasaka and Y. Takami. Durable and Hydrophobic Surface Modification by Plasma Polymers Deposited from Acetone/Hexafluoroacetone, Ethylene/Hexafluoroacetone, and Ethane/Hexafluoroacetone Mixture. *Journal of Applied Polymer Science*, 41: 965-973, 1990

(55) M. Sarmadi and Y. Kwon. Improved Water Repellency and Surface Dyeing of Polyester Fabrics by Plasma Treatment. *Textile Chemist and Colorist*, 25: 33-40, 1993

(56) Y. Iriyama, T. Yasuda, D. Cho and H. Yasuda. Plasma Surface Treatment on Nylon Fabrics by Fluorocarbon Compounds. *Journal of Applied Polymer Science*, 39: 249-264, 1990

(57) H. Wang, M. Rembold, and J. Wang. Characterization of Surface Properties of Plasma-Polymerized Fluorinated Hydrocarbon Layers: Surface Stability as a Requirement for Permanent Water Repellency, *Journal of Applied Polymer Science*, 49: 701-710, 1993

(58) M. McCord, Y. Hwang, L. Canup, Y. Qiu and M. Bourham. Surface Analysis of Cotton Fabrics Fluorinated in Atmospheric Plasma, *Journal of Applied Polymer Science*, 2002, In Press

(59) Discussion with Paolo Canonico, HTP Unitex

(60) P. Kassenbeck. Electrical Discharge Process and Its Application to Wool. *Bulletin Institut Textile De France*, 18(110): 7-33, 1964

(61) Q. Chen, K. Au, C. Yuen and K. Yeung. Development of Wool Shrinkproofing, 1969-99. *Textile Asia*, 31: 38-43, 2000

(62) K. Lee and A. Pavlath. Low Temperature Plasma Treatment of Wool. II. Effects of Variables on Shrinkage and Yarn Strength. *Journal of Polymer Science Part A-Polymer Chemistry*, 12: 2087-2090, 1972

(63) C. Kan, K. Chan, C. Yuen and M. Miao. Low Temperature Plasma on Wool Substrates: The Effect of the Nature of the Gas. *Textile Research Journal*, 69: 407-416, 1999

(64) K. Gregorski and A. Pavlath. Fabric Modification Using the Plasmod – The Effect of Extensive Treatment in Nitrogen and Oxygen Plasmas at Low Pressure. *Textile Research Journal*, 50: 42-46, 1980

(65) A. Hesse, H. Thomas and H. Hocker. Zero-AOX Shrinkproofing Treatment for Wool Top and Fabric, Part I: Glow Discharge Treatment. *Textile Research Journal*, 65, 355-361, 1995

(66) I. Zuchairah, M. Pailthorpe and S. David. Effect of Glow Discharge-Polymer Treatments on the Shrinkage Behavior and Physical Properties of Wool Fabric. *Textile Research Journal*, 67: 69-74, 1997

(67) T. Wakida, S. Tokino, S. Niu, H. Kawamura, Y. Sato and M. Lee. Surface Characteristics of Wool and Poly(ethylene Terephthalate) Fabrics and Film Treated with Low-Temperature Plasma under Atmospheric Pressure. *Textile Research Journal*, 63(8): 433-438, 1993

(68) Y. Nakashima, M. Tahara, H. Kimura and T. Takagishi. Morphology on the Surface of Wool Fibers Treated with Glow Discharge under Atmospheric Pressure. *Sen'i Gakkaishi*, 54(10): 496-501, 1998

(69) S. Tokino, T. Wakida, H. Uchiyama and M. Lee. Laundering Shrinkage of Wool Fabric Treated with Low-Temperature Plasmas under Atmospheric Pressure. *Journal of the Society of Dyer and Colourist*, 109(10): 334-335, 1993

(70) Metropolitan section. Plasma Treatment of Textiles: A Novel Approach to the Environmental Problems of Desizing. *Textile Chemist and Colorist*, 5: 239-248, 1973

(71) C. Kuo. The Study of Plasma Desizing. *Journal of China Textile Institute*, 9: 148-152, 1999

(72) Sando Iron Works Co., Ltd., Method and Apparatus for the Pretreatment of a Cloth. *US Patent*, 5,407,446, 1995

(73) Sando Iron Works Co., Ltd., Method and Apparatus for the Pretreatment of a Cloth. *US Patent*, 5,435,156, 1995

(74) C. Tomasino, J. Cuomo, C. Smith and G. Oehrlein. Plasma Treatments of Textiles. *Journal of Coated Fabrics*, 25: 115-126, 1995

(75) Z. Cai, Y. Hwang, Y. Park, C. Zhang, M. McCord and Y. Qiu. Preliminary Investigation of Atmospheric Pressure Plasma-Aided Desizing for Cotton Fabrics. *AATCC Review*, 2(12): 18-21 2002

(76) C. Simionescu, F. Denes, M. Macoveanu, G. Cazacu, M. Totolin, S. Percec and D. Balaur. Grafting of Rayon Fabrics with Phosphorus Containing Polymers in Cold Plasma in order to Obtain Flame-Retardant Materials. *Cellulose Chemistry and Technology*, 14: 869-883, 1980

(77) C. Simionescu, F. Denes, M. Macoveanu and I. Negulescu. Surface Modification and Grafting of Natrual and Synthetic Fibers and Fabrics under Cold Plasma Conditions, *Makromolekulare Chemie Supplement*, 8: 17-36, 1984

(78) R. Benerito, T. Ward, D. Soignet and O. Hinojosa. Modifications of Cotton Cellulose Surface by Use of Radiofrequency Cold Plasmas and Characterization of Surface Changes by ESCA. *Textile Research Journal*, 51: 224-232, 1981

(79) G. Akovali and G. Gundogan. Studies on Flame Retardancy of Polyacrylonitrile Fiber Treated by Flame Retardant Monomers in Cold Plasma. *Journal of Applied Polymer Science*, 41: 2011-2019, 1990

(80) L. Shi. An Approach Using CF_4/CH_4 Plasma-Induced Surface Modification to Impart Flame Retardancy to Polypropylene. *Journal of Polymer Engineering*, 20, 313-328, 2000

(81) L. Shi. Characterization of the Flame Retardancy of EVA Copolymer by Plasma Grafting of Acrylic Acid. *European Polymer Journal*, 36: 2611-2651, 2000

(82) D. Biro, G. Pleizier and Y. Deslandes. Application of the Microbond Technique. IV. Improved Fiber-Matrix Adhesion by RF Plasma Treatment of Organic Fibers. *Journal of Applied Polymer Science*, 47: 883-894, 1993

(83) M. Wertheimer and H. Schreiber. Surface Property Modification of Aromatic Polyamides by Microwave Plasmas. *Journal of Applied Polymer Science*, 26: 2087-2096, 1981

(84) S. Wu, G. Sheu and S. Shyu. Kevlar Fiber-Epoxy Adhesion and Its Effect on Composite Mechanical and Fracture Properties by Plasma and Chemical Treatment. *Journal of Applied Polymer Science*, 62, 1347-1360, 1996

(85) Y. Qiu, C. Zhang, Y. Hwang, B. Bures and M. McCord. The Effect of Atmospheric Pressure Helium Plasma Treatment on Surface and Mechanical Properties of Ultrahigh Modulus Polyethylene Fibers. *Journal of Adhesion Science and Technology*, 16(1): 99-107, 2002

(86) Y. Qiu, Y. Hwang, C. Zhang and M. McCord. The Effect of Atmospheric Pressure Oxygen-helium Plasma Treatment on Surface and Mechanical Properties of Ultrahigh Modulus Polyethylene Fibers. *Journal of Adhesion Science and Technology*, 16(4): 449-458, 2002

(87) Y. Hwang, Y. Qiu, C. Zhang, B. Jarrard, R. Stedeford, J. Tsai, Y. Park and M. McCord. The Effects of Atmospheric Pressure Helium Plasma Treatment on Adhesion and Mechanical Properties of Aramid Fibers. *Journal of Adhesion Science and Technology*, 2003, In Press

(88) Y. Hwang, Y. Qiu, C. Zhang and M. McCord. Effect of Atmospheric Pressure Helium + Oxygen + Air Plasma Treatments on Aramid/epoxy Interfacial Bonding and Single Fiber Strength. *Composites Science and Technology*, 2002, Submitted

(89) W. Thorsen. Modification of the Cuticle and Primary Wall of Cotton by Corona Treatment. *Textile Research Journal*, 44(6): 422-428, 1974

(90) S. Kubota and K. Emori. Abrasive Finishing of Cotton Fiber by Low Temperature Plasma. *Sen'i Gakkaishi*, 50: 57-62, 1994

(91) N. Yoon, Y. Lim, M. Tahara and T. Takagishi. Mechanical and Dyeing Properties of Wool and Cotton Fabrics Treated with Low Temperature Plasma and Enzymes. *Textile Research Journal*, 66: 329-336, 1996

(92) K. Wong, X. Tao, C. Yuen and K. Yeung. Effect of Plasma and Subsequent Enzymatic Treatments on Linen Fabrics. *Journal of the Society of Dyers and Colourist*, 116: 208-214, 2000

(93) H. Hocker, H. Thomas, A. Kusters and J. Herrling. Dyeing of Plasma Treated Wool. *Melliand Textilberichte*, 75: 506-512, 1994

(94) C. Kan, K. Chan, C. Yeun and M. Miao. Plasma Modification on Wool Fiber: Effect on Dyeing Properties. *Journal of the Society of Dyers and Colourist*, 114: 61-65, 1998

(95) C. Kan, K. Chan and C. Yeun. Effect of Low Temperature Plasma, Chlorination, and Polymer Treatments and their Combinations on Properties of Wool Fibers. *Textile Research Journal*, 68: 814-820, 1998

(96) H. Grzegorz, W. Urbanczyk, B. Lipp-Symonowicz and S. Kowalska. Influence of Low-Temperature Plasma on the Fine Structure and Dyeability of Polyester Fibers, *Melliand Textilberichte*, 64: 838-840, 1983

(97) T. Okuno, T. Yasuda and H. Yasuda. Effect of Crystallinity of PET and Nylon 66 Fibers on Plasma Etching and Dyeability Characteristics. *Textile Research Journal*, 62: 474-480, 1992

(98) M. Sarmadi, A. Denes and F. Denes. Improved Dyeing Properties of $SiCl_4$ (ST)-Plasma Treated Polyester Fabrics, *Textile Chemist and Colorist*, 28: 17-22, 1996

(99) T. Wakida, M. Lee, S. Niu, S. Kobayashi and S. Ogasawara. Microscopic Observation of Cross-Section of Dyed Wool and Nylon 6 Fibers after Treatment with Low-Temperature Plasma, *Sen'i Gakkaishi*, 50: 421-423, 1994

(100) T. Wakida, M. Lee, Y. Sato, S. Ogasawara, Y. Ge and S. Niu. Dyeing Properties of Oxygen Low-Temperature Plasma-Treated Wool and Nylon 6 Fibers with Acid and Basic Dyes. *Journal of the Society Dyers and Colourist*, 112: 233-236, 1996

(101) T. Wakida, S. Cho, S. Choi, S. Tokino and M. Lee. Effect of Low Temperature Plasma Treatment on Color of Wool and Nylon 6 Fabrics Dyed with Natural Dyes. *Textile Research Journal*, 68: 848-853, 1998

(102) J. Yip, K. Chan, K. Sin and K. Lau. Study of Physico-chemical Surface Treatments on Dyeing Properties of Polyamides. Part 1: Effect of Tetrafluoromethane Low Temperature Plasma. *Coloration Technology*, 118: 26-30, 2002

(103) G. Byrne and K. Brown. Modifications of Textiles by Glow-Discharge Reactions. *Journal of the Society Dyers and Colourist*, 88: 113-117, 1972

(104) M. Macoveanu, G. Cazacu and A. Ioanid. Grafting of Benzidine onto Binary Mixtures of Fabrics in Cold Plasma Conditions, III. *Cellulose Chemistry and Technology*, 19: 627-638, 1985

(105) A. Sarmadi, T. Ying and F. Denes. Surface Modification of Polypropylene Fabrics by Acrylonitrile Cold Plasma. *Textile Research Journal*, 63: 697-705, 1993

(106) J. Park, J. Kim and S. Song. Surface Modification of Polyester Fabric by Plasma Polymerization of Acrylic Acid in the Presence of Oxygen. *Journal of Korean Fiber Society*, 33: 790-797, 1996

(107) T. Oktem, H. Ayhan, N. Seventekin and E. Piskin. Modification of Polyester Fabrics by in situ Plasma or Post-plasma Polymerisation of Acrylic Acid, *Journal of the Society Dyers and Colourist*, 115: 274-279, 1999

(108) F. Seto, Y. Muraoka, N. Sakamoto, A. Kishida and M. Akashi. Surface Modification of Synthetic Fiber Nonwoven Fabrics with Poly(acrylic acid) Chains Prepared by Corona Discharge Induced Grafting. *Angewandte Makromolekulare Chemie*, 266: 56-62, 1999

(109) S. Park and J. Jin. Effect of Corona Discharge Treatment on the Dyeability of Low-Density Polyethylene Film. *Journal of Colloid and Interface Science*, 236: 155-160, 2001

(110) J. Ryu, J. Dai, K. Koo and T. Wakida. The Effect of Sputter Etching on the Surface Characteristics of Black-Dyed Polyamide Fabrics. *Journal of the Society Dyers and Colourist*, 108: 278-282, 1992

(111) S. Kobayashi, T. Wakida, S. Niu, S. Hazama, T. Ito and Y. Sasaki. The Effect of Sputter Etching on the Surface Characteristics of Dyed Aramide Fabrics. *Journal of the Society Dyers and Colourist*, 111: 72-76, 1995

(112) S. Kobayashi, T. Wakida, S. Niu, S. Hazama, C. Doi and Y. Sasaki. Change in Colour of Dyed Aramid Fabrics by Sputter Etching. *Journal of the Society Dyers and Colourist*, 111: 111-114, 1995

(113) M. Rabe, K. Greifeneder, K. Truckenmuller, B. Petasch and E. Rauchle. Waterproofing and Improvement of the Dye Fastness of Polyester Yarn by Plasma Polymerization. *Melliand Textilberichte*, 75: 513-517, 1994

(114) H. Lee, D. Kim and K. Lee. Anti-reflective Coating for the Deep Coloring of PET Fabrics Using an Atmospheric Pressure Plasma Technique. *Surface and Coatings Technology*, 142-144: 468-473, 2001

(115) T. Wakida, S. Tokino, S. Niu, M. Lee, H. Uchiyama and M. Kaneko. Dyeing Properties of Wool Treated with Low-Temperature Plasma Under Atmospheric Pressure. *Textile Research Journal*, 63: 438-442, 1993

(116) T. Chau, K. Kao, G. Blank and F. Madrid. Microwave Plasmas for Low-Temperaure Dry Sterilization. *Biomaterials*, 17: 1273-1277, 1996

(117) S. Shalaby. Radiation Effects on Polymers of Biomedical Significance. *Irradiation of Polymeric Material-American Chemistry Society Symposium Series*, 527: 315-319, 1993

(118) S. Adler, M. Scherrer and F. Daschner. Costs of Low-temperature Plasma Sterilization Compared with Other Sterilization Methods. *Journal of Hospital Infection*, 40: 125-134, 1998

(119) S. Gogolewski, P. Mainil-Varlet and J. Dillon. Sterility, Mechanical Properties, and Molecular Stability of Polylactide Internal-fixation Devices Treated with Low-temperature Plasmas. *Journal of Biomedical Materials Research*, 32: 227-235, 1996

(120) J. Fisher, E. Reeves, G. Isaac, K. Saum and W. Sanford. Comparison of the Wear of aged and Non-aged Ultrahigh Molecular Weight Polyethylene Sterilized by Gamma Irradiation and by Gas Plasma. *Journal of Materials Science-Materials in Medicine*, 8: 375-378, 1997

(121) M. Laroussi, G. Sayler, B. Glascock, B. McCurdy, M. Pearce, N. Bright, and C. Malott. Images of Biological Samples Undergoing Sterilization by a Glow Discharge at Atmospheric Pressure. *IEEE Transactions on Plasma Science*, 27: 34-35, 1999

(122) J. Roth, D. Sherman, R. Gadri, F. Karakaya, Z. Chen, T. Montie, K. Kelly-Wintenberg and P. Tsai. A Remote Exposure Reactor (RER) for Plasma Processing and Sterilization by Plasma Active Species at One Atmosphere. *IEEE Transactions on Plasma Science*, 28: 56-63, 2000

(123) H. Herrmann, I. Henins, J. Park and G. Selwyn. Decontamination of Chemical and Biological Warfare (CBW) Agents Using an Atmospheric Pressure Plasma Jet (APPJ). *Physics of Plasmas*, 6: 2284-2289, 1999

(124) S. Lerouge, M. Wertheimer, R. Marchand, M. Tabrizian and L. Yahia. Effect of Gas Composition on Spore Mortality and Etching during Low- pressure Plasma Sterilization. *Journal of Biomedical Materials Research*, 51: 128-135, 2000

(125) S. Moreau, M. Moisan, M. Tabrizian, J. Barbeau, J. Pelletier, A. Ricard and L. Yahia. Using the Flowing Afterglow of a Plasma to Inactivate Bacillus Subtilis Spores: Influence of the Operating Conditions. *Journal of Applied Physics*, 88: 1166-1174, 2000

(126) I. Soloshenko, V. Tsiolko, V. Khomich, A. Shchedrin, A. Ryabtsev, V. Bazhenov and I. Mikhno. Sterilization of Medical Products in Low-pressure Glow Discharges. *Plasma Physics Reports*, 26: 792-800, 2000

(127) P. Koulik, S. Begounov and S. Goloviatinskii. Atmospheric Plasma Sterilization and Deodorization of Dielectric Surface. *Plasma Chemistry and Plasma Processing*, 19: 311-326, 1999

(128) P. Koulik. Remarks Relative to the Use of Atmospheric Plasma-pulsed Discharge for PET Bottles Instant Sterilization. *Plasma Chemistry and Plasma Processing*, 20: 159-161, 2000

(129) M. Riekerink, J. Terlingen, H. Engbers and J. Feijen. Selective Etching of Semicrystalline Polymers: CF_4 Gas Plasma Treatment of Poly(ethylene). *Langmuir*, 15: 4847-4856, 1999

(130) D. Gray, V. Mohindra and H. Sawin. Redeposition Kinetics in Fluorocarbon Plasma Etching. *Journal of Vacuum Science and Technology A-Vacuum Surfaces and Films*, 12(2): 354-364, 1994

(131) J. Ding and N. Hershkowitz. Symmetric Rate Model for Fluorocarbon Plasma Etching of SiO_2. *Applied Physics Letters*, 68(12): 1619-1621, 1996

(132) B. Beake, J. Ling and G. Leggett. Scanning Force Microscopy Investigation of Poly(ethylene terephthalate) Modified by Argon Plasma Treatment. *Journal of Materials Chemistry*, 8(8): 1735-1742, 1998

(133) J. Kim, H. Park and S. Hyun. The Effects of Plasma Treatment on SiO_2 Aerogel Film Using Various Reactive (O_2, H_2, N_2) and Non-reactive (He, Ar) Gases. *Thin Solid Films*, 377-378: 525-529, 2000

(134) S. Carlotti and A. Mas. Improvement of Adhesion of PET Fibers to Rubber by Argon-Oxygen Plasma Treatment. *Journal of Applied Polymer Science*, 69: 2321-2330, 1998

(135) A. Wrobel, M. Kryszewski, W. Rakowski, M. Okoniewski and Z. Kubacki. Effect of Plasma Treatment on Surface Structure and Properties of Polyester Fabric. *Polymer*, 19: 908-912, 1978

(136) M. Padhye, N. Bhat and P. Mittal. Electron Microscopical Study of Plasma-Etched Polymers. *Textile Research Journal*, 46(7): 502-507, 1976

(137) N. Bhat and G. Nadiger. Effect of Nitrogen Plasma on the Morphology and Allied Textile Properties of Tasar Silk Fibers and Fabrics. *Textile Research Journal*, 48(12): 658-691, 1978

(138) J. Friedrich and J. Gähde. Investigation on Plasma Etching of Polymer. Part II. Effect of Plasma Parameters on the Degradation Rate and Uncovering of Supermolecular Polymer Structure. *Acta Polymerica*, 31: 52-58, 1980

(139) N. Inagaki, S. Tasaka, K. Narushima and K. Teranishi. Surface Modification of Poly(tetrafluoroethylene) with Pulsed Hydrogen Plasma. *Journal of Applied Polymer Science*, 83: 340-348, 2002

(140) M. Hudis. Surface Cross-linking of Polyethylene Using Hydrogen Glow Discharge. *Journal of Applied Polymer Science*, 16: 2397-2415, 1972

(141) J. Chen. Free Radicals of Fibers Treated with Low Temperature Plasma. *Journal of Applied Polymer Science*, 42: 2035-2037, 1991

(142) K. Johnsen, S. Kirkhorn, K. Olafsen, K. Redford and A. Stori. Modification of Polyolefin Surfaces by Plasma-induced Grafting. *Journal of Applied Polymer Science*, 59: 1651-1657, 1996

(143) Zubaidi and T. Hirotsu. Graft Polymerization of Hydrophilic Monomers onto Textile Fibers Treated by Glow Discharge Plasma. *Journal of Applied Polymer Science*, 61: 1579-1584, 1996

(144) S. Bugaev, A. Korotaev, K. Oskomov and N. Sochugov. A-C:H Films Deposited in the Plasma of Barrier and Surface Discharges at Atmospheric Pressure. *Surface and Coatings Technology*, 96: 123-128, 1997

(145) S. Stoykov, C. Eggs and U. Kortshagen. Plasma Chemistry and Growth of Nanosized Particles in a C_2H_2 RF Discharge. *Journal of Physics D-Applied Physics*, 34: 2160-2173, 2001

(146) J. Hopkins, R. Boyd and J. Badyal. Plasma Fluorination versus Oxygenation of Polypropylene. *Journal of Physical Chemistry*, 100: 6755-6759, 1996

(147) D. Clark and D. Hutton. Surface Modification by Plasma Techniques. I. The Interactions of a Hydrogen Plasma with Fluoropolymer Surface. *Journal of Polymer Science Part A-Polymer Chemistry*, 25: 2643-2644, 1987

(148) T. Ward and R. Benerito. Modification of Cotton by Radiofrequency Plasma of Ammonia. *Textile Research Journal*, 52: 256-263, 1982

(149) R. Wilken, A. Hollander and J. Behnisch. Surface Radical Analysis on Plasma-treated Polymers. *Surface and Coatings Technology*, 116-119: 991-995, 1999

(150) T. Wakida, K. Takeda, I. Tanaka and T. Takagishi. Free Radicals in Cellulose Fibers Treated in Low Temperature Plasma. *Textile Research Journal*, 59: 49-53, 1989

(151) J. Chen. Study on Free Radicals of Cotton and Wool Fibers Treated with Low-Temperature Plasma. *Journal of Applied Polymer Science*, 62: 1325-1329, 1996

(152) J. Lub, F. Vroonhoven and A. Benninghoven. The Interaction of Hydrogen and Ammonia Plasmas with Polymethacrylic Eesters, Studies by Static Secondary Ions Mass Spectrometry. *Journal of Polymer Science Part A-Polymer Chemistry*, 27: 4035-4049, 1989

(153) P. Gröning, O. Küttel, M. Collaud-Coen, G. Dietler and L. Schlapbach. Interaction of Low-energy ions (< 10eV) with Polymethylemethacrylate during Plasma Treatment. *Applied Surface Science*, 89: 83-91, 1995

(154) S. Idage and S. Badrinarayanan. Surface Modification of Polystyrene Using Nitrogen Plasma. An X-ray Photoelectron Spectroscopy Study. *Langmuir*, 14: 2780-2785, 1998

(155) T. Ward, H. Jung, O. Hinojosa and R. Benerito. Characterization and Use of Radio Frequency Plasma-Activated Natural Polymers. *Journal of Applied Polymer Science*, 23: 1987-2003, 1979

(156) G. Placinta, F. Arefi-khonsari, M. Gheorghiu, J. Amouroux and G. Popa. Surface Properties and the Stability of Poly(ethylene Terephthalate) Films Treated in Plasmas in Helium-Oxygen Mixture. *Journal of Applied Polymer Science*, 66: 1367-1375, 1997

(157) N. Inagaki, S. Tasaka and H. Kawai. Surface Modification of Aromatic Polyamide Film by Oxygen Plasma. *Journal of Polymer Science Part A-Polymer Chemistry*, 33: 2001-2011, 1995

(158) S. Wu, J. Xing, C. Zheng, G. Xu, G. Zheng and J. Xu. Plasma Modification of Aromatic Polyamide Reverse Osmosis Composite Membrane Surface. *Journal of Applied Polymer Science*, 64: 1923-1926, 1997

(159) D. Clark and A. Dilks. ESCA Applied to Polymers. XXIII. RF Glow Discharge Modification of Polymers in Pure Oxygen and Helium-Oxygen Mixture. *Journal of Polymer Science Part A-Polymer Chemistry*, 17: 957-976, 1979

(160) J. Friedrich, I. Loeschcke, H. Frommelt, H. Reiner, H. Zimmermann and P. Lutgen. Ageing and Degradation of Poly(ethylene terephthalate) in an Oxygen Plasma. *Polymer Degradation and Stability*, 31: 97-114, 1991

(161) A. Hollander, R. Wilken and J. Behnisch. Subsurface Chemistry in the Plasma Treatment of Polymers. *Surface and Coatings Technology*, 116-119: 788-791, 1999

(162) M. Gheorghiu, F. Arefi, J. Amouroux, G. Placinta, G. Popa and M. Tatoulian. Surface Cross Linking and Functionalization of Poly(ethylene terephthalate) in a Helium Discharge. *Plasma Sources Science and Technology*, 6: 8-19, 1997

(163) H. Yasuda, C. Lamaze and K. Sakaoku. Effect of Electrodeless Glow Discharge on Polymers. *Journal of Applied Polymer Science*, 17: 137-152, 1973

(164) T. Tamai, N. Ichinose, S. Kawanishi and K. Mizuno. Photochemical Oxygenation and Cross-Linking of Poly(4-trimethylsilymethylstyrene) Thin Film by UV Irradiation. *Macromolecules*, 33: 2881-2886, 2000

(165) B. Gupta, J. Hilborn, C. Hollenstein, J. Plummer, R. Houriet and N. Xanthopoulos. Surface Modification of Polyester Films by RF Plasma. *Journal of Applied Polymer Science*, 78: 1083-1091, 2000

(166) H. Yasuda and H. Marsh. ESCA Study of Polymer Surfaces Treated by Plasma. *Journal of Applied Polymer Science*, 15: 991-1019, 1997

(167) Y. Nakayama, F. Soeda, A. Ishitani and T. Ikegami. Surface Analysis of Plasma-Treated Poly(ethylene terephthalate) Film. *Polymer Engineering and Science*, 31: 812-817, 1991

(168) M. Shi, J. Christoud, Y. Holl and F. Clouet. Functionalization by Cold Plasmas of Polymer Model Surfaces (Hexatriacontane and Octadecyloctadecanoate) Studied by Contact Angle Measurements, XPS, and FTIR Spectroscopy. *Journal of Macromolecular Science-Pure and Applied Chemistry*, A(30): 219-239, 1993

(169) D. Clark and R. Wilson. Selective Surface Modification of Polymers by Means of Hydrogen and Oxygen Plasmas. *Journal of Polymer Science-Polymer Chemistry Edition 21*, 837-853, 1983

(170) S. Moon and J. Jang. Surface Characterization Method of Oxygen Plasma-Treated UHMPE Fiber Using Drift Spectroscopy. *Journal of Applied Polymer Science*, 68: 1117-1124, 1998

(171) R. Nuzzo and G. Smolinsky. Preparation and Characterization of Functionalized Polyethylene Surface. *Macromolecules*, 17: 1013-1019, 1984

(172) R. Goldblatt, L. Ferreiro, S. Nunes, R. Thomas, N. Chou, L. Buchwalter, F. Heidenreich and T. Chao. Characterization of Water Vapor Plasma-Modified Polyimide. *Journal of Applied Polymer Science*, 46: 2189-2202, 1992

(173) A. Mas, H. Jaaba, F. Schue, A. Belu, C. Kassis, R. Linton and J. Desimone. Poly(hydroxylbutyrate-co-9% Hydroxyvalerate) Film Surface Modification by Ar, O_2, H_2O/O_2, H_2O, and H_2O_2 Plasma Treatment. *Journal of Macromolecular Science-Pure and Applied Chemistry*, 34: 67-79, 1997

(174) J. Terlingen, H. Gerritsen, A. Hoffman and J. Feijen. Introduction of Functional Groups on Polyethylene Surface by a Carbon Dioxide Plasma Treatment. *Journal of Applied Polymer Science*, 57: 969-982, 1995

(175) Q. Le, J. Pireaux and R. Caudano. XPS Study of the PET Film Surface Modified by CO_2 Plasma: Effects of the Plasma Parameters and Ageing. *Journal of Adhesion Science and Technology*, 11: 735-751, 1997

(176) Q. Le, J. Pireaux, R. Caudano, P. Leclere, R. Lazzaroni. XPS/AFM Study of the PET Surface Modified by Oxygen and Carbon Dioxide Plasmas: Al/PET Adhesion. *Journal of Adhesion Science and Technology*, 12: 999-1023, 1998

(177) A. Klomp, J. Terlingen, G. Takens, A. Strikker, G. Engbers and J. Feijen. Treatment of PET Nonwoven with a Water Vapor or Carbon Dioxide Plasma. *Journal of Applied Polymer Science*, 75: 480-494, 2000

(178) S. O'Kell, T. Henshaw, G. Farrow, M. Aindow and C. Jones. Effects of Low-Power Plasma Treatment on Polyethylene Surfaces. *Surface and Interface Analysis*, 23: 319-327, 1995

(179) R. Foerch, N. McIntyre and R. Sodhi. Nitrogen Plasma Treatment of Polyethylene and Polystyrene in a Remote Plasma Reactor. *Journal of Applied Polymer Science*, 40: 1903-1915, 1990

(180) T. Yasuda, T. Okuno, K. Yoshida and H. Yasuda. A Study of Surface Dynamics of Polymers. II. Investigation by Plasma Surface Implantation of Fluorine-Containing Moieties. *Journal of Polymer Science Part B-Polymer Physics*, 26: 1781-1794, 1988

(181) S. Sigurdsson and R. Shishoo. Surface Properties of Polymers Treated with Tetrafluoromethane Plasma. *Journal of Applied Polymer Science*, 66: 1591-1601, 1977

(182) H. Yasuda, E. J. Charlson, E. M. Charlson, T. Yasuda, M. Miyama and T. Okuno. Dynamics of Surface Property Change in Response to Change in Environmental Conditions. *Langmuir*, 7: 2394-2400, 1991

(183) E. Winder and K. Gleason. Growth and Characterization of Fluorocarbon Thin Films Grown from Trifluoromethane (CHF_3) Using Pulsed-Plasma Enhance CVD. *Journal of Applied Polymer Science*, 78: 842-849, 2000

(184) E. Selli, G. Mazzone, C. Oliva, F. Martini, C. Riccardi, R. Barni, B. Marcandalli and M. Massafra. Characterisation of Poly(ethylene terephthalate) and Cotton Fibres after Cold SF_6 Plasma Treatment. *Journal of Materials Chemistry*, 11: 1985-1991, 2001

(185) F. Poncin-Epaillard, G. Legeay and J. Brosse. Plasma Modification of Cellulose Derivatives as Biomaterials. *Journal of Applied Polymer Science*, 44: 1513-1522, 1992

(186) D. Wilson, R. Williams and R. Pond. Plasma Modification of PTFE Surfaces Part I: Surfaces Immediately Following Plasma Treatment. *Surface and Interface Analysis*, 31: 385-396, 2001

(187) R. Paynter. Angle-resolved XPS Study of the Effect of X-radiation on the Aging of Polystyrene Exposed to an Oxygen/Argon Plasma. *Surface and Interface Analysis*, 33: 14-22, 2002

(188) M. Anand, R. Cohen and R. Baddour. Surface Modification of Low Density Polyethylene in a Fluorine Gas Plasma. *Polymer*, 22: 361-371, 1981

(189) J. McCarulley and H. Goldberg. Composition Depth Profiles of Plasma-Fluorinated Poly(ethylene terephthalate) Fibers. *Journal of Applied Polymer Science*, 53: 543-559, 1994

(190) R. Foerch, G. Kill and M. Walzak. Plasma Surface Modification of Polypropylene: Short-Term vs. Long-Term Plasma Treatment. *Journal of Adhesion Science and Technology*, 7: 1077-1089, 1993

(191) A. Mas, H. Jaaba, and F. Schue. Modification of Poly(3-hydroxybutyric acid)-co-(3-hydroxyvaleric acid) Film Surfaces in an Oxygen Low Pressure Plasma. *Macromolecular Chemistry and Physics*, 197: 2331-2341, 1996

(192) D. Piao, Y. Uyama and Y. Ikada. Aging of Plasma Treated Polymers. *Kobunshi Ronbunshu*, 48: 529-534, 1991

(193) F. Poncin-Epaollard, J. Brosse and T. Falher. Reactivity of Surface Groups Formed onto a Plasma Treated Poly(propylene) Film. *Macromolecular Chemistry and Physics*, 200: 989-996, 1999

(194) W. Brennan, W. Feast, H. Munro and S. Walker. Investigation of the Aging of Plasma Oxidized Peek. *Polymer*, 32: 1527-1530, 1991

(195) H. Yasuda, A. Sharma and T. Yasuda. Effect of Orientation and Mobility of Polymer Molecules at Surfaces on Contact Angle and Its Hysteresis. *Journal of Polymer Science-Polymer Physics Edition 19*, 1285-1291, 1981

(196) I. Gerenser. XPS Studies of in situ Plasma-Modified Polymer Surface. *Journal of Adhesion Science and Technology*, 7: 1019-1040, 1993

(197) D. Wilson, R. Williams and R. Pond. Plasma Modification of PTFE Surfaces, Part II: Plasma-treated Surfaces Following Storage in Air and PBS. *Surface and Interface Analysis*, 31: 397-408, 2001

(198) C. Chan, T. Ko and H. Hiraoka. Polymer Surface Modification by Plasma and Photons. *Surface Science Report*, 24: 1-54, 1996

(199) K. Sahre, K. Eichhorn, D. Pleul and F. Simon. The Chemical Structure and Stability of Plasma-Deposited Thin Hydrocarbon Layers on Polyethylene. *Journal of Adhesion Science and Technology*, 14: 867-878, 2000

(200) I. Retzko, J. Friedrich, A. Lippitz and W. Unger. Chemical Analysis of Plasma-Polymerized Films: The Application of X-ray Photoelectron Spectroscopy (XPS), X-ray Absorption Spectroscopy (NEXAFS) and Fourier Transform Infrared Spectroscopy (FTIR). *Journal of Electron Spectroscopy and Related Phenomena*, 121: 111-129, 2001

(201) H. Yasuda. Glow Discharge Polymerization. *Macromolecular Reviews Part D-Journal of Polymer Science*, 16: 199-293, 1981

(202) H. Kobayashi, A. Bell and M. Shen. Plasma Polymerization of Saturated and Unsaturated Hydrocarbons. *Macromolecules*, 7: 277-283, 1974

(203) Y. Haque and B. Ratner. Preparation and Properties of Plasma Deposited Films with Surface Energy Varying over a Wide Range. *Journal of Applied Polymer Science*, 32: 4369-4381, 1986

(204) T. Yasuda, M. Gazicki and H. Yasuda. Effects of Glow Discharges on Fibers and Fabrics. *Journal of Applied Polymer Science- Applied Polymer Symposia*, 38: 201-214, 1984

(205) T. Yasuda, T. Okuno and K. Yoshida. On the Ablation of Poly(ethylene terephthalate) Fiber by Air Plasma. *Sen'i Gakkaishi*, 42: T11-T17, 1986

(206) K. Wong, X. Tao, C. Yuen and K. Yeung. Low Temperature Plasma Treatment of Linen. *Textile Research Journal*, 69: 846-855, 1999

(207) D. Ferrante, S. Iannace and T. Monetta. Mechanical Strength of Cold Plasma Treated PET Fibers. *Journal of Materials Science*, 34: 175-179, 1999

(208) S. Dahl, D. Rats, J. Stebut, L. Martinu and J. Klemberg-Sapieha. Micromechanical Characterisation of Plasma Treated Polymer Surfaces. *Thin Solid Film*, 335-356: 290-294, 1999

(209) I. Negulescu, S. Despa, J. Chen and B. Collier. Characterizing Polyester Fabrics Treated in Electrical Discharges of Radio-Frequency Plasma. *Textile Research Journal*, 70: 1-7, 2000

(210) J. Yip, K. Chan, K. Sin and K. Lau. Low Temperature Plasma-Treated Nylon Fabrics. *Journal of Materials Processing Technology*, 123: 5-12, 2002

(211) R. Stone and J. Barrett Jr.. U.S.D.A. Study Reveals Interesting Effects of Gas Plasma Radiation on Cotton Yarn. *Textile Bulletin*, 1: 65-69, 1962

(212) G. Abbott. Open-End Spun Corona-Treated Cotton. *Textile Research Journal*, 53(9): 566-567, 1977

(213) W. Thorsen. Improvement of Cotton Spinnability, Strength, and Adhesion Resistance by Corona Treatment. *Textile Research Journal*, 41(5): 455-458, 1971

(214) M. McCord, Y. Hwang, P. Hauser, Y. Qiu, J. Cuomo, O. Hankins and M. Bourham and L. Canup. Modifying Nylon and Polypropylene Fabrics with Atmospheric Pressure Plasma. *Textile Research Journal*, 72(6): 491-498, 2002

(215) M. Shenton and G. Steven. Surface Modification of Polymer Surface: Atmospsheric Plasma versus Vacuum Plasma Treatments. *Journal of Physics D-Applied Physics*, 34: 2761-2768, 2001

IV. SURFACE MODIFICATION OF ORGANIC POLYMER FILMS TREATED IN ATMOSPHERIC PLASMAS[1]

1. Abstract

Interaction of atmospherically generated plasma with polyethylene terephthalate (PET) films has been studied in this paper, using helium and oxygenated-helium plasmas. The interaction took place inside a closed ventilation plasma chamber at variable exposure times. The percent of the samples' weight change have shown initial increase followed by a decreasing percent as exposure time is extended. Contact angle measurement showed that wettability increased rapidly up to 1 minute then remained constant with increased exposure time.

Atomic Force Microscopy (AFM) was used to characterize changes in the surface morphology of PET films, where increased roughness and surface re-deposition were observed. Surface functionalization and cross-linking were examined by X-ray Photoelectron Spectroscopy (XPS). In both plasma treatments functionalization is induced after chain-scission. Chain scission may be responsible for the generation of particles as a result of etching and these particles may be a source of re-deposition on the surface and. Re-deposition affects the weight loss (%), roughness, carbon content and functional groups during plasma exposure. Cross-linking is exposure time and helium content dependent. Additional cross-linking took place at longer exposure times.

[1] This paper was presented at 202nd The Electrochemical Society Meeting (Salt Lake City, Utah, USA, October 20-25, 2002), and is submitted to Journal of the Electrochemical Society (2003).

2. Introduction

Material surfaces immersed in atmospheric plasmas may be subject to various forms of interactions including, but not limited to, electron and ion impact, radicals-surface interactions, ultraviolet and photon transport, etching, implantation, deposition and re-deposition [1,2]. For textile materials, these interactions may result in surface etching, chain scission, polymerization, cross-linking, development of functional groups, surface roughness, etc.; Figure 1 shows an illustration of such possible interactions.

Surface etching by reactive species may break molecular chains and the derivative particles are mixed with the plasma. When active species reach surface of substrate, new functional groups can be generated by molecular chain scission, atom substitution and recombination. Free radicals can also promote polymerization. Photons from UV-radiation may also introduce cross-linking between molecules on the substrate surface. It is very complicated to determine, characterize and assess all plasma parameters and interactions affecting changes in the substrate properties.

Plasma treatment of textile materials and surface modifications has growing interest as a novel technique to replace chemical wet methods. In polymer surface modification, various techniques were commonly used including wet chemical methods, RF-vacuum plasmas, ion beam irradiation, and corona and flame treatments [3-15]. In wet chemical processing, large amount of toxic solvents are required [13]. RF vacuum plasma and ion beam techniques are conducted under vacuum, leading to high cost and limiting treatments to batch processing. The corona and flame treatments have problems with treatment uniformity and limited application [3]. Atmospheric pressure plasma systems (microwave-coupled atmospheric pressure plasma [3,4] and atmospheric pressure glow discharge [12]) provide an

appealing alternative to vacuum systems as they provide the possibility for achieving the same surface effects while allowing continuous processing at lower cost [14]. While vacuum plasma surface modification of polymers is well documented [5–11], effects and mechanisms of atmospheric plasma treatment have not completely been characterized [3,4,12].

This study focuses on the physical and chemical effects of atmospheric pressure plasma on organic polymer films. Plasma treated films were characterized using surface analytical techniques to determine the nature of the plasma-surface interactions and the possible mechanisms responsible for observed surface changes.

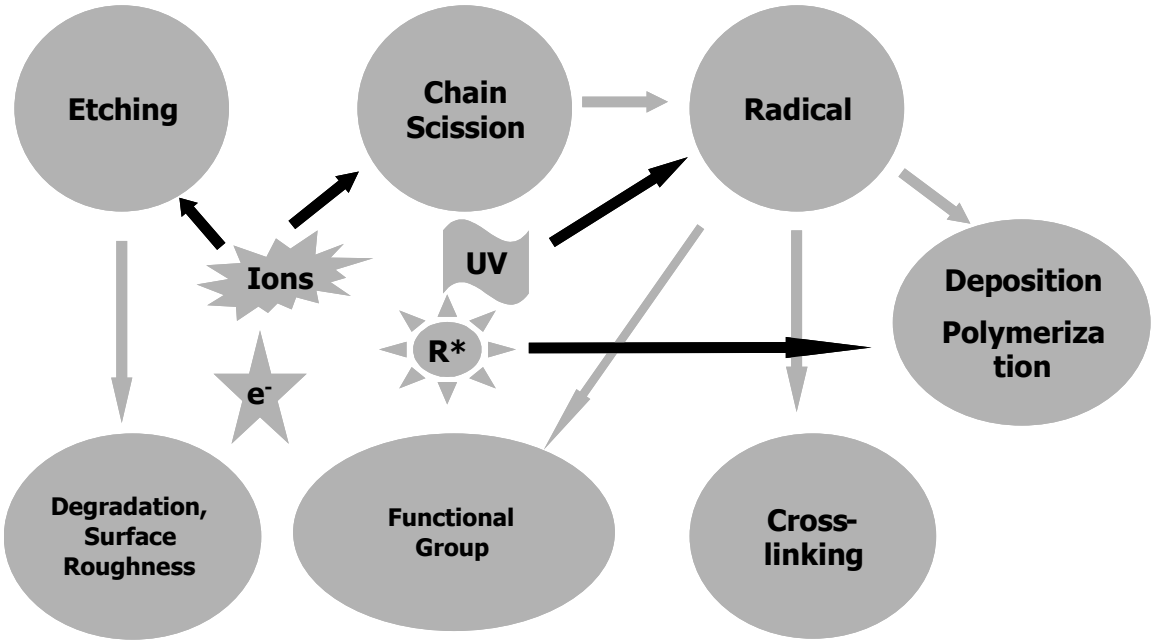

Figure 1. Mechanism of Plasma-Substrate Interaction

3. Experimental

PET films (MELINEX® S/200, thickness 50 μm) were supplied by DuPont Teijin Films™. The films were washed prior to plasma exposure by acetone solution for 3 minutes and dried at ambient temperature. Experiments were conducted using the NC State University atmospheric pressure plasma device. Figure 2 shows a schematic of the experimental device in closed ventilation geometry [15]. The plasma was generated with He/Air and He/O_2 (oxygenated helium with helium being the seed gas) at 10 kHz with 7.8 kV_{rms} across the plates at constant gas flow rate. The exposure time was varied between 0 and 5 min. at 0.5 min. intervals.

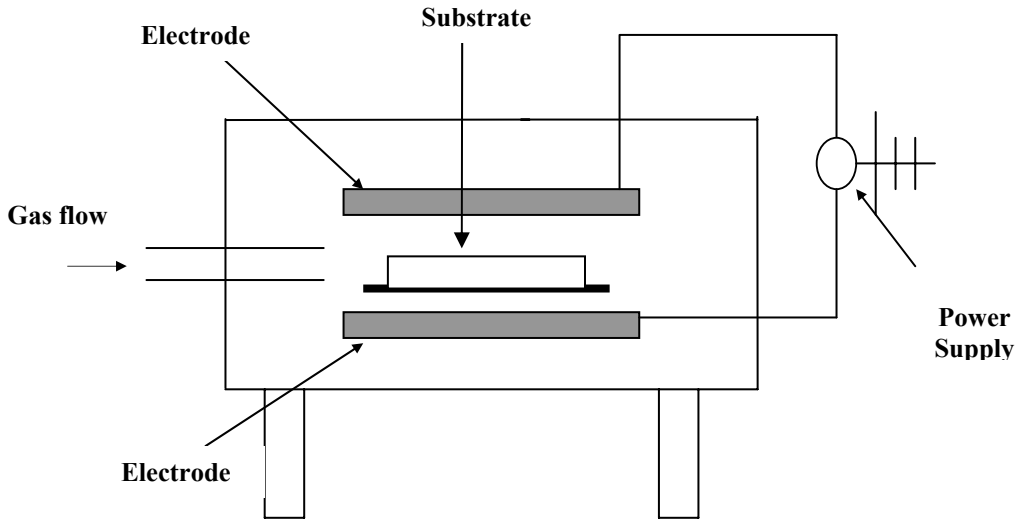

Figure 2. Atmospheric Pressure Plasma System Diagram (Closed Ventilation)

Following plasma treatment, the PET film weight loss (%) was determined as follow:

$$Weight\ Loss(\%) = \frac{(W_0 - W_i)}{W_0} \times 100 \qquad (1)$$

where W_0 is the initial weight of the PET film and W_i is the weight of the PET film after plasma treatment.

Surface wettability was characterized by contact angle measurement using a goniometer (Model A-100 by Ramé-Hart, Inc.) by the sessile drop technique using a 1 μL distilled water droplet on the PET film. The contact angle was measured in 5 different places to determine hydrophobicity.

Chemical composition analysis of the PET film surface was performed with Perkin Elmer PHI 5400 XPS (X-ray Photoelectron Spectroscopy). The x-ray source was Mg_α (1,253.6 eV) with 45° take-off angle. The references of XPS spectra were used with respect of 285.0 eV for C_{1s}, observed in hydrocarbon polymers. Sensitive factors (S) for XPS transition were $S(C_{1s})$= 0.296, $S(N_{1s})$=0.477 and $S(O_{1s})$ = 0.711. O/C, N/C and (O+N)/C atomic rates were estimated from the relative intensities of the O_{1s}, N_{1s} and C_{1s} core levels. C_{1s} deconvolution analyses were conducted to examine the functionalization on PET film surface after plasma treatments.

Surface morphology of PET films was analyzed using Hitachi model S-3200 scanning electron microscopy (SEM) with magnifications up to 10,000× at 5.0 kV. The surface roughness was examined using atomic force microscopy (AFM - JEOL JSPM-5200), and a silicon nitride tip was used as a probe with scanned areas of 1 μm^2 and 5 μm^2 at 10^{-3} Pa

pressure. A root mean square of the surface roughness (RMS) was calculated from the roughness profile using following equation:

$$RMS = \sqrt{\frac{1}{L}\int_0^L Z(x)^2\,dx} \qquad (2)$$

where L is the scanning distance.

4. Results

4.1 Weight Loss (%)

The PET film weight was measured before and after plasma treatment under close ventilation conditions and plotted versus exposure time (Figure 3). The weight loss (%) of PET films treated by He/Air plasma increases with increased exposure time to reach a maximum at 1 min., while the weight loss (%) increases up to 2 min. exposure time for He/O_2 plasma treatment. These results show that oxygen has a greater etching effect than air. At longer exposure time, the weight loss (%) of PET films decreases and reaches the equilibrium state after conditioned exposure for both gas plasma treatments. This suggests simultaneous etching and re-deposition processes in plasma-substrate interaction.

4.2 Surface Morphology Change

As shown in Figure 4, SEM pictures did not show a change in PET film surface roughness, however, AFM pictures showed changes as a result of plasma exposure as shown in Figure 5. The He/O_2 plasma treatment leads to higher surface roughness than that of

He/Air gas. As shown in Figure 6, the surface roughness initially increased after plasma treatment for both gases in 1 and 5 μm^2 scans, and then decreased again, which may be attributed to a re-deposition effect as shown in Figure 7.

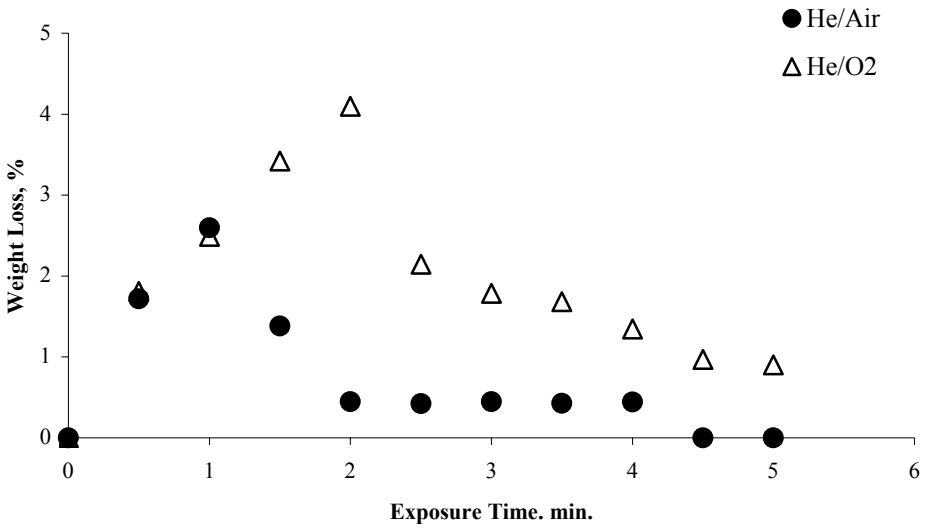

Figure 3. Weight Loss (%) of PET Film Treated by Atmospheric Pressure Plasma

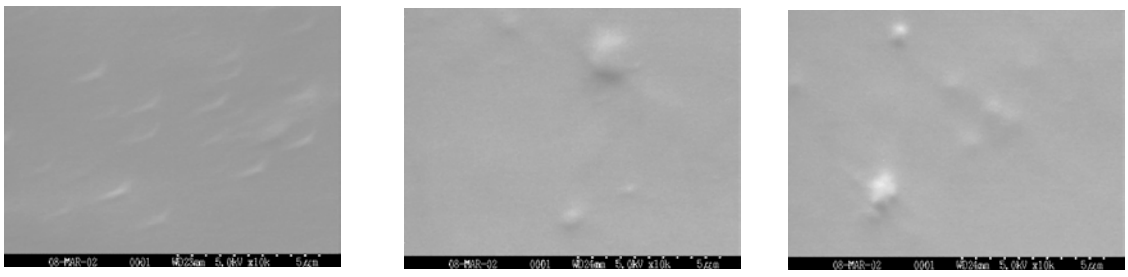

(a) PET Film Control (b) He/Air 4 min. (c) He/O_2 5 min.

Figure 4. Scanning Electron Microscopy (SEM) Pictures of PET Films

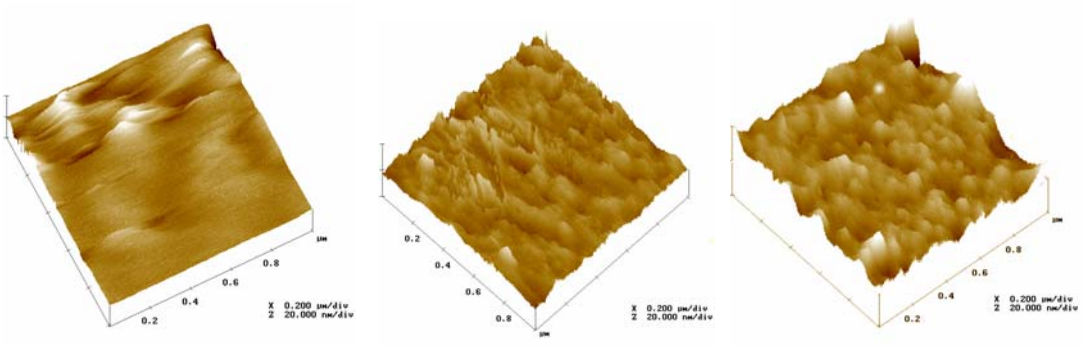

(a) PET Film Control (b) He/Air 3 min. (c) He/O_2 2 min.

Figure 5. AFM Images of Control and Atmospheric Pressure Plasma Treated PET Films

4.3 Wettability

Wettability is affected by chemical changes (functionalization) induced by plasma exposure. As shown in Figure 8, contact angles of plasma treated PET films decreased with increased exposure time as compared to the control sample. It is also noted that He/O_2 gas treatment leads to higher wettability than He/Air gas treatment up to 1 min. exposure time. He/O_2 gas has higher oxygen content, that is, it can have more chemical interaction with the molecules on PET film surface. However, after 1 min. exposure time, there is no further wettability enhancement in both gas plasma treatments.

(a)

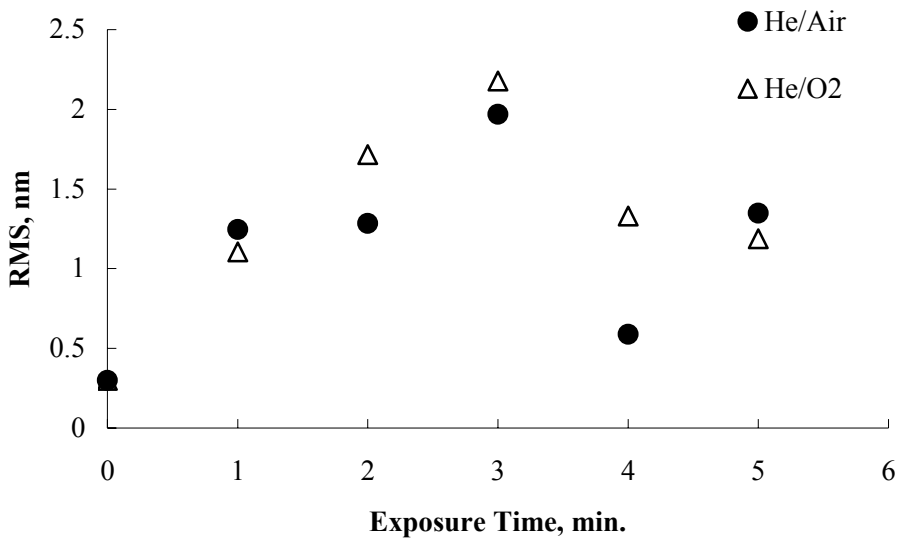

(b)

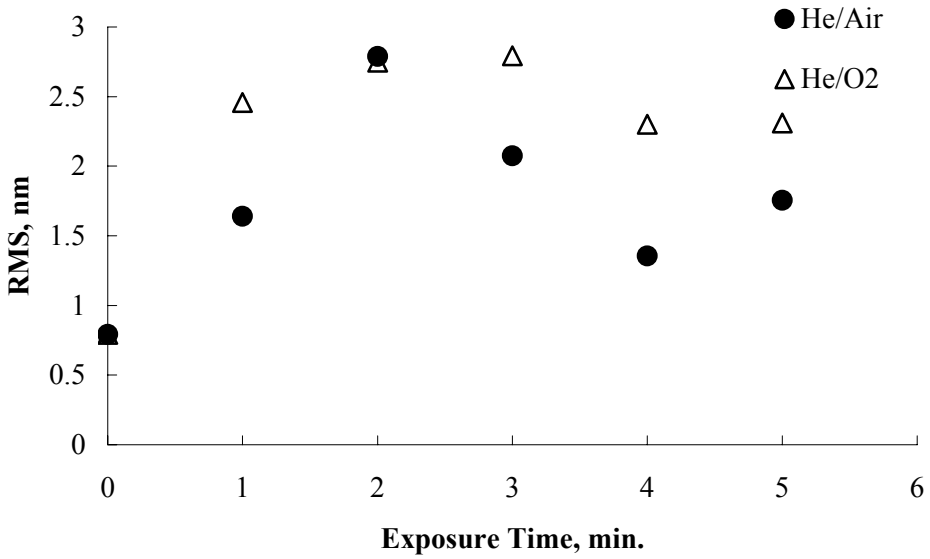

Figure 6. Surface Roughness (RMS) of Plasma Treated PET Films by AFM: (a) 1 μm^2 Scanning and (b) 5 μm^2 Scanning

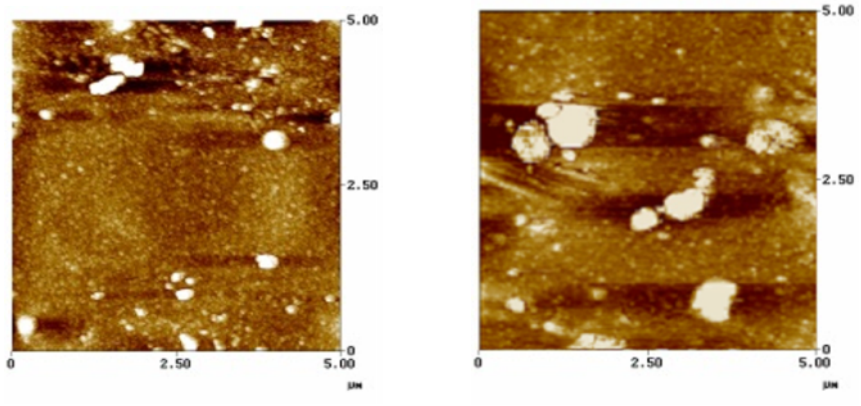

(a) He/Air Plasma 5 min. (b)He/O_2 Plasma 5 min.

Figure 7. AFM Pictures of Re-deposited Nano-Size Particles on Plasma Treated PET Films

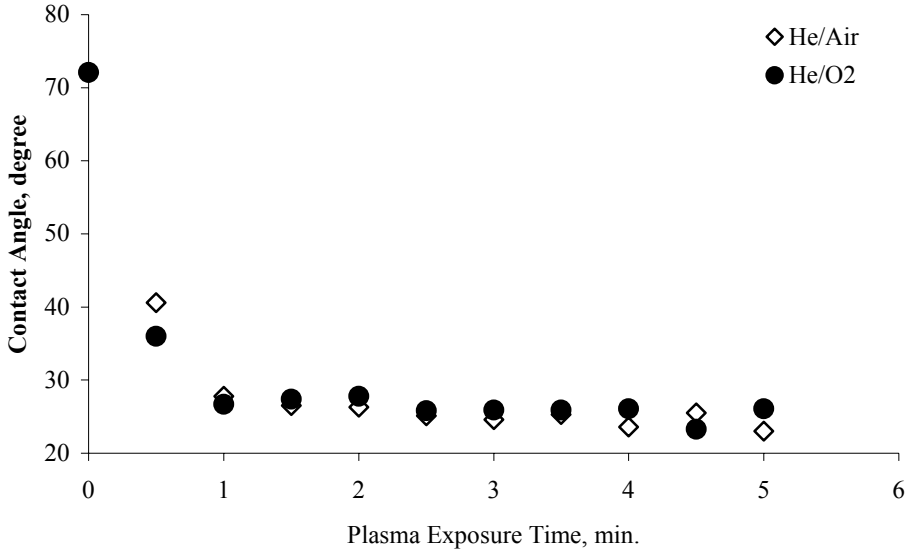

Figure 8. Contact Angle Measurement of Plasma Treated PET Films

4.4 Chemical Composition Change on PET Film Surface

XPS analysis showed apparent chemical composition change (Tables 1 and 2). The carbon contents (C_{1s}) of plasma treated PET films decreased at treatment times up to 1 min. for He/Air plasma exposure and up to 2 min. for the He/O_2 plasma, then increased again. The nitrogen content (N_{1s}) increment shows that N_2 related chemical reactions were involved because N_2 gas exists in atmospheric pressure plasma. The oxygen content (O_{1s}) increased up to 1min. exposure time and decreased again for He/Air plasma, while He/O_2 plasma treatment resulted in the highest O_{1s} at a 2 min. exposure time. He/O_2 plasma generated lower carbon content and higher oxygen content on PET film than He/Air plasma because oxygen content is higher in He/O_2 plasma.

Table 1. Relative Chemical Composition and Atomic Ratio Determined by XPS for PET Film Treated by He/Air Atmospheric Pressure Plasma

Exposure Time, min.	Chemical Composition, %			Atomic Ratio		
	C_{1s}	N_{1s}	O_{1s}	O/C	N/C	(O+N)/C
Control	86.3	0.2	13.5	0.16	0.00	0.16
0.5	86.6	0.3	13.1	0.15	0.00	0.15
1.0	64.0	3.3	32.7	0.51	0.05	0.56
1.5	65.2	7.7	27.1	0.42	0.12	0.53
2.0	71.5	6.9	21.6	0.30	0.10	0.40
2.5	76.0	8.8	15.2	0.20	0.12	0.32
3.0	76.3	7.3	16.5	0.22	0.10	0.31
3.5	78.9	6.6	14.5	0.18	0.08	0.27
4.0	75.1	4.9	20.0	0.27	0.07	0.33
4.5	77.4	3.9	18.7	0.24	0.05	0.29
5.0	82.2	2.5	15.3	0.19	0.03	0.22

Table 2. Relative Chemical Composition and Atomic Ratio Determined by XPS for PET Film Treated by He/O_2 Atmospheric Pressure Plasma

Exposure Time, min.	Chemical Composition, %			Atomic Ratio		
	C_{1s}	N_{1s}	O_{1s}	O/C	N/C	(O+N)/C
Control	86.3	0.2	13.5	0.16	0.00	0.16
0.5	84.6	0.4	15.0	0.18	0.00	0.18
1.0	60.8	2.8	37.2	0.61	0.05	0.66
1.5	53.4	5.5	41.1	0.77	0.10	0.87
2.0	50.8	4.8	44.4	0.87	0.09	0.97
2.5	51.9	5.1	43.9	0.85	0.10	0.94
3.0	54.4	3.3	42.3	0.78	0.06	0.84
3.5	56.6	4.4	39.0	0.69	0.08	0.77
4.0	58.0	4.1	37.9	0.65	0.07	0.72
4.5	56.2	5.9	37.9	0.67	0.10	0.78
5.0	57.6	5.8	36.6	0.64	0.10	0.74

C_{1s} deconvolution analysis shows functional group change of PET films (Figure 9) and formation of new functional group (Tables 3 and 4). C-C bonds decreased up to 1 min. in the He/Air plasma and up to 2 min. for the He/O_2 plasma then increased again. The He/O_2 plasma treatment led to higher reduction of C-C bond than He/Air plasma at longer exposure time. However, C-O bond showed little change in both He/Air and He/O_2 plasma treatments. The C-OH group increased then decreased again in both He/Air and He/O_2 plasmas as did C=O/CH=O bonds. The He/O_2 plasma can generate C-OH group than He/Air plasma. Plasma treated PET films showed a lower COO- bond content than control PET film. New functional group, OCOO-, was formed on PET films in both gas plasma treatments.

(a)

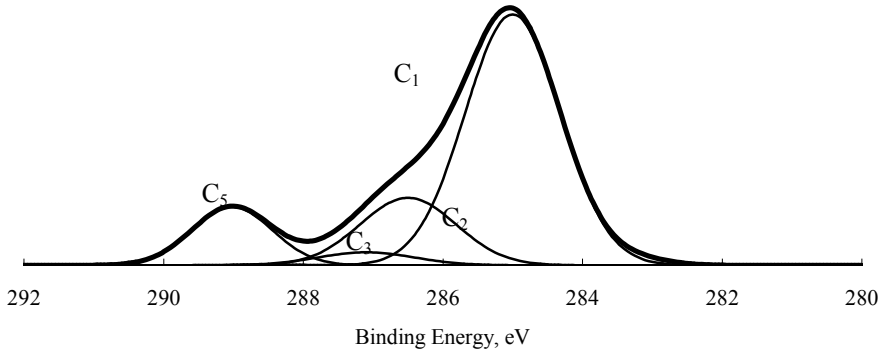

(b)

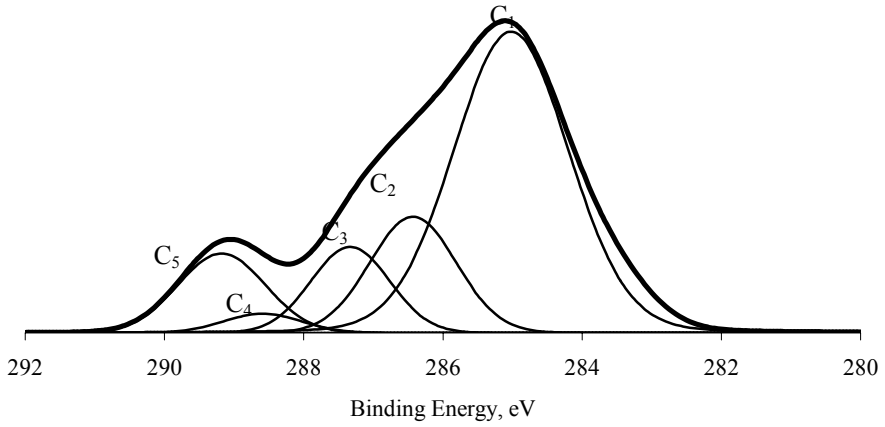

(c)

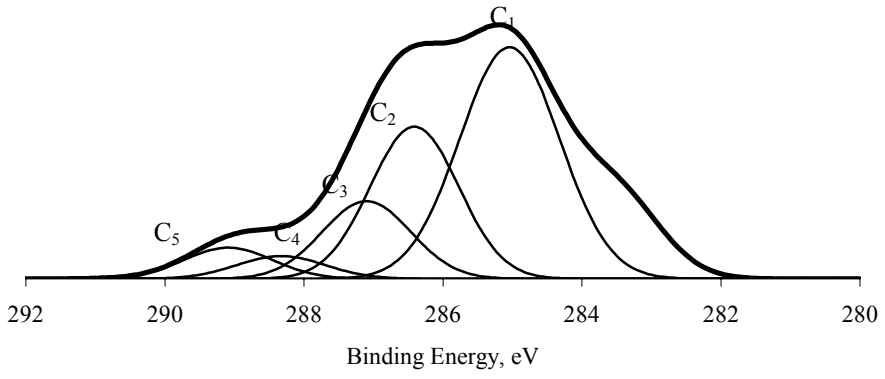

C_1 = -C-C- (285.0 eV), C_2 = -C-O- (286.5 eV), C_3 = -COH (287.1 eV),
C_4 = -C=O/-CH=O (288.5 eV), C_5 = -COO- (289.2 eV), C_6 = -O-COO- (290.4 eV)

Figure 9. C_{1s} Deconvolution Analysis of PET Films Treated by Atmospheric Pressure Plasma: (a) Control, (b) He/Air 1.0 min., and (c) He/O_2 2.0 min.

Table 3. Deconvolution of C_{1s} Spectra for PET Film Treated by He/Air Atmospheric Pressure Plasma

Exposure Time, min.	Relative Chemical Bond Area of C_{1s}, %					
	-C-C- (285.0 eV)	-C-O- (286.5 eV)	C-OH (287.1eV)	C=O/CH=O (288.50 eV)	COO- (289.4 eV)	-OCOO- (290.4 eV)
Control	65.2	17.6	4.3	0.2	12.7	0
0.5	64.2	18.1	6.1	1.1	10.5	0
1.0	56.5	15.8	14.5	2.3	10.9	0
1.5	56.8	17.1	16.0	2.8	7.2	0.1
2.0	57.6	14.9	15.3	2.5	9.4	0.3
2.5	57.6	11.3	17.4	3.8	9.0	0.9
3.0	58.7	14.5	13.3	4.3	8.7	0.5
3.5	62.2	15.5	9.9	3.7	8.6	0.1
4.0	62.8	13.9	10.6	1.8	10.6	0.3
4.5	63.9	12.8	11.3	3.3	8.4	0.3
5.0	59.7	18.6	8.6	1.8	11.3	0

Table 4. Deconvolution of C_{1s} Spectra for PET Film Treated by He/O_2 Atmospheric Pressure Plasma

Exposure Time, min.	Relative Chemical Bond Area of C_{1s}, %					
	-C-C- (285.0 eV)	-C-O- (286.5 eV)	C-OH (287.1eV)	C=O/CH=O (288.5 eV)	COO- (289.4 eV)	-OCOO- (290.4 eV)
Control	65.2	17.6	4.3	0.2	12.7	0
0.5	63.3	12.8	11.4	2.0	10.2	0.3
1.0	60.9	15.3	12.0	3.3	8.3	0.2
1.5	57.8	15.8	14.2	2.9	9.0	0.3
2.0	41.7	24.3	25.3	3.6	5.0	0.1
2.5	49.7	16.1	20.6	2.9	10.6	0.1
3.0	50.5	14.8	20.8	3.5	10.3	0.1
3.5	50.0	17.5	19.0	4.2	9.2	0.1
4.0	52.0	15.6	18.9	2.6	10.7	0.2
4.5	57.4	14.3	18.0	2.5	7.5	0.3
5.0	60.0	13.4	15.2	3.4	7.7	0.3

5. Discussion

5.1 Etching and Re-deposition

Weight loss due to plasma treatment is attributed to physical etching effects. As most conventional polymer films consist of crystalline and amorphous region, the etching effect would be selective and is dominated on amorphous over crystalline regions, which are softer and could be easily removed [16]. Initially, active species are likely to attack both regions concurrently, but with different etching rates. It is also possible that particles knocked off from molecular chain scission by etching can be re-deposited on the surface. Thus, it likely that the observed weight change is a result of weight loss by etching and weight gain by re-deposition occurring simultaneously and may be explained by the following equation:

$$L_P(t) = L_E(t) - G_D(t) \qquad (3)$$

where, L_P(t) is the weight loss rate of the substrate after plasma exposure, L_E(t) is the weight loss rate by etching and G_D(t) is the weight gain rate by re-deposition. The weight loss of the substrate by plasma treatment can be divided into weight loss at amorphous and crystalline region as follows [16,18]:

$$L_E(t) = (1-f)\cdot L_{AE}(t) + f\cdot L_{CE}(t) = [L_{CE}(t) - L_{AE}(t)]\cdot f + L_{AE}(t) \qquad (4)$$

where, L_{AE}(t) is weight loss rate on amorphous region, L_{CE}(t) is weight loss rate on crystalline region and f is the crystalline fraction. Also, L_{AE}(t) > L_{CE}(t). This etching model was applied to a two-phase material to explain the linear dependence of the etching rate of a polymer

surface on percent crystallinity, assuming that the etching rates of crystalline and amorphous phases remain constant during the etching process. Even etching behavior of polymer surface could be explained by this model, it seems that other parameters would be ignored in etching process. Based on the results (Figure 3), the etching process could be affected by not only substrate conditions (temperature of substrate, roughness, and chemical composition [16]) but also surface restructuring by re-deposition.

In this study, all plasma treatments were conducted in a closed-ventilation geometry. Assuming all gas molecules and particles broken off from surface would be trapped in the plasma chamber, thus, the etched particles coexist with active gas particles. The density of molecular particles by etching increases along the exposure time, and becomes involved into re-deposition on the surface. This condition is similar to the those results obtained for the deposition of fluorocarbon gas on polymeric film, which showed linear relations with flow rate and exposure time [18], and the deposition rate was reached to the maximum point as the monomer gas flow rate increases then decreased at higher flow rate [19]. Based on weight loss (%) trend of PET film, plasma treatment under atmospheric pressure can lead to three regions can be classified; (1) etching dominated region (R_E, $L_E > G_D$), (2) re-deposition dominated region (R_D, $L_E < G_D$), and (3) equilibrium region (R_{eq}, $L_E = G_D$).

This corresponds to roughness (Figure 6) and carbon content (Tables 1 and 2) of PET film surface. The roughness of PET film increased initially during etching (R_E) then decreased again during deposition (R_D). The re-deposition could induce coating or deposited material on the surface of the PET film, and reduce roughness. Figure 7 shows re-deposited apparent nano-size particles on treated PET films. As shown in Tables 1 and 2, carbon content of PET film decreased during etching (R_E), but increased again as a result of

deposition (R_D). With further increase in the plasma exposure time, the re-deposited layer could also increase further.

5.2 Chain Scission and Funtionalization

Ion bombardment into substrate surface during exposure to atmospheric plasma introduces not only etching but also chain scission of molecules on the substrate's surface, leading to the formation of active sites such as radicals. These active sites can interact with reactive particles in the plasma and generate new functional groups. The general possible interaction positions in PET molecule are illustrated as follows:

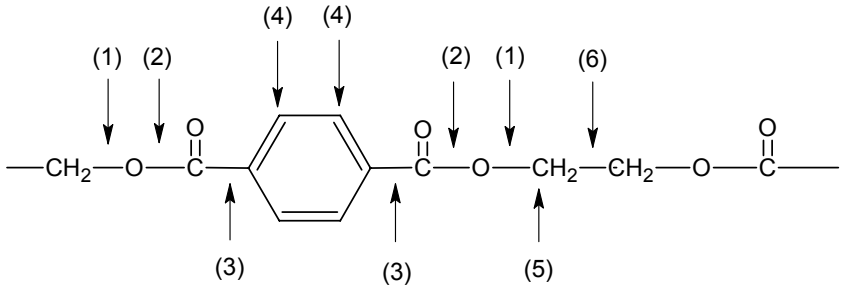

These interaction positions on PET molecules are attacked by plasma reactive particles generated by Penning transfer in helium containing plasma, leading to excitation and ionization of oxygen as follows [10]:

$$He^m + O_2 \rightarrow He + O^* + O^+ + e$$

$$He^+ + O^2 \rightarrow He^+ + O + O^*$$

$$He^+ + O^2 \rightarrow He + O^+ + O^*$$

And reactions at PET surface can render other chemical byproducts as follows:

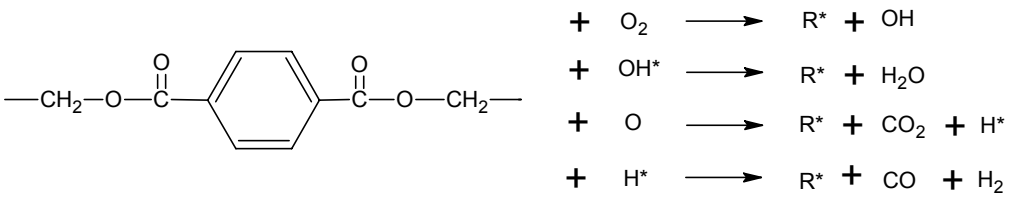

Generally, these chemical reactions could take a place in relatively weaker chemical bonds by chain scission. Chain scissions in PET molecule generate radicals, which are reactive with plasma particles. Among chemical bonds of PET is the C=C bond, which has the highest bonding energy as shown in Table 5, and thus has the lowest possibility of chain scission. Therefore, at positions (1), (2), (3) and (6) (C-C, C-O and C-H), there is higher probability of chain scission. Possible chain scission processes and their derivatives are summarized in Figure 10. Among the derivatives, $\bullet CH_2\text{-}CH_2\bullet$ radical or $CH_2{=}CH_2$ gas can be a source of re-deposition on PET film surface. In addition, the radicals generated by chain scission can render new functional group and change of functional groups following reactions with active species in the plasma. From the XPS deconvolution analyses of treated PET films, plasma treatment reduced -COO bond and increased –OH group (Figures 11 and 12).

5.3 Cross-linking

In this study, helium was used as the seed plasma gas. Helium is known to be the most proficient inert gas for cross-linking of polymeric materials because of abundance of UV radiation from large amount of energy generated by ion neutralization, Auger

deexcitation and Penning ionization [9,10]. Figure 13 shows the possible cross-linking reaction at position 4 and 5. As shown in Figure 14, C-C group decreased at shorter plasma exposure time, but additional formation of C-C group was obtained at longer exposure time. In addition, He/Air plasma treatment provided higher portion of C-C group than He/O_2 plasma, because He/Air plasma has higher helium content leading to higher possibility of cross-linking formation.

Table 5. Bond Energies of Common Chemical Bonds in Polymers [20]

Chemical Bond	Bond Energy, eV
C-H	4.3
C-C	3.6
C-O	3.7
N-H	4.0
O-H	4.7
C=C	6.3
C-N	3.5

(a)

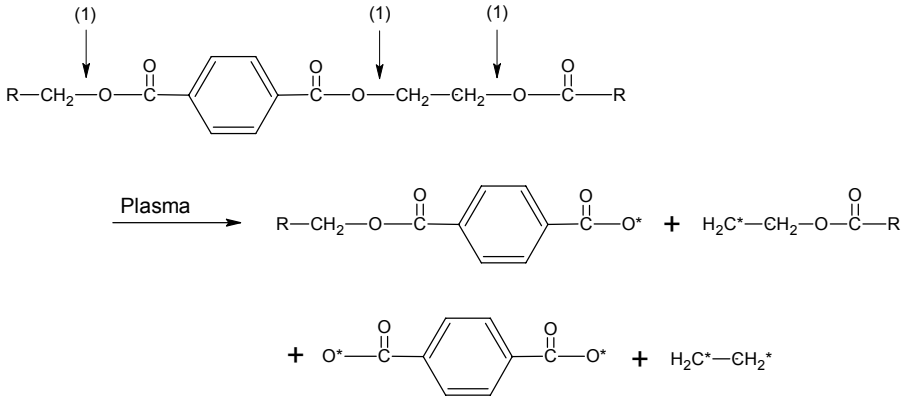

Figure 10. Chain Scission Processes and Derivatives in PET Molecules by Helium Containing Plasma Treatment [7,8,10]: (a) Position 1, (b) Position 2, (c) Position 3, and (d) Position 6 - Continued

(b)

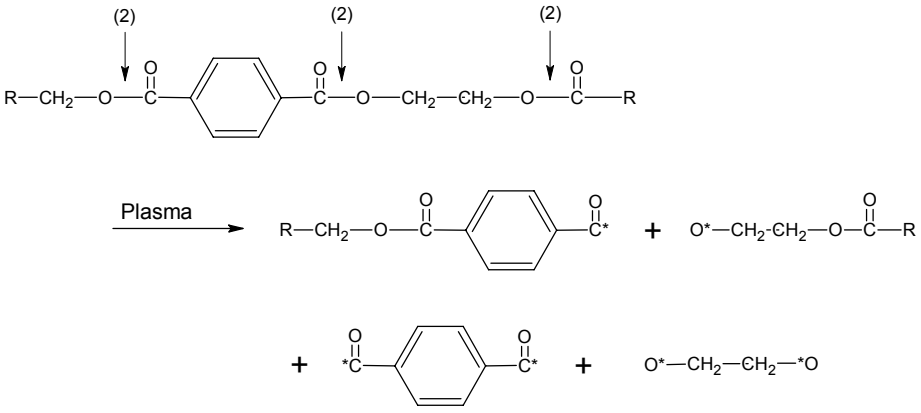

(c)

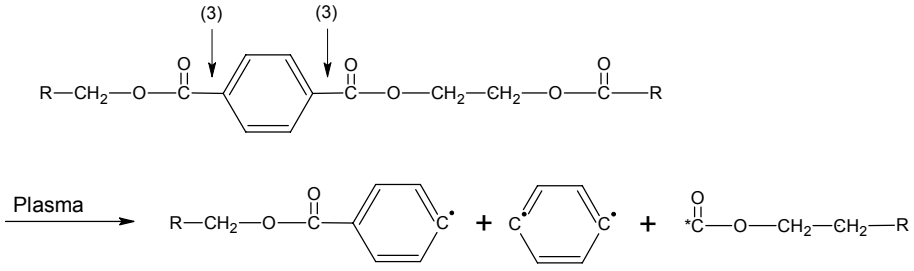

(d)

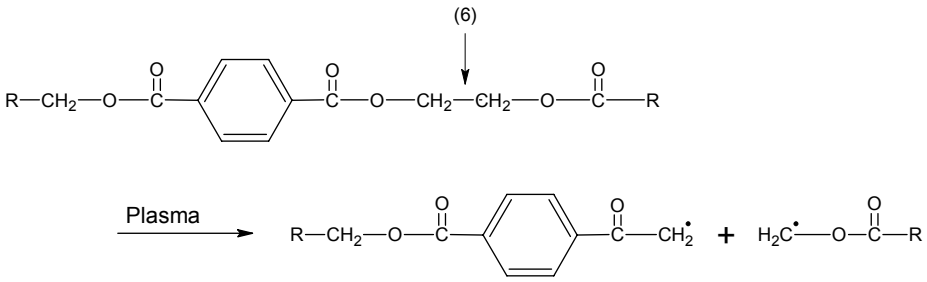

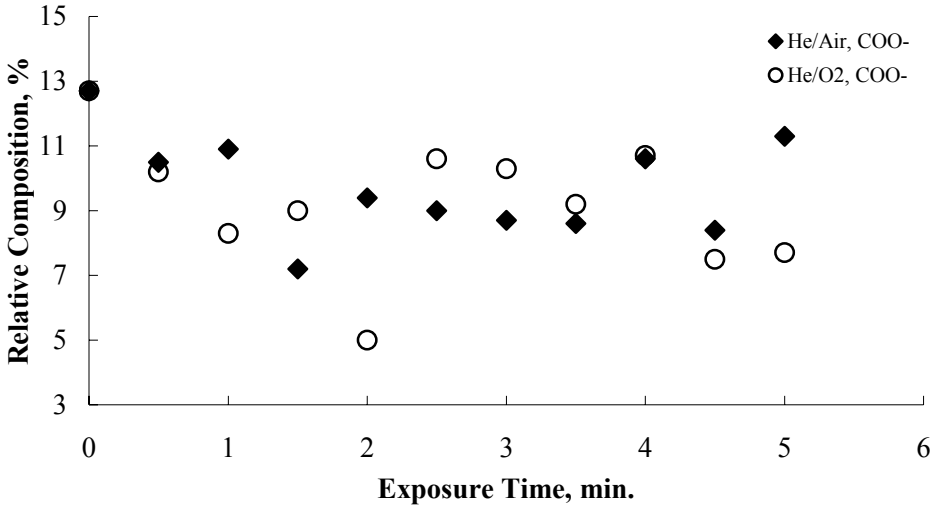

Figure 11. –COOH Group in C_{1s} Deconvolution Analysis of Plasma Treated PET Films

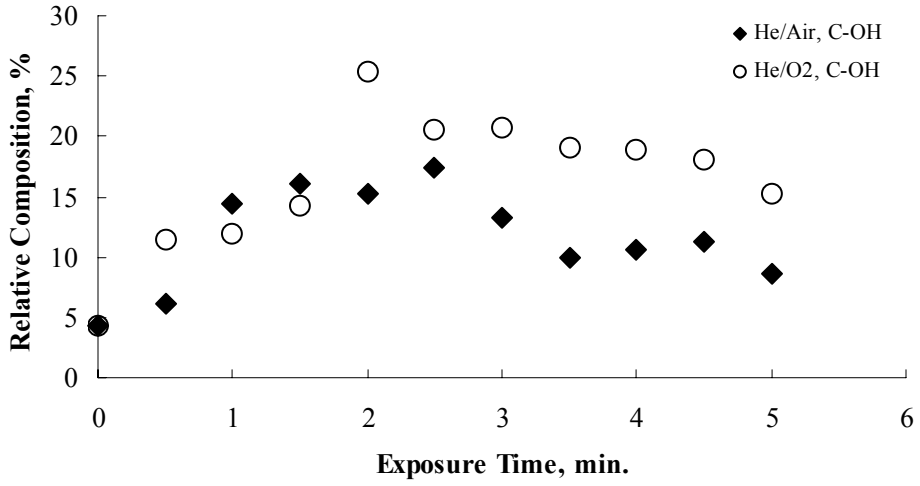

Figure 12. –C-OH Group in C_{1s} Deconvolution Analysis of Plasma Treated PET Films

(a)

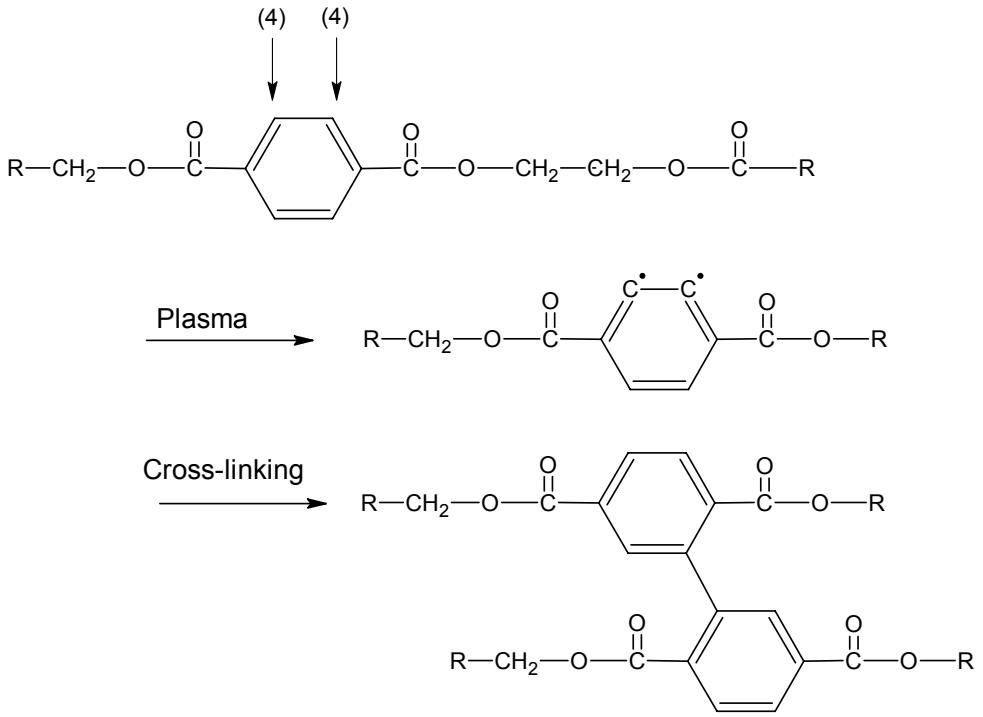

(b)

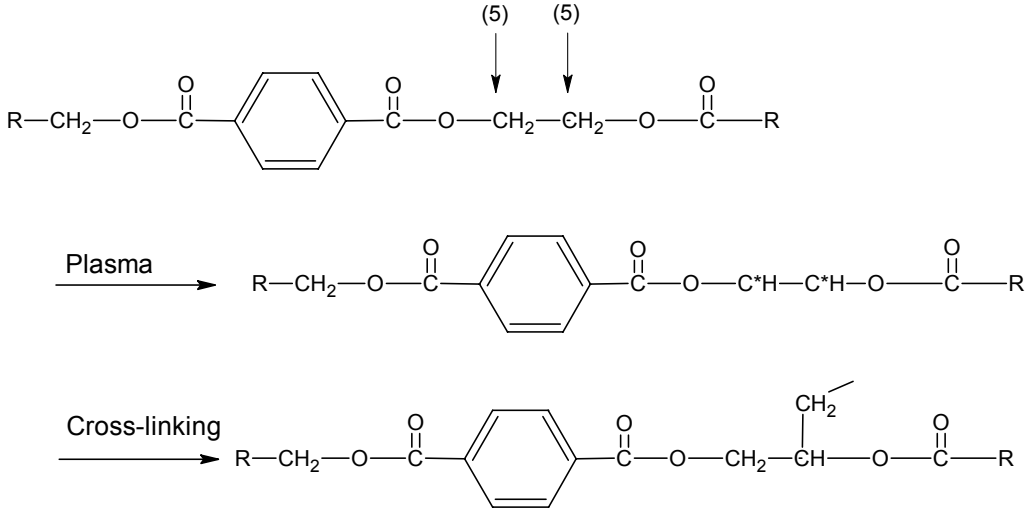

Figure 13. Possible Cross-linking Positions in PET Molecules by He Containing Plasma [7,10]: (a) Recombination between Benzene Rings and (b) Combination with other chains

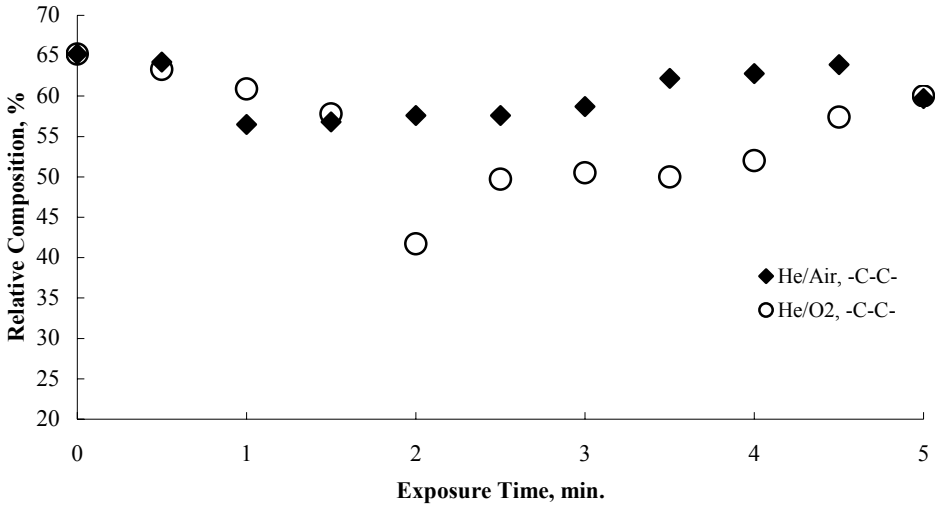

Figure 14. –C-C Bond in C_{1s} Deconvolution Analysis of Plasma Treated PET Films

6. Conclusion

In this study, XPS and AFM results revealed that the properties of the surface were changed in terms of roughness, chemical composition, cross-linking and re-deposition. Thus, it is expected that the surface condition could be changed during plasma treatment, and surface etching process could also be affected. In this study, only re-deposition behavior is considered to explain weight loss trend along exposure time. In plasma treatment, the density of etched particles coming from substrate surface would increase in plasma bulk over the maximum plasma exposure time. Thus, re-deposition increases with an increment of exposure time and density of active particles by breaking off on the substrate surface.

In atmospheric pressure plasma treatment of PET film, weight loss (%) results showed a different trend in closed ventilation condition. For commercial applications, plasma

exposure time should be minimized and the effect of plasma should be maximized. The maximum wettability change can be obtained within 1 min. exposure time for both He/air and HeO_2 plasmas. From XPS analysis, it is apparent that cross-linking and deposition take place concurrently. The increment of C-C bonds is due to new C-C bond construction resulting in cross-linking between benzene rings presumably caused by UV radiation during plasma treatment. The cross-linking is inevitable because the atmospheric plasma system employed in this study uses He gas as an initiator to generate the plasma. Surface roughness changes induced by etching were evident after plasma treatment. Re-deposition may either increase or decrease surface roughness, and also affect functional group generation. The $–CH_2-CH_2-$ segment of the PET chain may be broken down and converted into a $•CH_2-CH_2•$ radical or $CH_2=CH_2$ gas, which is then able to react with radicals on the PET molecule.

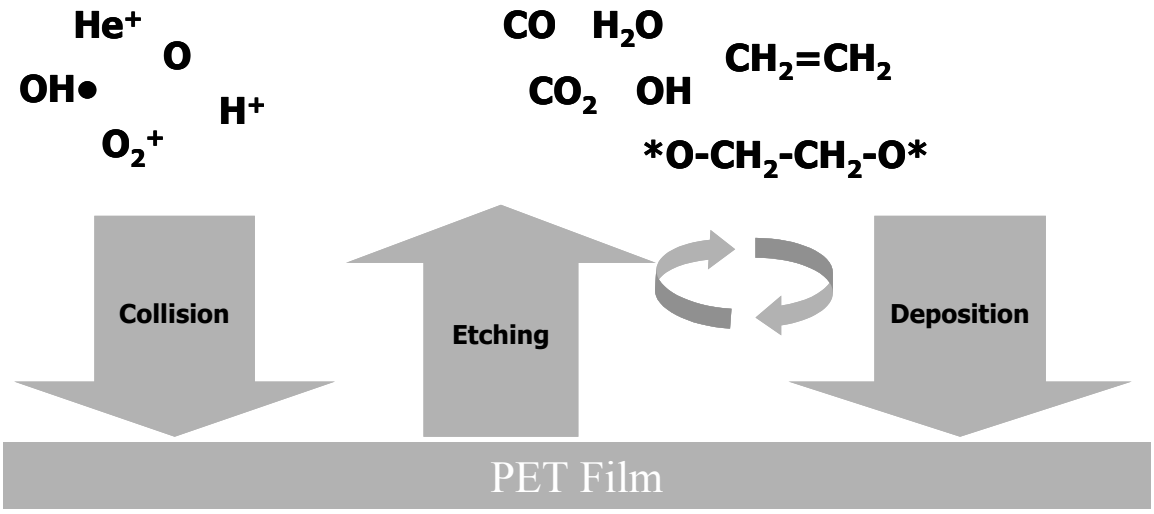

Figure 15. Mechanism of Re-deposition by Etched Species

Acknowledgement

Financial support for the project is given by the National Textile Center and North Carolina State University.

7. References

(1) M. Lieberman and A. Lichtenberg. *Principles of Plasma Discharges and Materials Processing*, John Wiley & Sons, New York, 1994

(2) J. Roth. *Industrial Plasma Engineering*, Vol. 1: Principles, Institute of Physics Publishing, Bristol, UK (1995), and *Industrial Plasma Engineering* Vol. 2: Application to Nonthermal Plasma Processing, Institute of Physics Publishing, Bristol, UK, 2001

(3) M. Shenton, M. Lovell-Hoare and G. Steven. Adhesion Enhancement of Polymer Surfaces by Atmospheric Plasma Treatment. *Journal of Physics D-Applied Physics*, 34: 2754-2760, 2001

(4) M. Shenton and G. Steven. Surface Modification of Polymer Surface: Atmospsheric Plasma versus Vacuum Plasma Treatments. *Journal of Physics D-Applied Physics*, 34: 2761-2768, 2001

(5) E. Selli, G. Mazzone, C. Oliva, F. Martini, C. Riccardi, R. Barni, B. Marcandalli and M. Massafra. Characterisation of Poly(ethylene terephthalate) and Cotton Fibres after Cold SF_6 Plasma Treatment. *Journal of Materials Chemistry*, 11: 1985-1991, 2001

(6) B. Gupta, J. Hilborn, C. Hollenstein, J. Plummer, R. Houriet and N. Xanthopoulos. Surface Modification of Polyester Films by RF Plasma. *Journal of Applied Polymer Science*, 78: 1083-1091, 2000

(7) S. Weidner, G. Kühn, R. Decker, D. Roessner and J. Friedrich. Influence of Plasma Treatment on the Molar Mass of Poly(ethylene terephthalate) Investigated by Different Chromatographic and Spectroscopic Methods. *Journal of Polymer Science Part A-Polymer Chemistry*, 36: 1639-1648, 1998

(8) M. Gheorghiu, F. Arefi, J. Amouroux, G. Placinta, G. Popa and M. Tatoulian. Surface Cross Linking and Functionalization of Poly(ethylene terephthalate) in a Helium Discharge. *Plasma Sources Science and Technology*, 6: 8-19, 1997

(9) D. Clark and A. Dilks. ESCA Applied to Polymers. XXIII. RF Glow Discharge Modification of Polymers in Pure Oxygen and Helium-Oxygen Mixture. *Journal of Polymer Science Part A-Polymer Chemistry*, 17: 957-976, 1979

(10) G. Placinta, F. Arefi-khonsari, M. Gheorghiu, J. Amouroux and G. Popa. Surface Properties and the Stability of Poly(ethylene Terephthalate) Films Treated in Plasmas in Helium-Oxygen Mixture. *Journal of Applied Polymer Science*, 66: 1367-1375, 1997

(11) A. Hollander, R. Wilken and J. Behnisch. Subsurface Chemistry in the Plasma Treatment of Polymers. *Surface and Coatings Technology*, 116-119: 788-791, 1999

(12) R. Gardri, J. Roth, T. Monti, K. Kelly-Wintenberg, P. Tsai, D. Helfritch, P. Feldman, D. Sherman, F. Karakaya and Z. Chen. Sterilization and Plasma Processing of Room Temperature Surfaces with a One Atmosphere Uniform Glow Discharge Plasma (OAUGDP). *Surface and Coatings Technology*, 131: 528-542, 2000

(13) A. Kruse, G. Kruger, A. Baalmann and O. Hennemann. Surface pretreatment of plastics for adhesive bonding. *Journal of Adhesion Science and Technology*, 9: 1611-1621, 1995

(14) M. Shenton, G. Steven, N. Wright and X. Duan. Chemical-Surface Modification of Polymers Using Atmospheric Pressure Nonequilibrium Plasmas and Comparisons with Vacuum Plasmas. *Journal of Polymer Science Part A-Polymer Chemistry*, 40: 95-109, 2002

(15) M. McCord, Y. Hwang, P. Hauser, Y. Qiu, J. Cuomo, O. Hankins and M. Bourham and L. Canup. Modifying Nylon and Polypropylene Fabrics with Atmospheric Pressure Plasma. *Textile Research Journal*, 72(6): 491-498, 2002

(16) M. Riekerink, J. Terlingen, H. Engbers and J. Feijen. Selective Etching of Semicrystalline Polymers: CF_4 Gas Plasma Treatment of Poly(ethylene). *Langmuir*, 15: 4847-4856, 1999

(17) S. Herbert, D. Shinozaki and R. Collactott. Fine-scale Morphology of Ultraviolet-ozone Etched Polyethylene. *Journal of Materials Science*, 31(17): 4655-4661, 1996

(18) R. Chen, V. Gorelik and M. Silverstein. Plasma Polymerization of Hexafluoropropylene: Film Deposition and Structure. *Journal of Applied Polymer Science*, 56: 615-623, 1995

(19) K. Donohoe and T. Wydeven. Plasma Polymerization of Ethylene in an Atmospheric Pressure-Pulsed Discharge. *Journal of Applied Polymer Science*, 23: 2591-2601,1979

(20) A. Buchman, H. Dodiuk, M. Rotel and J. Zahavi. *Polymer Surface and Interfaces: Characterization, Modification and Application*, 37-69, 1997 (K. Mittal and K.Lee (Edition))

V. EFFECTS OF ATMOSPHERIC PRESSURE HELIUM/AIR PLASMA TREATMENT ON ADHESION AND MECHNICAL PROPERTIES OF ARAMID FIBERS[1]

1. Abstract

In order to investigate the effect of atmospheric pressure plasmas on adhesion between aramid fibers and epoxy, aramid fibers were treated with atmospheric pressure helium/air for 15, 30 and 60 seconds on a capacitively-coupled device at a frequency of 5.0 kHz and He outlet pressure of 3.43kPa. SEM analysis at 10,000 × magnification showed that no significant surface morphological change resulted from the plasma treatments. XPS analysis showed a decrease in carbon content and an increase in oxygen content. Deconvolution analysis of C_{1s}, N_{1s} and O_{1s} peaks showed an increase in surface hydroxyl groups that can interact with epoxy resin. The microbond test showed that the plasma treatment for 60 seconds increased interfacial shear strength by 109% over that of the control (untreated). The atmospheric pressure plasma increased single fiber tensile strength by 16 – 26 %.

Key words:

Atmospheric pressure plasma, Interfacial shear strength, Fiber/matrix interface, Aramid fibers

[1] Effects of Atmospheric Pressure Helium/Air Plasma Treatment on Adhesion and Mechanical Properties of Aramid Fibers, Journal of Adhesion Science and Technology (2003), In Press

2. Introduction

Low-pressure plasma (low temperature) treatments have been extensively used in research and industry for modification of fiber surfaces [1-4]. These treatments are applied for surface modifications such as micro-roughness (ablation and etching), introduction of new chemical functional groups, polymerization (cross-linking), and coating (deposition). Although low-pressure plasma treatments are highly effective, it is necessary to carry them out under a low pressure or a high vacuum. Therefore, for processing of most materials, a low pressure plasma treatment is likely to be a batch process, which is time and energy consuming and, therefore, may not be cost-effective for many applications.

On the other hand, atmospheric pressure plasmas can treat materials continuously at a temperature no higher than 40ºC without a vacuum system. A carrier gas such as helium is frequently used to initiate the plasma. The treatment gases are subsequently introduced into the plasma zone. Atmospheric pressure plasma is more difficult to control than low-pressure plasmas because an unknown quantity of air, mixed with the carrier and the treatment gases, could induce complex interactions, which may influence the effectiveness of the treatment.

In our previous studies, we found that ultra-high modulus polyethylene (UHMPE) fibers treated by He/air and He/O_2/air atmospheric pressure plasmas showed a significant increase in interfacial shear strength with epoxy [5,6]. It was found that the surface chemical composition of the UHMPE fibers was altered by both He/air and He/O_2/air plasma treatments significantly. Tensile strength of the fibers was not affected by He/air plasma treatment but for the He/O_2/air treated group it was reduced due to development of micro-cracks on the surface of the fibers.

Aramid or poly *p*-phenylene terephthalamide (PPTA) fibers have high tensile strength and tensile modulus, high thermal resistance, and low density. However, aramid fibers have poor interfacial bonding with most of the commercially available resins used in composites. These limitations lead to poor out-of-plane (off-axial) strength of the composites. In order to enhance the aramid/matrix interfacial strength, various fiber surface modification techniques have been investigated such as bromine treatment [7], deposition of coatings [8], chemical modifications [9-11], plasma-aided grafting [12-15] and low-pressure plasma treatments [16-22]. Although all these methods for surface modification increased aramid/matrix interfacial strength, they often had negative effects on tensile strength of aramid fibers [18-20]. Low-pressure plasma treatments using various gases (NH_3, H_2O, O_2, Air, Ar and Ar/NH_3) can greatly improve the interfacial strength between aramid and epoxy resin by not only generating possible reactive chemical groups, such as –COOH, -OH, and -NH_2, but also by roughening fiber surfaces . In addition, cross-linking of molecules on the surface of aramid fibers occurs after low-pressure oxygen plasma treatment [18,21].

Little has been reported in literature on the effect of atmospheric pressure plasma on aramid fiber with regard to improving interfacial bonding of the fiber to any matrix in composites. Helium is one of the most frequently used carrier gases in atmospheric pressure plasma and, therefore, its effect on the surface of any fiber is important for setting up a baseline for atmospheric pressure plasma treatments using various treatment gases. This study was designed to investigate the effect of atmospheric pressure He/air plasma on aramid fiber surface morphology, tensile strength, surface chemical composition and interfacial bond strength of the fiber to epoxy resin. Based on the results of X-ray Photoelectron Spectroscopy

(XPS) analysis, potential interactions between atmospheric pressure plasma and PPTA molecules are discussed.

3. Experimental

3.1. Plasma Treatment

Kevlar® 49 fibers were employed in the experiment. To eliminate finishes and surface contamination, the fibers were washed for 5 min with acetone, and then stored in a vacuum oven for 12 hours to remove the remaining acetone in the fiber. The atmospheric pressure plasma treatments were carried out in a capacitively-coupled device. This device operates at low-frequencies (audible) between 1 and 12 kHz. The plates were located in a closed but not sealed plexiglass chamber and, therefore, the pressure inside the chamber was the same as atmospheric pressure (10^5 Pa). In this study, the frequency was set at 5.0 kHz and the outlet pressure of He was maintained at 3.43 kPa. The temperature of the electrons in the plasma was 3.56 eV (1 eV = 11604K), although the overall temperature of the plasma was lower than 40°C. The average density of the electrons was $8.03\times10^{13}/m^3$ for all treatments. The power density was $5.382 kW/m^2$. During the treatment, samples were placed between the two electrodes. The fibers were treated for 15, 30 and 60 seconds in He/air plasma. After the treatment, the fibers were immediately placed into a clean Ziploc® plastic bag which was sealed to minimize potential contamination.

3.2. Sample Preparation for Microbond Test

Immediately after the plasma treatment, microbond samples were prepared on a frame as described in [25] with DER 331 and DER 732 (bisphenol-A type epoxy) provided by Dow

Chemical in a ratio of 70:30, and 12 phr (parts per a hundred resin parts) of hardener DEH 26. After placing the beads on the fibers, the samples were cured for 3 hours at 80°C and post-cured for 2 hours at 100°C.

3.3. Microscopic Examination

The diameters of the fibers, the lengths of the epoxy beads, and the contact angle between epoxy and the fiber were measured from digital images of the fibers and the beads taken with an Anti-Mould Nikon Labophot2-POL polarized light microscope equipped with a Kodak MDS 290 digital photomicrography system. The surfaces of the fibers were examined using a HITACHI S-3200N Scanning Electron Microscope at 10,000× magnification.

3.4. XPS Analysis

The chemical composition of the fiber surfaces was analyzed with a Perkin Elmer PHI 5400 XPS spectrometer. The x-ray source was Mg, and the take-off angle was 45°. The pressure in the XPS chamber was between 10^{-9} and 10^{-10} torr. The data acquisition was carried out with an RBD Enterprises Model 147 Controlling System.

3.5. Interfacial Bond Strength Test and Single Fiber Tensile Test

The microbond test was performed at a crosshead speed of 1 mm/min on a Sintech universal-testing machine with a load cell of 0.5 N capacity. Fiber tensile test was carried out at a gauge length of 5 cm and a strain rate of 0.05/min using the same test machine with a load cell of 25 N capacity. The test was carried out at 20°C and 65% relative humidity.

3.6. Statistical Analysis

One-way analysis of variance (ANOVA) and Fisher's pair-wise multiple comparison were used to compare the interfacial shear strengths and tensile strengths of the fibers among different treatment groups. A P-value less than 0.05 was considered significant.

4. Results and Discussion

4.1. Microscopy Examination

Figure 1 shows the SEM micrographs of surfaces of aramid fibers untreated and treated by He/air atmospheric pressure plasma. Both the control sample and plasma treated samples show smooth surfaces. Therefore, no surface morphology change can be observed after plasma treatment at the magnification used. This is consistent with what has been reported in the literature when He/air and He/O_2/air atmospheric pressure plasma treatments were applied to nylon 66 fibers [26]. However, UHMPE fibers treated with He/air and He/O_2/air atmospheric pressure plasmas showed rougher surfaces [5,6]. Aramid fibers have high crystallinity and more stable molecular structure and, therefore, may not be as susceptible to etching by atmospheric pressure plasma as UHMPE fibers.

4.2. XPS Analysis

Plasma treatment of aramid fibers has been reported to introduce new functional groups that could interact chemically with epoxy resin as shown in Figure 2 [11,12]. XPS analysis results on chemical composition change on the aramid fiber surface are shown in Table 1. Based on the PPTA molecular structure, both O/C and N/C should be 0.143 (1/7).

However, these ratios for the untreated aramid fiber are higher than the theoretical value. This could be due either to finishing agents remaining on the fiber or contamination.

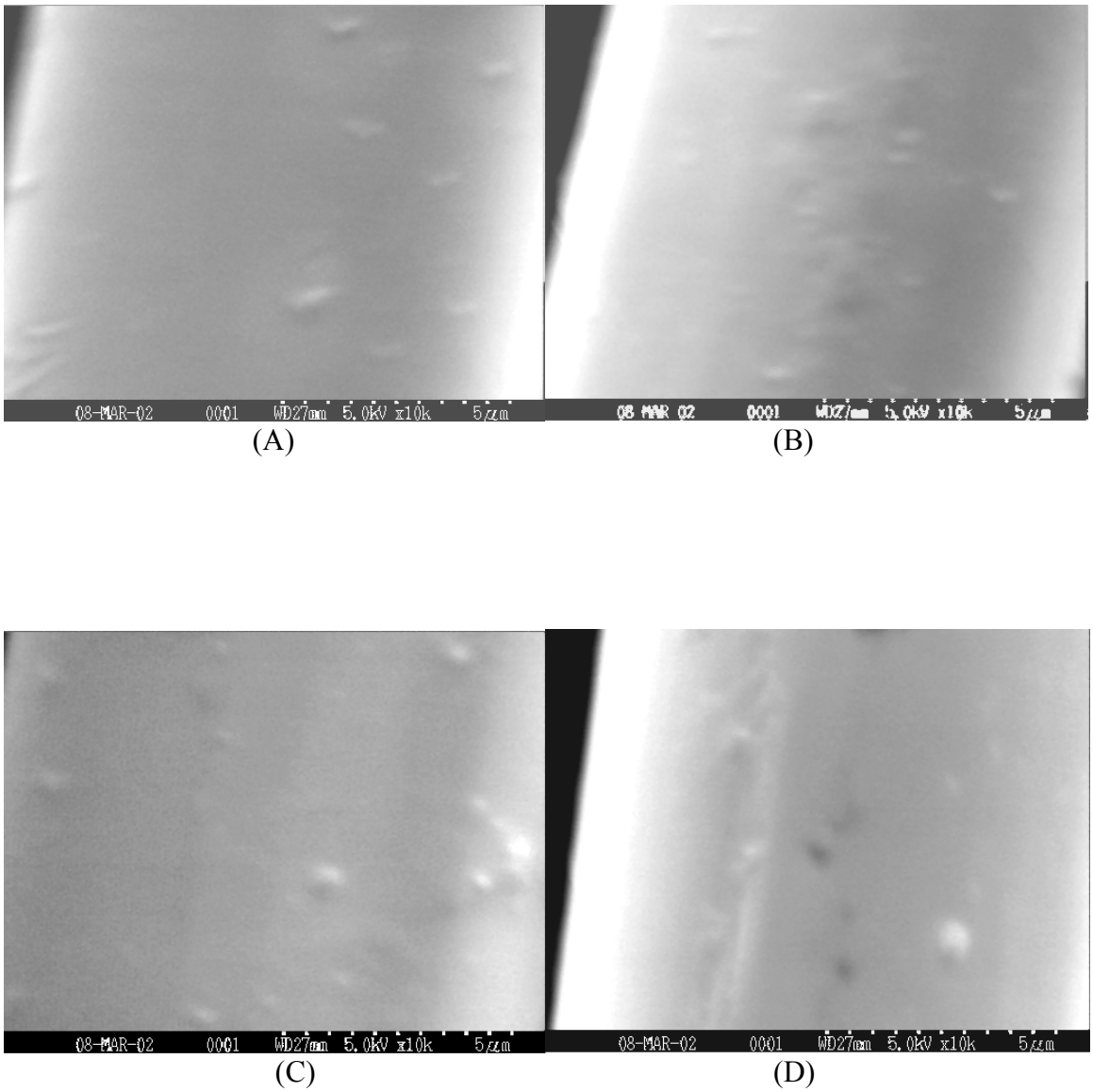

(A) (B)

(C) (D)

Figure 1. SEM Micrographs of Aramid Fiber Surfaces: (A) untreated, (B) He/Air-15 sec, (C) He/Air -30 sec (D) He/Air-60 sec.

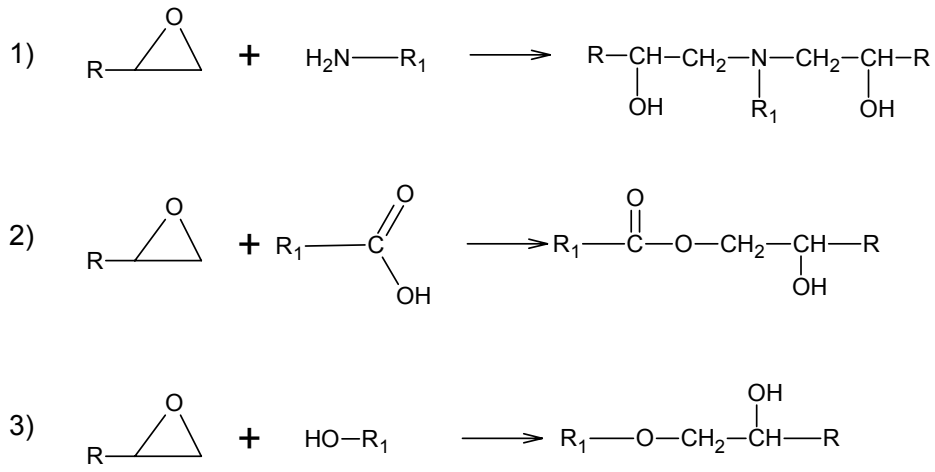

Figure 2. Possible Chemical Interactions of Epoxy Resin with the Plasma Treated Aramid Fiber Surface.

Table 1. Relative Chemical Composition and Atomic Ratios Determined by XPS for Aramid Fibers Untreated and Treated with Atmospheric Pressure Plasmas

Treatment	Chemical Composition, %			Atomic Ratio, %		
	C_{1s}	O_{1s}	N_{1s}	O/C	N/C	(O+N)/C
Control	89.5	7.6	2.9	8.5	3.2	11.7
He/Air 15 sec.	88.0	9.1	2.9	10.3	3.3	13.6
He/Air 30 sec.	87.5	8.1	4.4	9.3	5.0	14.3
He/Air 60 sec.	87.3	7.6	5.1	8.7	5.8	14.5

After He/air atmospheric pressure plasma treatments, the O/C and N/C ratios are either increased or unchanged as shown in Table 1. The N/C ratios for the plasma treatment groups are lower than the theoretical ratio of PPTA molecules, indicating a disruption of surface molecular structure due to chain scission and cross-linking. In order to examine the chemical interactions during the plasma treatment, the deconvolution analysis of C_{1s}, N_{1s}, and O_{1s} peaks was performed (Tables 2-4). The aramid fiber surface after treatments has five potential carbon-containing components with binding energies of 285.0 eV (-C-**C**-C-), 286.3 eV (-C-**C**-N/-**C**-O-), 287.8 eV (-**C**ONH-), 288.3 eV (-**C**=O) and 289.1 eV (-**C**OO-) [12,27,28]. In addition, four potential oxygen-containing components exist in the aramid molecule with binding energies of 531.6 eV (-C**O**NH-), 532.8 eV (**O**=C-OH), 533.7 eV (-C-**O**H) and 534.3 eV (O=C-**O**H) [12,27]. The N_{1s} has two potential deconvoluted peaks with binding energies of 400.3 eV (-CO**N**H-) and 401.4 eV (-**N**H_2) [12,27].

Table 2 presents the results of C_{1s} peak deconvolution analysis that show a distinct change of functional groups on aramid fiber surface after plasma treatment. The peak areas of -C-**C**-C- and -**C**ONH- decreased after plasma treatment while those of -C-**C**-N/-**C**-O-, -**C**=O and -**C**OO- increased. N_{1s} peak deconvolution analysis (Table 3) showed that the peak areas of –CO**N**H- group decreased and that of Ph–**N**H_2 group increased after plasma treatments. In O_{1s} peak deconvolution analysis (Table 4), the peak areas of **O**=C-OH, -C-**O**H and –CO**O**- increased while that of –C**O**NH decreased. All deconvolution analyses showed that the plasma treatments reduced the number of amide groups while augmented other oxygen related bonds.

Table 2. Results of Deconvolution of C_{1s} Peaks for Aramid Fibers Untreated and Treated with Atmospheric Pressure Plasmas

Treatment	Relative Area Corresponding to Different Chemical Bonds, %				
	-C-C-	-C-C-N/-C-O-	-CONH-	-C=O	-COO-
Control	74.9	13.1	11.3	0.5	0.2
He/Air, 15 sec.	73.1	19.0	4.8	1.3	1.8
He/Air, 30 sec.	63.5	27.0	3.4	2.6	3.5
He/Air, 60 sec.	65.5	25.0	2.3	3.6	3.6

Table 3. Results of Deconvolution of N_{1s} Peaks for Aramid Fibers Untreated and Treated with Atmospheric Pressure Plasmas

Treatment	Relative Area Corresponding to Different Chemical Bonds, %	
	-CO<u>N</u>H-	Ph-<u>N</u>H_2
Control	91.1	8.9
He/Air, 15 sec.	83.9	16.1
He/Air, 30 sec.	81.6	18.4
He/Air, 60 sec.	80.3	19.7

Table 4. Results of Deconvolution of O_{1s} peaks for Aramid Fibers Untreated and Treated with Atmospheric Pressure Plasmas

Treatment	Relative Area Corresponding to Different Chemical Bonds, %			
	-CONH-	-C=O/O=C-OH	-C-OH	-COO-
Control	57.7	30.0	9.7	2.6
He/Air, 15 sec.	49.1	33.5	11.7	5.7
He/Air, 30 sec.	47.4	34.1	12.3	6.1
He/Air, 60 sec.	42.7	34.8	14.5	8.0

According to the PPTA molecular structure, possible chemical interactions could occur at four positions as shown in Figure 3 [12,22,28]. Figure 4 shows possible interactions for –OH groups in PPTA molecules. The free radicals could be generated by photons (UV-radiation) at position 1, and chain scission and radical formation could be induced simultaneously at position 3. The –OH groups can be produced by interactions with OH• radicals in the plasma. Figure 5 explains the reduction of –CONH- groups by plasma treatment and formation of new functional groups. Due to the interaction between PPTA molecules and photons in the plasma, the chain scission could occur at position 2 [22,28]. The chemical interactions of PPTA molecules with active species in the plasma bulk (OH•, H•, CO, excited molecular oxygen $O_2(1\Delta g)$ and $O_2(1\Sigma g)$, and oxygen atom) generate –COOH and -NH_2 groups at chain ends. These mechanisms are considered to be responsible for the chemical composition changes revealed by XPS deconvolution analysis (Tables 2-4).

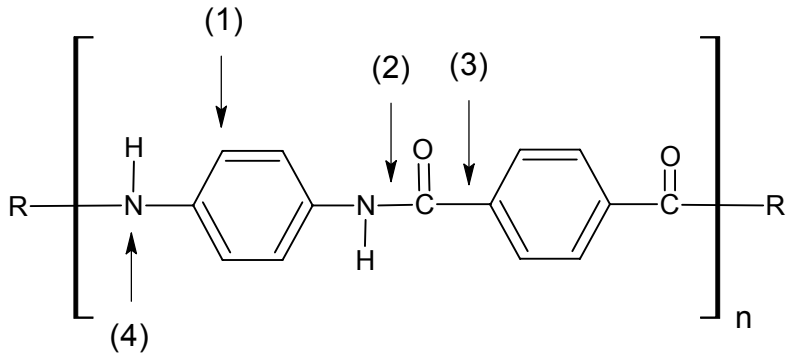

Figure 3. Potential Reaction Sites (1-4) in Kevlar Molecular Structure.

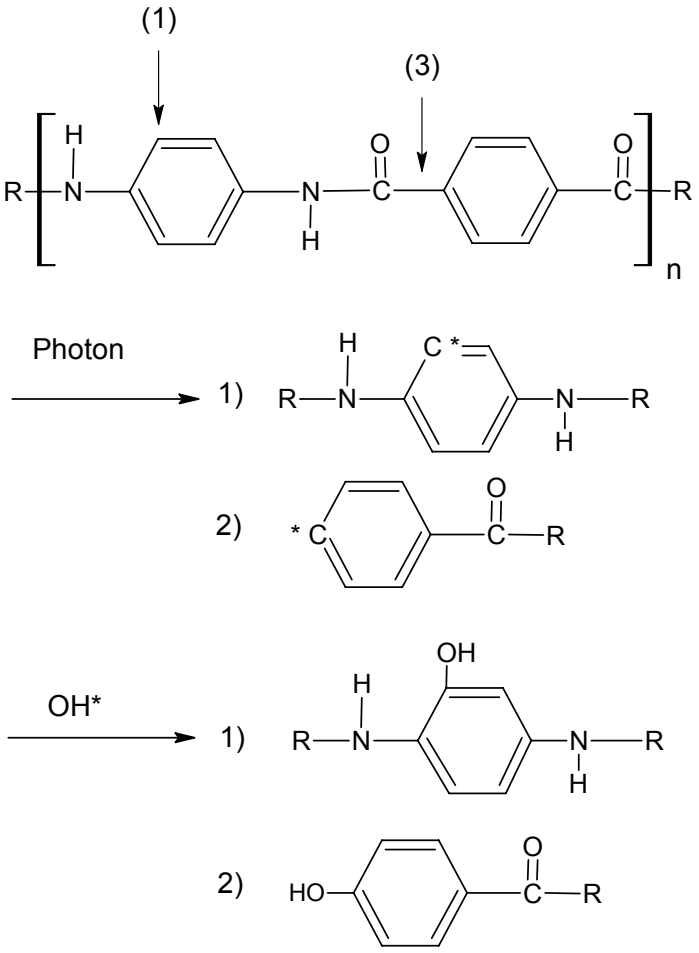

Figure 4. Possible Reaction Mechanism for –OH Group Generation at Positions 1 and 3 in Kevlar Molecular Structure

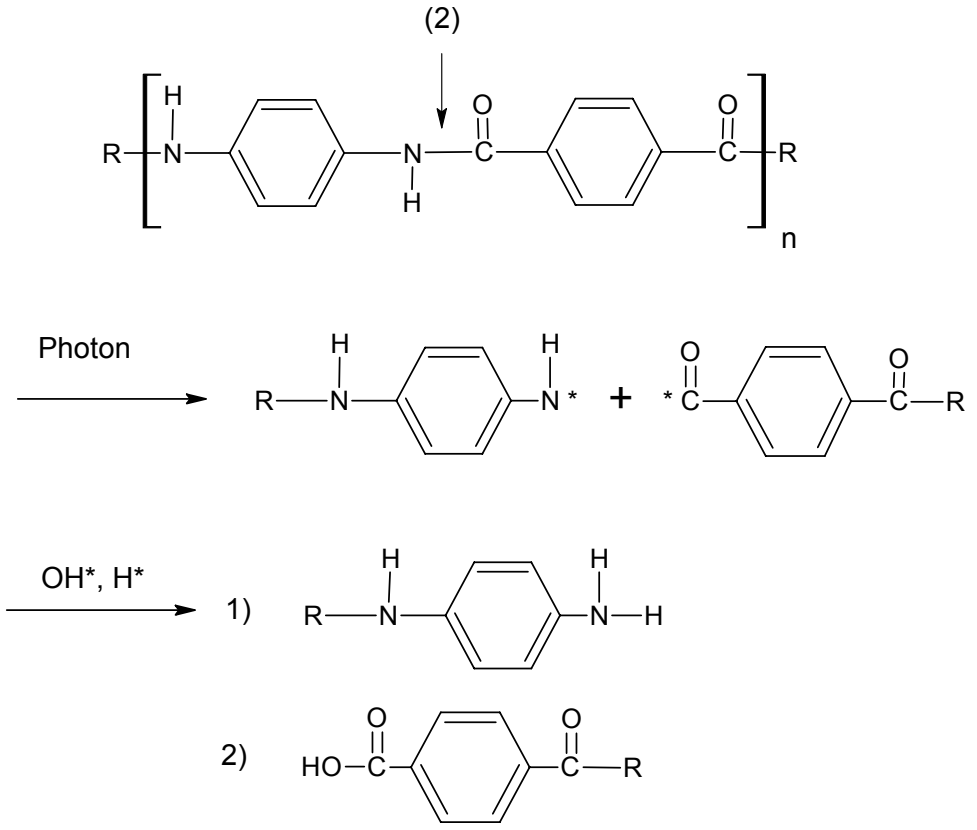

Figure 5. Possible Chain Scission and Interactions at Position 2 in Kevlar Molecular Structures

4.3 Wettability of Fibers by Epoxy

The wettability of the aramid fibers by epoxy resin was determined by the contact angle measurements between the epoxy beads and the fiber and the results are shown in Table 5. The lower the contact angle, the higher the wettability of the aramid fiber by the epoxy. The contact angles on He plasma treated samples were significantly ($P < 0.05$) lower than those of control groups, indicating an improved wettability.

Table 5. Contact Angles between Epoxy Beads and Aramid Fibers

Treatment	Contact Angle
Control	60.7
He/Air, 15 sec.	55.7
He/Air, 30 sec.	55.7
He/Air, 60 sec.	46.4

4.4. Microbond Test

Typical plot load-displacement curves for the control and 60 sec He/Air plasma treated samples in the microbond tests are shown in Figure 6. The interfacial shear strengths (IFSS) or debonding shear stresses, τ_i, for all treatment groups are presented in Table 6. The IFSS was calculated using the following equation derived from the well-known shear-lag model [29]:

$$\tau_i = \frac{nP_{\max}\coth(nL/r)}{2A} \qquad (1)$$

where P_{max} is the peak load, A is the cross-sectional area of the fiber, L is the imbedded length, r is the equivalent fiber radius calculated from the fiber cross-sectional area and n is defined as

$$n = \left[\frac{E_m}{E_f(1+\nu_m)\ln(R/r)}\right]^{1/2} \qquad (2)$$

where

E_m = 1.4 GPa is the Young's modulus of the matrix reported in [30],

ν_m = 0.4 is the Poisson's ratio of the matrix measured in our laboratory,

E_f = 130 GPa is the tensile modulus of the fiber [29],

R = the radius of the epoxy beads observed under microscope, and

r is the apparent radius of the fiber calculated from fiber cross section micrographs.

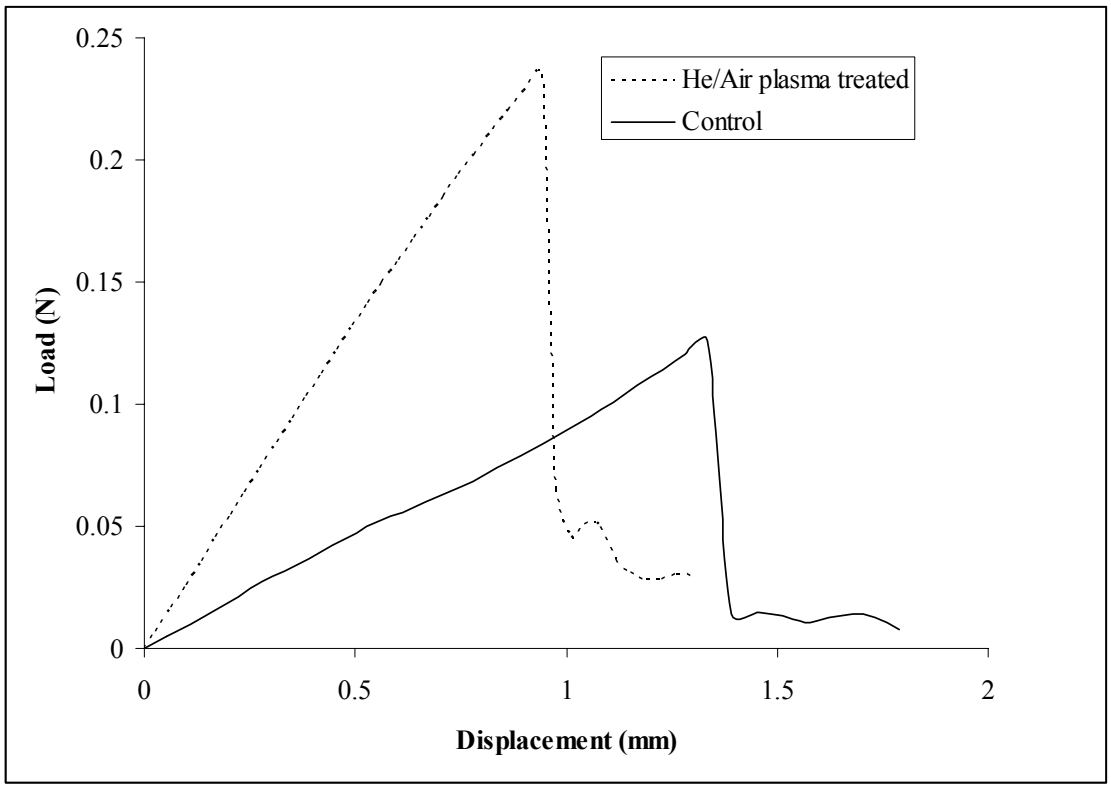

Figure 6. Typical Load-Displacement Curves for the Control and 60-seconds He/Air Plasma Treated Samples in the Microbond Test.

For comparison purpose, also presented in Table 6 is the average IFSS over the length of the fiber calculated as

$$\bar{\tau}_i = \frac{P_{\max}}{S_f L} \qquad (3)$$

where S_f is the circumference length of the fiber. The average IFSS indeed decreased with the increase of imbedded length.

Table 6. Interfacial Shear Strength Data

Treatment	Number of specimens	IFSS (MPa)			
		Shear-lag model		Average over the imbedded length	
		Mean	Standard deviation	Mean	Standard deviation
Control	16	16.58	16.22	9.92	10.08
He/Air 15 sec.	28	30.64	18.51	12.78	9.21
He/Air 30 sec.	19	24.00	20.33	12.58	11.62
He/Air 60 sec.	20	34.62	19.29	17.74	9.49

The 60 sec He/air atmospheric plasma treated group showed a 109 % higher IFSS ($P < 0.05$) than those of the control group (Table 6). No statistically significant difference was observed between the control and the 15 and 30 sec plasma treated groups although the IFSS for the plasma treated groups tends to be higher than the control group. Compared with the

IFSS values of aramid fibers by low-pressure air [18] and O_2 [20] plasmas reported in the literature, the IFSS increased more in the atmospheric pressure plasmas treatments. Plasma treatments can increase the IFSS by creating micro-roughness and introducing functional groups on the fiber surface. The micro-roughness on the fiber surface by the ablation effect of the plasma increases the surface area leading to the increase of friction force and mechanical keying. The chemical change on the fiber surface increases potential bonding sites with the epoxy as well as hydrophilicity of the fiber, leading to a better wetting of the fiber by the epoxy. In this study, SEM micrographs at 10,000 × magnification did not show significant surface morphology change on aramid fiber surfaces after plasma treatments (Figure 1). However, XPS results showed that atmospheric pressure plasma treatments introduced functional groups that not only improve hydrophilicity of the fiber surface but also form covalent bonds with epoxy resin, resulting in an increased IFSS.

4.5. Single Fiber Tensile Strength

The tensile strength of the aramid fiber increased by 15.7 to 26.1 % ($P < 0.05$) by He/air plasma treatment (Table 7). Generally, fiber tensile strength is reduced due to ablation or etching effect of plasma treatments. Kupper and Schwartz [31] reported that aramid fiber strength was not affected by RF low pressure Ar, N_2, and CO_2 plasmas. Sheu and Shyu [20] found that low pressure NH_3, O_2 or H_2O plasmas reduced only slightly the tensile strength of aramid fibers (less than 10%). In our experiment, we found that the strength of nylon fabric was increased slightly by atmospheric pressure He/Air plasma treatment [26].

Table 7. Single Aramid Fiber Tensile Strength

Treatment	Number of specimens	Tensile strength (GPa)		
		Mean	Standard Deviation	Increase from control (%)
Control	19	2.99	0.59	-
He/Air 15 sec.	19	3.77	0.99	26.1
He/Air 30 sec.	20	3.46	1.24	15.7
He/Air 60 sec.	20	3.77	0.67	26.1

There was no significant etching observed among all the plasma treated groups and, therefore, no such negative effect on fiber tensile strength should be expected here. The etching effect of atmospheric pressure plasma is not nearly as aggressive as that of a low pressure plasma because the activated particles in an atmospheric pressure plasma cannot be accelerated as much as in a low pressure plasma. This is due to higher probability of inelastic collisions of the particles with non-active particles existing in atmospheric plasmas. In addition, He molecules are small compared to Ar molecules used in Kupper and Schwartz's study and thus have a considerably milder etching effect.

Aramid fibers are known to be composed of fibrils or microfibers in its micro-structure. The bonding between these fibrils is rather weak, which makes the fibers susceptible to damage due to external abrasion as well as causes low compression strength. The weak inter-fibril bonds also limit the degree of improvement in aramid/matrix interfacial

bond strength since the fibrils on surface of the fiber can be peeled away before the fiber/matrix interface fails [32,33]. To improve interfibril bond strength, Mathur and Netravali [34] used epoxy and bismaleimide to infiltrate the interfibril space of aramid fibers after swelling the fibers with concentrated sulfuric acid. They also increased interfibrillar adhesion of aramid fibers using a low pressure NH_3 plasma. They reported that both the fiber tensile and compression strengths were increased because the plasma treatments could potentially improve the interfibrillar adhesion or cohesion and thus improve the fiber tensile strength as well as the IFSS. This result is also consistent with the observations in our previous studies on other fibers [5,26] in which the tensile strengths of UHMPE fibers and nylon fabrics increased under certain conditions of He/air plasma treatment. It is obvious that the mechanism of how atmospheric pressure plasmas alter aramid fiber mechanical properties needs to be studied further.

Helium is the most efficient inert gas for cross-linking on polymer surfaces compared with Ar which has bigger molecular size and thus may have greater degradation effect [35,36]. During the He/air plasma treatment, an intense ultraviolet radiation is emitted, which induces cross-linking reaction on the surface of the fibrils. Potential cross-linking mechanisms on PPTA surfaces have been proposed [22,35-37].

5. Conclusion

The effects of atmospheric pressure He/air plasma treatment of aramid fibers were investigated. No obvious surface morphology change was observed at 10,000 × magnification after the plasma treatments. Oxygen atomic content and density of hydrophilic groups (-COOH, -OH and $-NH_2$) on the aramid fibers increased after He/air plasma treatment.

He/air atmospheric pressure plasma treatment for 60 seconds increased the interfacial shear strength (IFSS) of aramid fiber/epoxy matrix interface by approximately 109%. The plasma treated aramid fibers showed significantly higher single fiber tensile strength than that of the control group, which is likely due to an improved inter-fibril bond strength.

Acknowledgement

This project is sponsored by the National Textile Center and North Carolina State University.

6. References

(1) K. Mittal (Ed.). *Polymer Surface Modification: Relevance to Adhesion, Volume 2*. VSP, Utrecht, The Netherlands, 2000

(2) M. Strobel, C. Lyons and K Mittal. (Eds.) *Plasma Surface Modification of Polymers: Relevance to Adhesion*. VSP, Utrecht, The Netherlands, 1994

(3) U. Gaur and T. Davidson. Interfacial Effects of Plasma Treated Fiber Pull-out. *Material Research Society Symposium Proceedings*, 170, 309-314. 1990

(4) S. Lee, T Kang and T Yoon. Effect of Surface Area on the Interfacial Adhesion of UHMWPE Fibers. *Journal of Polymer Engineering,* 18: 49-61, 1998

(5) Y. Qiu, C. Zhang, Y. Hwang, B. Bures and M. McCord. The Effect of Atmospheric Pressure Helium Plasma Treatment on Surface and Mechanical Properties of Ultrahigh Modulus Polyethylene Fibers. *Journal of Adhesion Science and Technology*, 16(1): 99-107, 2002

(6) Y. Qiu, Y. Hwang, C. Zhang and M. McCord. The Effect of Atmospheric Pressure Oxygen-helium Plasma Treatment on Surface and Mechanical Properties of Ultrahigh Modulus Polyethylene Fibers. *Journal of Adhesion Science and Technology*, 16(4): 449-458, 2002

(7) M. Breznick, J. Banbaji, H. Guttmann and G. Marom. Surface-Treatment Technique for Aramid Fiber, *Polymer Communications*, 28: 55-56, 1987

(8) Y. Mai and F. Castino. The Debonding and Pull-out Properties of Coated Kevlar

Fibers from an Expoxy-Resin Matrix. *Journal of Materials Science Letters*, 4: 505-508, 1985

(9) T. Lin, S. Wu, J. Lai, and S. Shyu. The Effect of Chemical Treatment on Reinforcement/matrix Interaction in Kevlar-fiber/bismaleimide Composites. *Composites Science and Technology*, 60: 1873-1878, 2000

(10) S. Wu, G. Sheu and S. Shyu. Kevlar Fiber-Epoxy Adhesion and Its Effect on Composite Mechanical and Fracture Properties by Plasma and Chemical Treatment. *Journal of Applied Polymer Science*, 62, 1347-1360, 1996

(11) G. Sheu, T. Lin, S. Shyu and J. Lai. Improvement of Adhesion of Kevlar Fiber to Epoxy by Chemical Modification. *Journal of Adhesion Science and Technology*, 8: 511-530, 1994

(12) Q. Wang, S. Kaliaguine and A. Aitkadi. Catalytic Grafting-A New Technique for Polymer Fiber Composites. 1. Polyethylene-Asbestos Composites. *Journal of Applied Polymer Science*, 44: 1107-1119, 1992

(13) M. Mori, Y. Uyama and Y. Ikada. Surface Modification of Aramid Fiber by Graft-polymerization. *Polymer*, 35: 5336-5341, 1994

(14) H. Salehimobarakeh, A. Aitkadi, and J. Brisson. Improvement of Mechanical Properties of Composites through Polyamide Grafting onto Kevlar Fibers, *Polymer Engineering and Science*, 36: 778-785, 1996

(15) K. Yamada, T. Haraguchi and T. Kajiyama. Plasma-graft Polymerization of Vinyl Monomers with Reactive Groups onto a Surface of Poly(p-phenylene terephthalamide) Fiber. *Journal of Applied Polymer Science*, 60: 1847-1853, 1996

(16) G. Rallis, P. Tarantili and A. Andreopoulos. Epoxy Resin Composites with Surface Modified Aramid Fibres. *Advanced Composites Letter*, 9: 127-133, 2000

(17) B. Jang. Control of Interfacial Adhesion in Continuous Carbon and Kevlar Fiber Reinforced Polymer Composites. *Composites Science and Technology*, 44: 333-349, 1992

(18) D. Biro, G. Pleizier and Y. Deslandes. Application of the Microbond Technique. 4. Improved Fiber Matrix Adhesion by RF Plasma Treatment of Organic Fibers. *Journal of Applied Polymer Science*, 47: 883-894, 1993

(19) J. Finch, G. Poulsen and W. Pitt. Degradation of Organic Fibers in Radio-Frequency Plasma. *SAMPE Quarterly-Society for the Advancement of Material and Process Engineering*, 23: 48-53, 1992

(20) G. Sheu and S. Shyu. Surface-Properties and Interfacial Adhesion Studies of Aramid

Fiber Modified by Gas Plasma. *Composites Science and Technology*, 52: 489-497, 1994

(21) N. Inagaki, S. Tasaka and H. Kawai. Surface Modification of Aromatic Polyamide Film by Oxygen Plasma. *Journal of Polymer Science Part A-Polymer Chemistry*, 33: 2001-2011, 1995

(22) S. Wu, J. Xing, C. Zheng, G. Xu, G. Zheng and J. Xu. Plasma Modification of Aromatic Polyamide Reverse Osmosis Composite Membrane Surface. *Journal of Applied Polymer Science*, 64: 1923-1926, 1997

(23) Q. Wang, A. Aitkadi and S. Kaliaguine. Catalytic Grafting-A New Technique for Polymer Fiber Composites. 2. Plasma Treated UHMPE Fibers Polyeethylene Composites. *Journal of Applied Polymer Science*, 45: 1023-1033, 1992

(24) W. Pitt, J. Lakenan and A. Strong. The Influence of Plasma Gas Species on the Adhesion of Thermoplastic to Organic Fibers. *Journal of Applied Polymer Science*, 48: 845-856, 1993

(25) Y. Qiu, S. Deflon and P. Schwartz. Plasma Surface-Treatment of Poly(p-phenylene benzobisthiozol) Fibers. *Journal of Adhesion Science and Technology*, 7: 1041-1049, 1993

(26) M. McCord, Y. Hwang, P. Hauser, Y. Qiu, J. Cuomo, O. Hankins and M. Bourham and L. Canup. Modifying Nylon and Polypropylene Fabrics with Atmospheric Pressure Plasma. *Textile Research Journal*, 72(6): 491-498, 2002

(27) D. Clark, B. Cromarty and Dilks. ESCA Applied Polymers. 24. Theoretical Investigation of Molecular Core Binding and Relaxation Energies in a Series of Oxygen-Containing Organic-Molecules of Interest in the Study of Surface Oxidation of Polymers. *Journal of Polymer Science Part A-Polymer Chemistry*, 16: 3173-3184 (1978)

(28) N. Inagaki, S. Tasaka, H. Kawai and Y. Yamada. Surface Modification of Aromatic Polyamide Film by Remote Oxygen Plasma. *Journal of Applied Polymer Science*, 64: 831-840 (1997)

(29) D. Hull and T. Clyne. *An Introduction to Composite Materials*, 2 Ed., 133-155. Cambridge University Press, Cambridge, 1996

(30) Y. Qiu and P. Schwartz. Single-Fiber Pull-out from a Microcomposite Test. *Composites Science and Technology*, 48: 5-10, 1993

(31) K. Kupper and P. Schwartz. Modification of the Fiber Matrix Interface of p-Aramid Fiber Using Gas Plasma. *Journal of Adhesion Science and Technology*, 5: 165-176, 1991

(32) J. Kalantar and L. Drzal. The Bonding Mechanism of Aramid Fibers to Epoxy Matrices. 2. An Experimental Investigation. *Journal of Materials Science*, 25: 4194-4202, 1990

(33) J. Kalantar and L. Drzal. The Bonding Mechanism of Aramid Fibers to Epoxy Matrices. 1. A Review of the Literature. *Journal of Materials Science*, 25: 4186-4193, 1990

(34) A. Mathur and A. Netravali. Modification of Mechanical Properties of Kevlar Fiber by Polymer Infiltration. *Journal of Materials and Science*, 5: 1265-1274, 1996

(35) S. Weidner, G. Kühn, R. Decker, D. Roessner and J. Friedrich. Influence of Plasma Treatment on the Molar Mass of Poly(ethylene terephthalate) Investigated by Different Chromatographic and Spectroscopic Methods. *Journal of Polymer Science Part A-Polymer Chemistry*, 36: 1639-1648, 1998

(36) M. Gheorghiu, F. Arefi, J. Amouroux, G. Placinta, G. Popa and M. Tatoulian. Surface Cross Linking and Functionalization of Poly(ethylene terephthalate) in a Helium Discharge. *Plasma Sources Science and Technology*, 6: 8-19, 1997

(37) G. Placinta, F. Arefi-khonsari, M. Gheorghiu, J. Amouroux and G. Popa. Surface Properties and the Stability of Poly(ethylene Terephthalate) Films Treated in Plasmas in Helium-Oxygen Mixture. *Journal of Applied Polymer Science*, 66: 1367-1375, 1997

VI. STUDY OF PLASMA-POLYMERIC SUBSTRATE INTERACTION IN CAPACITIVELY-COUPLED ATMOSPHERIC PRESSURE PLASMA

1. Introduction

Plasma-substrate interactions have been studied for over 30 years, since plasma modification of polymers enhances their surface properties (wettability, adhesion, hydrophobicity, oleophobicity, biocompatibility, permeability, dyeability etc.) without alteration of bulk properties by means of etching/cleaning, polymerization, coating/deposition, etc. instead of using any wet chemical processes. Surface modification is derived by physical and chemical interactions between substrate surface and plasma particles such as ions, atoms, ozone, metastables of atomic and molecules, UV-radiation and molecules. Etching is achieved by ion bombardment on substrate surface, leading to surface roughness [1] and weight loss [2]. Functionalization is achieved by chemical interactions between molecular radicals generated by plasma and active particles in plasma [3-6]. In addition, UV-radiation generates cross-linking on the subsurface of substrate by recombination of radicals [7,8]. Low-pressure plasmas are conducted under vacuum and thus most likely a batch process, leading to high cost and application limits. However, atmospheric pressure plasma systems can reduce processing cost, while achieving similar surface treatment effects in a continuous process [9]. Nevertheless, unlike the low-pressure plasma [7,13-18] plasma-substrate interactions in atmospheric plasma treatment have not been completely characterized [10-12].

Our preliminary study [19] showed that there was a competition between etching and re-deposition in atmospheric pressure plasma, and its mechanism was proposed. In addition, it was proposed that helium gas might play an important role in formation of cross-links in

plasma [16,18]. In this study, etching/re-deposition behavior in capacitively-coupled atmospheric pressure plasma was confirmed by surface analytical techniques. The effect of cross-linking formation influencing on physical properties and surface wettability ageing of a given substrate was investigated at plasma exposure times and gas flow rates.

2. Experimental

PET films (MELINEX® S/200 supplied by DuPont Teijin Films™, thickness: 50 μm, 28x22 cm^2) and silicon wafer (diameter = 1 inch) were treated by He and He/O_2 atmospheric pressure plasma after cleaning with acetone solution for 3 minute and drying at ambient temperature. PET film and silicon wafer on the film were placed together in the middle of two parallel electrode plates with distance of 3.5 cm during plasma treatment in a capacitively-coupled atmospheric pressure plasma system as shown in Figure 1.

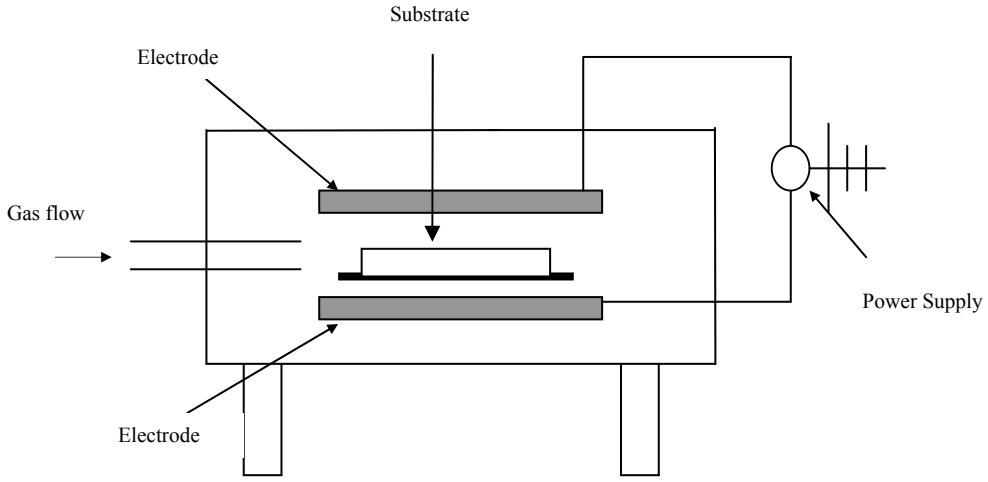

Figure 1. Schematic Diagram of Capacitively-Coupled Atmospheric Pressure Plasma System

The atmospheric pressure plasma treatment was performed with various treatment conditions as illustrated in Table 1. The plasma was generated with He and He/O_2 gas at 5 kHz with 7.8 kV_{rms} across the plates.

Table 1. Experimental Design of PET Films and Silicon Wafer Treated by He and He/O_2 Atmospheric Pressure Plasmas

Conditions		Plasma Treatment	
		He	He/O_2
Frequency, kHz		5	
Experiment Set 1	He Flow Rate, lpm*	4, 8 and 12	12
	O_2 Flow Rate, lpm	-	0.1,0.2 and 0.3
	Exposure Time, min.	3	3
Experiment Set 2	He Flow Rate, lpm	12	12
	O_2 Flow Rate, lpm	-	0.3
	Exposure Time, min.	1,2,3,4 and 5	

*lpm = liter per minute

After plasma treatment, the PET films were exposed to air at ambient temperature for weight loss (%) and weighed in 1 and 2 days after plasma treatment. After 2-day storage, the PET films were dried in an oven at 80 ºC for 24 hours, and then weighed. PET film weight loss (%) was determined using the following equation:

$$Weight\ Loss(\%) = \frac{(W_0 - W_i)}{W_0} \times 100 \qquad (1)$$

where W_0 is a control PET film weight and W_i is a plasma treated PET film weight after storage.

Contact angle measurements were performed on plasma treated PET films for surface wettability and ageing process using a goniometer (Model A-100 by Ramé-Hart, Inc.) by the sessile drop technique. After dropping a 1 μL distilled water droplet on PET film, the contact angle of the droplet was observed through the telescope. The contact angles were measured in 5 different places on the film surface. The greater contact angle, the greater the hydrophobicity.

Chemical composition on the PET film and silicon wafer surfaces were analyzed by Perkin Elmer PHI 5400 X-ray Photoelectron Spectroscopy (XPS) photospectrometer. The X-ray source was Mg_α (1,253.6 eV) with the take-off angle, 30-60°. The anode voltage was 15 kV and the power was 300W. The holding pressure of the XPS chamber was between 10^{-9} and 10^{-10} torr. The possible scanning area was variable from 200 microns diameter to 30 mm, and the scanning depth is about 1-10 nm. The Computer Acquisition was equipped with a RBD Enterprises Model 147 Controlling System. This allowed for the system control and data acquisition to be performed in an easy-to-use Windows™-based environment. The references of XPS spectra were used with respect to 284.5 eV for C_{1s}, observed in hydrocarbon polymers. Sensitive factors (S) for XPS transition were $S(C_{1s})$= 0.296, $S(N_{1s})$=0.477 and $S(O_{1s})$ = 0.711. O/C, N/C and (O+N)/C atomic rates were estimated from the relative intensities of the O_{1s}, N_{1s} and C_{1s} core levels. The C_{1s} deconvolution analyses were conducted to examine the functionalization on PET film and silicon wafer surfaces after

plasma treatments. The angle resolved XPS technique was used to characterize the depth of PET film surface modification. The higher angle, the larger the detection depth.

Surface morphology of PET films and silicon wafers was analyzed by atomic force microscopy (AFM) (JEOL JSPM-5200). The silicon nitride tip was used as a probe, and areas of 1 μm^2 and 5 μm^2 were scanned under a pressure of 10^{-3} Pa. Surface roughness was determined by root mean square of surface roughness (RMS) and surface area ratio (%). RMS was calculated from the roughness profile by following equation:

$$RMS = \sqrt{\frac{1}{N}\sum_{0}^{N}(Z_i - Z_{ave})^2} \qquad (2)$$

where Z_{ave} is the average of the Z values within the given area, Z_i is the current Z value, and N is the number of points within a given area. Surface area ratio (%), the percentage of the three-dimensional surface area to the two-dimensional surface area produced by projecting the surface onto the threshold plane, was estimated by the following equation:

$$Surface\ Area\ Ratio(\%) = \frac{\sum(surface\ area) - \sum(projected\ area)}{\sum(surface\ area)} \times 100 \quad (3)$$

The PET film tensile strength test was performed based on ASTM method D-882 (Standard Test Method for Tensile Properties of Thin Plastic Sheeting). Crosshead speed is 25 mm/min with a gauge length of 5 cm on a Sintech universal-testing machine. The specimen size is 2.54 x 10 cm and 5 specimens were tested for each group. The test was carried out at 20°C and 65% relative humidity. For statistical analysis, one-way analysis of

variance (ANOVA) and Turkey pair-wise multiple comparison were used to compare the tensile strengths and initial modulus of the PET films among different treatment groups. A P-value smaller than 0.05 was considered significant.

3. Results

3.1 Weight Loss (%)

3.1.1 Weight Loss (%) after Plasma Treatment

The PET films were weighed after and before plasma treatment. Figure 2 shows weight loss (%) of plasma treated PET films as function of flow rates of helium and oxygen gases. The weight loss (%) increased with an increase of flow rate in both He and He/O_2 plasma treatments, because density of plasma particles increased with an increase of flow rate, resulting in an increase of etching effect.

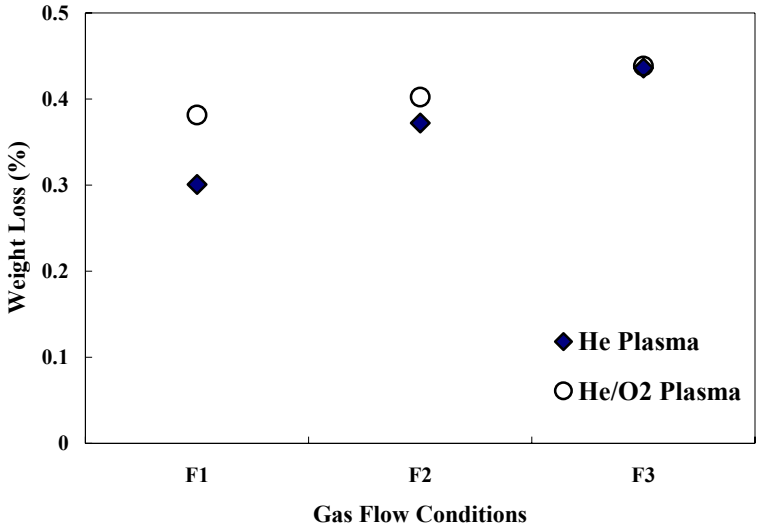

Figure 2. Weight Loss (%) of Plasma Treated PET Film with Gas Flow Conditions (F1: He=4 lpm and He/O_2=12/0.1 lpm, F2: He=8 lpm and He/O_2=12/0.2 lpm, F3: He =12 lpm and He/O_2=12/0.3 lpm)

Figure 3 illustrates the weight loss (%) of PET films as a function of exposure time for He and He/O_2 plasma treatments. The weight loss (%) of plasma treated films increases initially for both plasma treatments, and reach a maximum at 3 min. for He plasma and 4 min. for He/O_2 plasma. In He/O_2 plasma, the maximum weight loss (%) is obtained at longer exposure time than He plasma. He/O_2 plasma has higher oxygen content, involving in more etching effect on PET film surface. At longer exposure time, the weight loss (%) of PET films decreases for both plasma treatments. These results suggest simultaneous etching and re-deposition processes in plasma-substrate interaction, and the similar results showed in previous study [19].

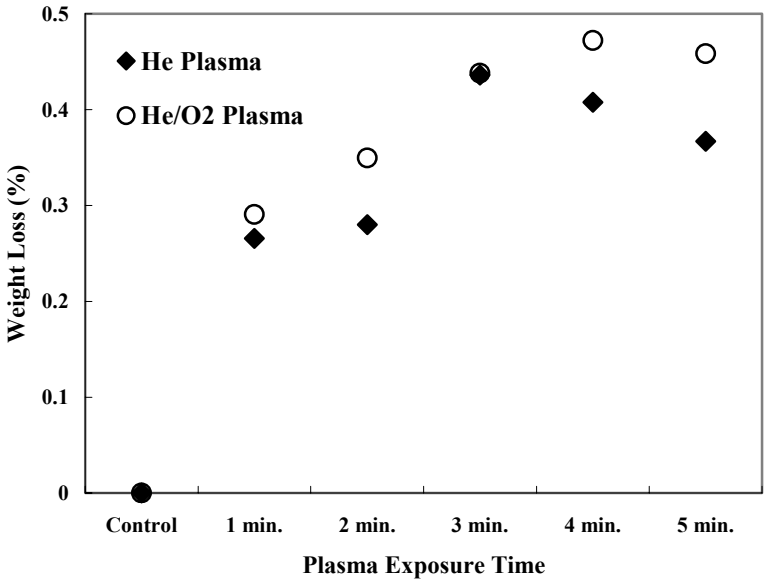

Figure 3. Weight Loss (%) of Plasma Treated PET Film with Exposure Time
(Flow Rate: He=12 lpm, He/O_2=12/0.3 lpm)

3.1.2 Influence of Ageing on Weight Loss (%)

Table 2 shows the weight loss (%) recovery as a function of storage time of plasma treated PET films exposed to air after plasma treatment. The weight loss (%) decreased with an increase of storage time for both plasma treatments, however, increased again after drying in oven. After storage of 2 days, weights of the films exceed those of untreated. The recovery of weight loss (%) in storage by ageing is related to moisture regain, coming from hydrogen bonding between water moisture in air and hydrophilic functional groups generated by plasma treatment. However, after drying in oven, weight loss (%) of the films was not recovered up to those of right after plasma treatments in all plasma conditions. The first layer of molecules on film surface is likely boned to the film with covalent bonds that cannot be removed by drying.

3.2 Surface Wettability (Contact Angle)

3.2.1 Wettability of Plasma Treated PET Film

Wettability of plasma treated PET films was estimated by contact angle measurement. Figures 4 and 5 show the dynamic contact angle as a function of flow rate and exposure time. Contact angles of plasma treated PET films decreased after plasma treatment, however, there is no further wettability enhancement with an increase of flow rate for both plasmas. Wettability of plasma treated PET films increased with an increase of exposure time for both plasmas. Contact angles dropped rapidly after 1 min. exposure time, and then leveled off thereafter. He/O_2 gas treatment leads to a higher wettability than He gas treatment at 1 min. exposure time. It is noted that He/O_2 gas has higher oxygen content, generating more hydrophilic functional groups by more chemical interaction with the molecules on PET film

surface. However, after 1 min. exposure time, wettability enhancement increased slightly in both gas plasma treatments. In addition, there is no difference between two gases.

Table 2. Weight Loss (%) of Plasma Treated PET Films with Different Storage Conditions (He/O_2: He flow rate = 12 lpm)

Gas	Exposure Time, min.	Flow, lpm	After Plasma	1 Day	2 Day	2 Day + Drying
He	3	4	0.301	0.075	0.000	0.011
		8	0.372	0.089	0.021	0.104
		12	0.436	0.109	-0.060	0.160
He/O_2	3	0.1	0.381	0.038	-0.005	0.027
		0.2	0.402	0.109	-0.022	0.114
		0.3	0.438	0.114	-0.044	0.213
He	1	12	0.266	0.043	-0.021	0.051
	2	12	0.280	0.077	-0.022	0.095
	3	12	0.436	0.109	-0.060	0.160
	4	12	0.408	0.101	-0.038	0.116
	5	12	0.367	0.083	-0.044	0.071
He/O_2	1	0.3	0.291	0.053	-0.011	0.092
	2	0.3	0.349	0.079	-0.023	0.137
	3	0.3	0.438	0.114	-0.044	0.213
	4	0.3	0.472	0.191	-0.090	0.285
	5	0.3	0.459	0.165	-0.058	0.117

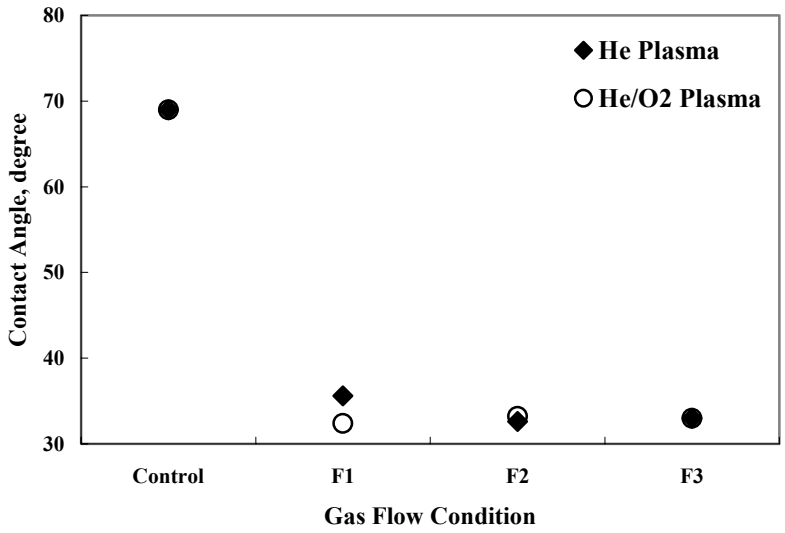

Figure 4. Wettability on Plasma Treated PET Film Surface with Different Gas Flow Condition (F1: He=4 lpm and He/O_2=12/0.1 lpm, F2: He=8 lpm and He/O_2=12/0.2 lpm, F3: He =12 lpm and He/O_2=12/0.3 lpm)

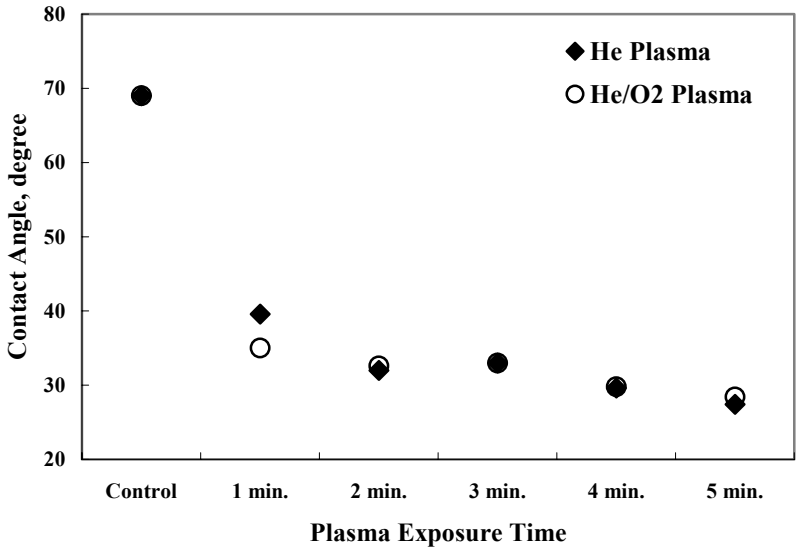

Figure 5. Wettability on Plasma Treated PET Film Surface with Different Exposure Time (He:12 lpm and He/O_2: He=12 lpm and O_2=0.3 lpm)

3.2.2 Change of Wettability on Plasma Treated PET Film due to Ageing

Contact angle increased with an increase of storage time at all flow rates and exposure times for both gas plasmas as shown in Figures 6 and 7. For He plasma treatment at 4 lpm helium flow rate, the wettability recovery was faster and reached at equilibrium state after 4-day storage, while continuously increased along storage time at higher flow rates. Figure 6-(b) shows that contact angles of He plasma treated films increased with an increase of storage time at all exposure times. Ageing processes of 1 and 2 min. plasma exposed films becomes steady after 4-day storage, however, wettability of the films treated for longer exposure time increased continuously for longer storage time. In addition, the films treated for longer exposure time showed lower contact angle than those treated of shorter time.

For He/O_2 plasma treatment (Figure 7), contact angle increased with an increase of ageing time at all oxygen flow rates, however, the ageing process was faster at higher flow rate than at lower flow rate. Contact angle becomes equilibrium after 30-day storage at 0.1 and 0.2 lpm oxygen flow rates, while it increased continuously along storage time at 0.3 lpm oxygen flow rate. Although wettability of He/O_2 plasma treated films decreased along storage time at all exposure times, the ageing behaviors are different from those of He plasma treated films. The films treated for longer exposure time showed faster ageing process and higher contact angle in He/O_2 plasma treatment than those of shorter exposed films. However, wettability of He/O_2 plasma treated films was lower than those of He plasma treated films after 2-day storage. In addition, longer He/O_2 plasma exposed PET films were shown faster loss of wettability than He plasma treated. This behavior might result from cross-linking formation that can limit re-orientation of oxidized functional groups to subsurface.

(a)

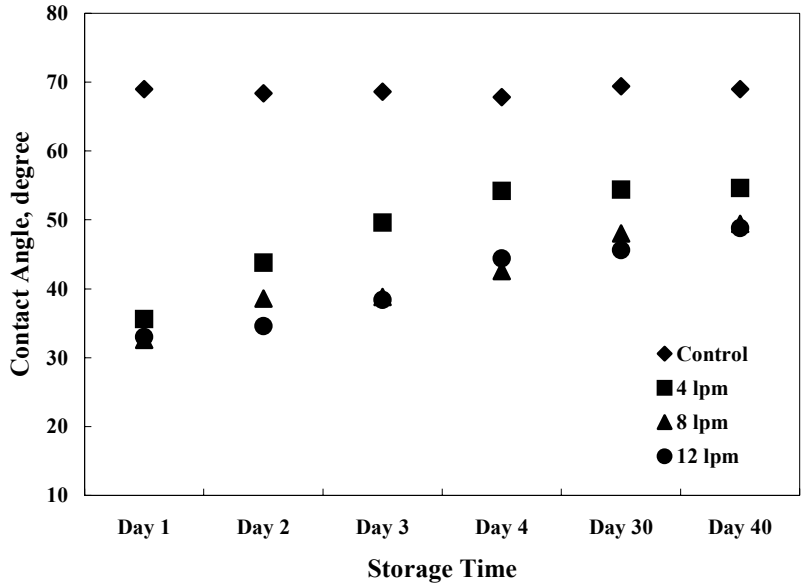

(b)

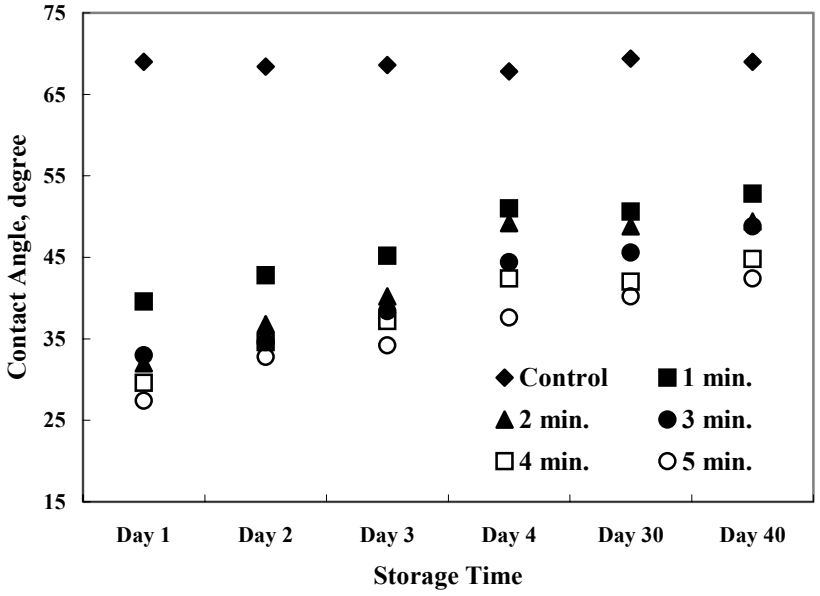

Figure 6. Contact Angle Change on He Plasma Treated PET Films with Different Gas Flow Rate: (a) Flow Rate and (b) Exposure Time (He Flow Rate = 12 lpm)

(a)

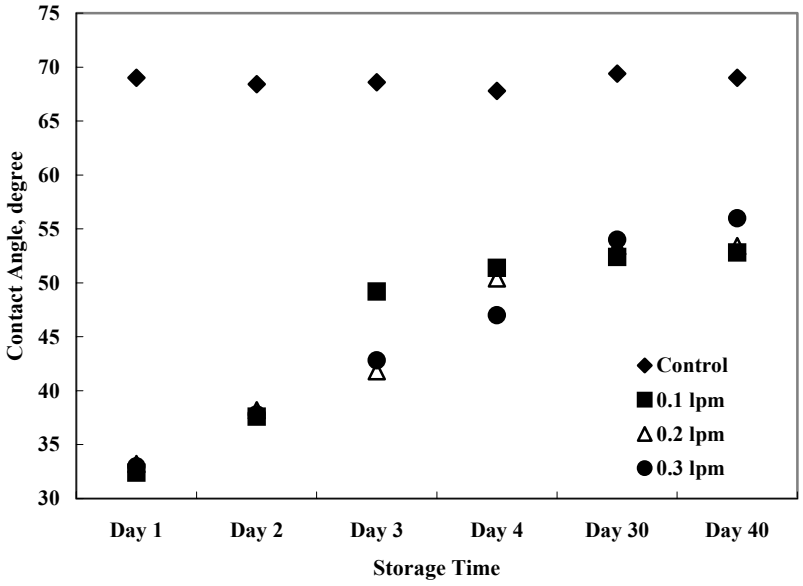

(b)

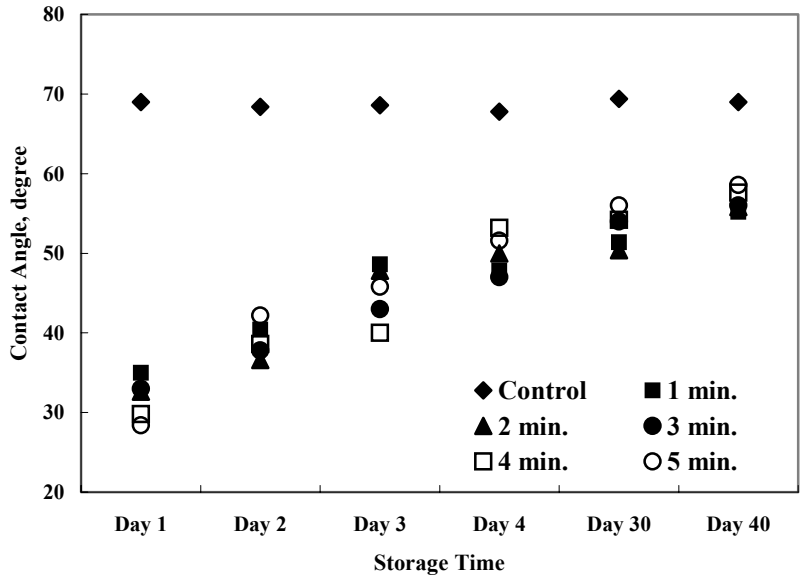

Figure 7. Contact Angle Change on He/O_2 Plasma Treated PET Films with Different Exposure Time (He Flow Rate = 12 lpm): (a) Flow Rate and (b) Exposure Time

3.3 Surface Chemical Analysis by X-ray Photoelectron Spectroscopy (XPS)

3.3.1 Surface Chemical Analysis and Depth Profile of PET Film

Chemical analysis and depth profile of plasma treated PET films were conducted by X-ray Photoelectron Spectroscopy (XPS). Table 3 shows significant chemical composition change on PET films surface after plasma treatments. The carbon contents (C_{1s}) of plasma treated PET films decreased with an increase of exposure time at 30 degree of XPS resolved angle (outer surface of PET film) for both plasmas. The nitrogen content (N_{1s}) increment resulted from nitrogen related chemical reactions because N_2 gas exists in atmospheric pressure plasma. The oxygen content (O_{1s}), O/C and (O+N)/C increased after plasma treatment for both gas plasmas. He/O_2 plasma generated lower carbon content and higher oxygen content on PET film than He plasma because oxygen content is higher in He/O_2 plasma. In addition, silicon content (Si_{2p3}) increased after both plasma treatments and was higher in He/O_2 plasma. The increment of silicon content might be derived from re-deposition of etched silicon particles from silicon wafer.

The carbon contents of plasma treated films increased and oxygen contents decreased with an increase of penetration depth. In addition, He/O_2 plasma treated films had lower carbon content and higher oxygen content (O/C and (O+N)/C) than He plasma. This implies that the surface modification depth of He/O_2 plasma is deeper than He plasma. The deeper modification of He/O_2 plasma may be due to higher reactivity of oxygen in plasma, determined by higher oxygen particle density involving in chemical interaction between plasma and substrate.

Table 3. Chemical Composition of Plasma Treated PET Films by XPS Angle Resolved Analysis (He plasma: He Flow Rate = 12 lpm, He/O_2 plasma: He Flow Rate=12 lpm and O_2 Flow Rate = 0.3 lpm): (a) 30 degree, (b) 45 degree and (c) 60 degree

(a)

Plasma Condition	Chemical Composition, %				Atomic Ratio	
	C_{1s}	N_{1s}	O_{1s}	Si_{2p3}	O/C	(O+N)/C
Control	95.7	0.0	4.3	0.0	0.04	0.04
He 1 min.	84.6	2.1	12.1	1.3	0.14	0.17
He 3 min.	82.6	2.1	13.0	2.2	0.16	0.18
He 5 min.	84.4	1.1	13.3	1.2	0.16	0.17
He/O_2 1 min.	77.8	1.3	19.5	1.5	0.25	0.27
He/O_2 3 min.	78.9	2.1	14.3	4.7	0.18	0.21
He/O_2 5 min.	71.4	4.3	17.0	7.3	0.24	0.30

(b)

Plasma Condition	Chemical Composition, %				Atomic Ratio	
	C_{1s}	N_{1s}	O_{1s}	Si_{2p3}	O/C	(O+N)/C
Control	85.0	0.0	15.0	0.0	0.18	0.18
He 1 min.	84.5	1.4	14.0	0.0	0.17	0.18
He 3 min.	84.5	1.4	12.9	1.1	0.15	0.17
He 5 min.	84.5	0.9	13.4	1.2	0.16	0.17
He/O_2 1 min.	78.8	1.4	18.4	1.4	0.23	0.25
He/O_2 3 min.	83.6	0.8	13.6	2.0	0.16	0.17
He/O_2 5 min.	82.1	1.5	14.8	1.6	0.18	0.20

(c)

Plasma Condition	Chemical Composition, %				Atomic Ratio	
	C_{1s}	N_{1s}	O_{1s}	Si_{2p3}	O/C	(O+N)/C
Control	85.3	0.0	14.7	0.0	0.17	0.17
He 1 min.	85.5	1.2	13.3	0.0	0.16	0.17
He 3 min.	86.2	1.1	12.7	0.0	0.15	0.16
He 5 min.	86.1	0.8	13.1	0.0	0.15	0.16
He/O_2 1 min.	81.0	0.8	16.8	1.4	0.21	0.22
He/O_2 3 min.	84.4	0.8	13.2	1.6	0.16	0.17
He/O_2 5 min.	83.9	0.7	14.3	1.0	0.17	0.18

Table 4. Deconvolution Analysis of Plasma Treated PET Films by XPS Angle Resolved Analysis (He plasma: He Flow Rate = 12 lpm, He/O_2 plasma: He Flow Rate=12 lpm and O_2 Flow Rate = 0.3 lpm): (a) 30 degree, (b) 45 degree and (c) 60 degree

(a)

Plasma Condition	Bonding Composition, %						
	C-C	C-O	C-OH	C=O/ CH=O	COO	OCOO	C-Si
Control	74.0	12.3	4.8	4.5	3.8	0.6	0.0
He 1 min.	63.5	12.2	6.5	5.6	8.4	2.0	1.7
He 3 min.	66.5	10.8	8.0	6.8	4.2	1.0	2.6
He 5 min.	65.5	9.4	8.2	6.9	6.7	1.0	2.3
He/O_2 1 min.	62.8	8.7	9.1	7.3	5.9	2.2	4.1
He/O_2 3 min.	65.0	8.1	10.5	5.3	5.3	1.4	4.5
He/O_2 5 min.	68.1	6.8	10.5	6.3	4.6	0.9	2.8

(b)

Plasma Condition	Bonding Composition, %						
	C-C	C-O	C-OH	C=O/ CH=O	COO	OCOO	C-Si
Control	64.2	14.7	4.4	3.8	12.6	0.3	0.0
He 1 min.	64.0	14.5	6.1	9.3	5.6	0.5	0.0
He 3 min.	67.3	11.0	7.1	7.0	6.2	0.4	0.8
He 5 min.	68.2	10.3	5.3	7.5	6.5	1.2	1.1
He/O_2 1 min.	64.1	10.4	8.0	6.6	8.6	1.1	1.2
He/O_2 3 min.	66.2	8.2	8.7	6.5	7.4	0.7	2.4
He/O_2 5 min.	64.6	9.4	9.0	6.2	8.1	1.3	1.4

(c)

Plasma Condition	Bonding Composition, %						
	C-C	C-O	C-OH	C=O/ CH=O	COO	OCOO	C-Si
Control	64.3	14.3	2.5	6.8	12.1	0.0	0.0
He 1 min.	66.4	14.2	3.9	9.1	5.5	0.8	0.0
He 3 min.	67.9	12.4	4.4	9.6	4.0	1.7	0.0
He 5 min.	69.3	11.1	4.4	8.0	7.2	0.0	0.0
He/O_2 1 min.	67.8	10.0	7.4	5.8	7.0	1.4	0.6
He/O_2 3 min.	66.3	8.8	7.1	7.7	7.9	0.6	1.6
He/O_2 5 min.	65.8	10.1	6.9	7.0	8.6	0.7	0.9

C_{1s} deconvolution analysis shows functional group change of PET films and formation of new functional groups (Table 4). The control sample has lower contents of oxidized functional groups (C-O, COO and C=O) and higher C-C group in outer surface than subsurface. The higher C-OH content in outer surface might be due to contamination. The outmost surface of control PET film is relatively stable due to ageing, that is, the functional groups on the polymer surface are likely to be reoriented by the migration of oxidized molecules and the diffusion of oxidized functional groups into polymer bulk [20,21]. C-C bond decreased up to 1 min. for both gas plasmas then increased again at 30 degree of XPS resolved angle. He/O_2 plasma treatment led to higher reduction of C-C bond than He plasma at longer exposure time. The reduction of C-O bond in He plasma was smaller than He/O_2 plasma along exposure time. C-OH group increased in both gas plasmas as well as C=O/CH=O bonds. He/O_2 plasma generated higher content of C-OH group than He plasma. New functional groups (C-OH, CH=O, OCOO and C-Si) were formed on PET films in both gas plasmas. C-Si group is generated from re-deposition of silicon particles, and the content is higher in He/O_2 plasma, corresponding to an increase of silicon content.

At higher XPS resolved angles, plasma treated PET films had higher C-C bond content than untreated. For He plasma treatment, C-C bond increased with an increase of plasma exposure time. He/O_2 plasma treatment led to lower content of C-C than He plasma. The intensities of C-O and COO groups decreased for both gas plasmas while C=O/CH=O and C-OH groups increased.

Table 5. Chemical Composition of Silicon Wafer Treated by Atmospheric Plasma (He/O_2 plasma: He Flow Rate=12 lpm)

Gas	Exposure Time, min.	Flow, lpm	Chemical Composition, %				Atomic Ratio			
			C_{1s}	N_{1s}	O_{1s}	Si_{2p3}	O/C	C/Si	O/Si	(C+O)/Si
	Control		5.3	0.0	16.5	78.2	3.11	0.07	0.21	0.28
He	3	4	14.6	1.0	25.5	58.9	1.75	0.25	0.43	0.68
		8	16.1	1.5	21.4	61.0	1.33	0.26	0.35	0.61
		12	17.2	1.4	25.0	56.4	1.45	0.30	0.44	0.75
He/O_2	3	0.1	14.9	1.2	20.3	63.6	1.36	0.23	0.32	0.55
		0.2	15.6	0.8	22.4	61.2	1.44	0.25	0.37	0.62
		0.3	32.7	1.2	18.7	47.4	0.57	0.69	0.39	1.08
He	1	12	16.1	1.5	21.4	61.0	1.33	0.26	0.35	0.61
	2	12	16.9	0.7	25.2	57.2	1.49	0.30	0.44	0.74
	3	12	17.2	1.4	25.0	56.4	1.45	0.30	0.44	0.75
	4	12	20.4	1.5	13.6	64.5	0.67	0.32	0.21	0.53
	5	12	31.4	1.0	18.7	48.9	0.60	0.64	0.38	1.02
He/O_2	1	0.3	23.8	1.6	22.0	52.6	0.92	0.45	0.42	0.87
	2	0.3	24.6	0.6	21.4	53.4	0.87	0.46	0.40	0.86
	3	0.3	32.7	1.2	18.7	47.4	0.57	0.69	0.39	1.08
	4	0.3	42.3	0.0	10.8	46.9	0.26	0.90	0.23	1.13
	5	0.3	47.7	1.9	17.8	32.6	0.37	1.46	0.55	2.01

3.3.2 Surface Chemical Analysis of Silicon Wafer

The silicon wafers exposed to both gas plasmas with PET films were analyzed by XPS. It is shown that carbon content (C_{1s}) increased with increase of flow rate and exposure time while silicon content (Si_{2p3}) decreased after plasma treatment (Table 5). In addition, oxygen content (O_{1s}) and nitrogen content (N_{1s}) increased after both plasma treatments. The increment of carbon content (C_{1s}) is related to the fact that carbon-containing particles are deposited from PET film surface to silicon wafer through plasma treatment, and oxygen content (O_{1s}) increasing shows that oxidation is carried out concurrently with re-deposition. For He/O_2 plasma treatment, the increments of carbon content (C_{1s}) and C/Si are higher while oxygen content (O_{1s}) and O/Si are lower at longer exposure times than He plasma. Moreover, (C+O)/Si of He/O_2 plasma treated silicon is higher while O/C is lower than those of He plasma treated. This behavior results from higher re-deposition rate of carbon-containing particles through greater chain-scission and etching effect on PET film surface due to reactivity of oxygen. It is also re-deposition and surface oxidation occurred simultaneously.

3.3.3 Surface Chemical Change by Ageing

Surface chemical change of PET films stored for 3 and 40 days was examined along the film depth by XPS resolved angle analysis (Table 6). The surface of the control sample is already stabled due to the diffusion or migration of oxidized functional groups into subsurface of the film. Carbon content (C_{1s}) is the highest, and oxygen content (O_{1s}) is the lowest at 30 degree resolved angle, while the lowest carbon content (C_{1s}) and the highest oxygen content (O_{1s}) at 45 degree. The similar results also are found in 40-day stored samples after plasma treatment. The outer surface of PET film (30 degree) has a reduction of

carbon content (C_{1s}) and an increase of oxygen content (O_{1s}) at 1 and 2 min. exposure times. However, after 40-day storage, both treated films have lower carbon content (C_{1s}) and higher oxygen content (O_{1s}) at 30 degree than 45 degree. These results are corresponding to O/C and (O+N)/C values.

Table 6. Chemical Composition Change along Ageing Time of Plasma Treated PET Films by XPS Angle Resolved Analysis (He Flow Rate = 12 lpm)

Condition	Ageing, Day	Angle, degree	Chemical Composition, %				Atomic Ratio	
			C_{1s}	N_{1s}	O_{1s}	Si_{2p3}	O/C	(O+N)/C
Control	-	30	95.7	0.0	4.3	0.0	0.04	0.04
		45	85.0	0.0	15.0	0.0	0.18	0.18
		60	85.3	0.0	14.7	0.0	0.17	0.17
		75	86.8	0.0	13.2	0.0	0.15	0.15
He 1 min.	3	30	82.2	1.1	14.5	2.2	0.18	0.19
		45	84.3	1.4	12.2	2.1	0.14	0.16
		60	84.1	0.0	12.8	3.1	0.15	0.15
		75	84.1	0.7	13.1	2.1	0.16	0.16
	40	30	84.6	2.1	12.1	1.3	0.14	0.17
		45	84.5	1.4	14.0	0.0	0.17	0.18
		60	85.5	1.2	13.3	0.0	0.16	0.17
He 2 min.	3	30	69.9	3.6	15.1	11.4	0.22	0.27
		45	81.5	1.1	14.2	3.2	0.17	0.19
		60	82.8	0.0	14.1	3.1	0.17	0.17
		75	83.9	1.0	13.2	1.9	0.16	0.17
	40	30	82.6	2.1	14.0	1.2	0.17	0.19
		45	82.2	1.4	15.8	0.6	0.19	0.21
		60	87.5	1.1	12.4	0.0	0.14	0.15

3.4 Surface Morphology Analysis by Atomic Force Microscopy (AFM)

3.4.1 Surface Morphology Change of PET Film

Atomic force microscopy (AFM) was used to determine the surface morphology change of PET film through plasma treatment. Table 7 shows the changes of surface roughness (RMS) and surface area ratio (%) of PET film. AFM pictures (Figure 8), also, show the change of surface structure as a result of plasma exposure. The surface roughness and surface area ratio (%) increased with an increase of flow rate for both gas plasmas. He/O_2 plasma led to an increase of the surface roughness along exposure time at 1 μm^2 scanning. However, the surface roughness increased initially and then decreased again in He plasma. At 5 μm^2 scanning area, both gas plasmas rendered initial increase of surface roughness and a reduction at exposure time of 5 min., resulting from a re-deposition effect (predicted nano-scale particles on PET film surface) as shown in Figure 8. He/O_2 plasma treatment leads to higher surface roughness than He plasma along exposure time due to higher reactivity of oxygen.

Surface area ratio (%) of plasma treated film also represents surface roughness change. Regardless of small change by plasma treatments, surface area increased with an increase of flow rate for both plasma treatments. However, as exposure time increases, surface area increased initially, and then decreased again for both gas plasmas.

Table 7. Surface Roughness (RMS) and Increase of Surface Area (%) of Plasma Treated PET Film (He/O_2 plasma: He Flow Rate=12 lpm)

Gas	Exposure Time, min.	Flow, lpm	Scanning Area, μm^2			
			1		5	
			RMS	Surface Area Ratio (%)	RMS	Surface Area Ratio (%)
Control	-	-	0.95	0.46	1.63	0.08
He	3	4	1.04	0.36	4.18	0.03
		8	1.39	0.38	4.55	0.06
		12	2.13	1.86	4.92	0.64
He/O_2	3	0.1	1.07	0.37	3.17	0.19
		0.2	1.53	0.88	4.52	0.33
		0.3	1.74	2.12	4.98	0.69
He	1	12	0.54	0.04	2.58	0.06
	2	12	1.07	0.23	3.19	0.13
	3	12	2.13	1.86	4.92	0.64
	4	12	1.13	2.34	4.52	0.38
	5	12	0.88	0.61	3.23	0.35
He/O_2	1	0.3	0.55	0.34	3.73	0.21
	2	0.3	1.17	1.79	4.18	0.38
	3	0.3	1.74	2.12	4.98	0.69
	4	0.3	2.14	1.98	7.54	1.22
	5	0.3	3.6	0.37	4.72	0.33

(a)

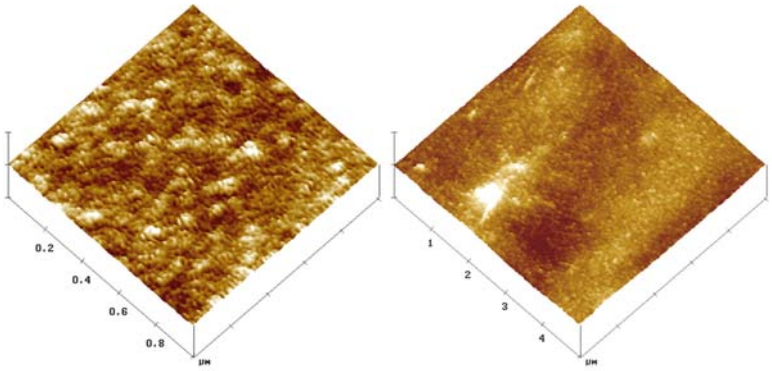

1 µm^2 Scanning 5 µm^2 Scanning

(b)

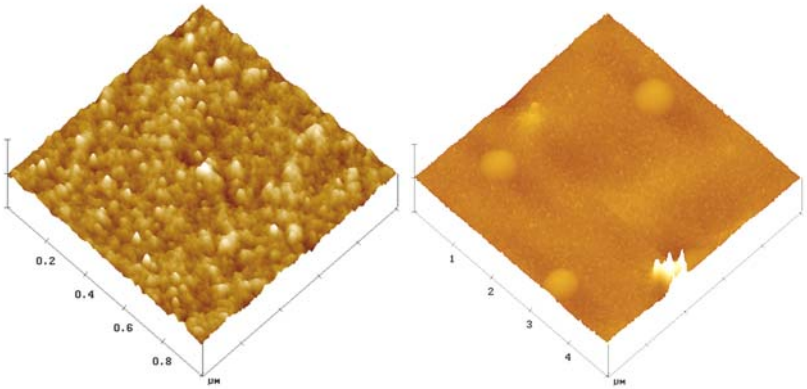

1 µm^2 Scanning 5 µm^2 Scanning

(c)

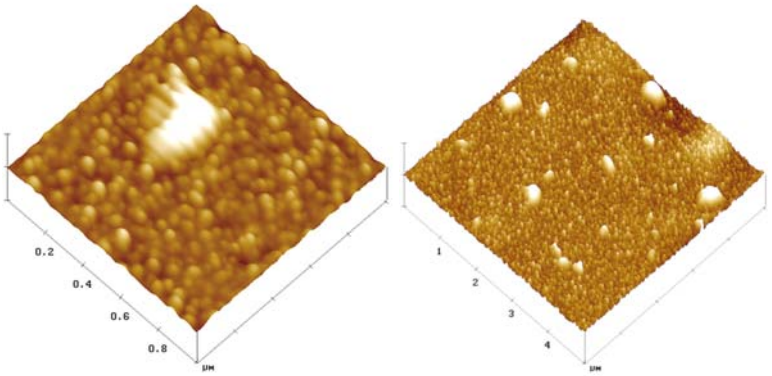

1 µm^2 Scanning 5 µm^2 Scanning

Figure 8. AFM Pictures of PET Films:(a) Control, (b) He 5 min. and (c) He/O_2 5 min. (He Flow Rate=12 lpm and O_2 Flow Rate = 0.3 lpm)

3.4.2 Surface Morphology Change of Silicon Wafer

The surface morphology change of silicon wafer was examined by Atomic force microscopy (AFM). The results show the changes of surface roughness (RMS) of silicon wafer (Table 8 and Figure 9). At scanning area 1 μm^2, the surface roughness of plasma treated silicon wafer became smoother with an increase of flow rate for both gas plasmas. He plasma led to a reduction of surface roughness with an increase of exposure time, however, in He/O_2 plasma, surface roughness decreased initially and then increased again.

Table 8. Surface Roughness (RMS) of Silicon Wafer
(He/O_2 plasma: He Flow Rate=12 lpm)

Gas	Exposure Time, min.	Flow, lpm	Scanning Area, μm^2	
			1	5
Control	-	-	0.715	3.624
He	3	4	0.293	2.117
		8	0.260	1.586
		12	0.150	2.034
He/O_2	3	0.1	0.234	2.668
		0.2	0.177	5.548
		0.3	0.190	6.176
He	1	12	0.628	2.849
	2	12	0.459	1.875
	3	12	0.150	2.034
	4	12	0.147	4.668
	5	12	0.115	3.121
He/O_2	1	0.3	0.410	1.747
	2	0.3	0.484	3.433
	3	0.3	0.190	6.176
	4	0.3	1.058	5.232
	5	0.3	0.551	8.041

(a)

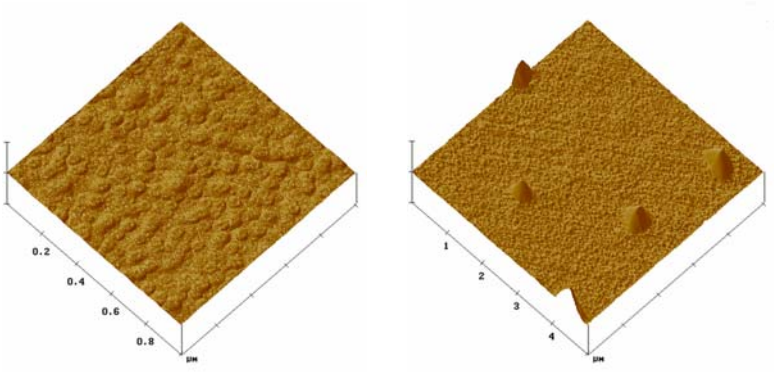

1 μm^2 Scanning 5 μm^2 Scanning

(b)

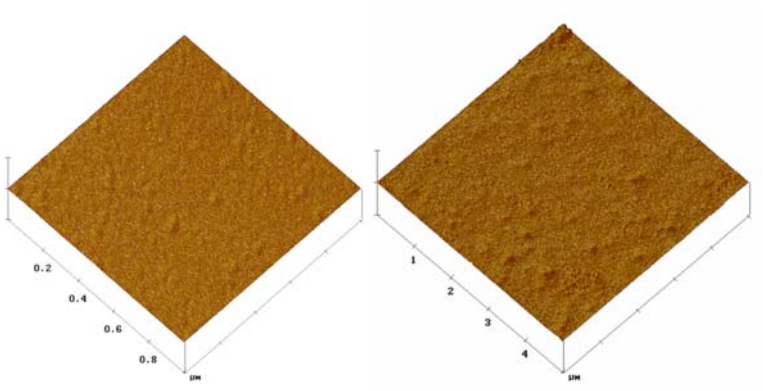

1 μm^2 Scanning 5 μm^2 Scanning

(c)

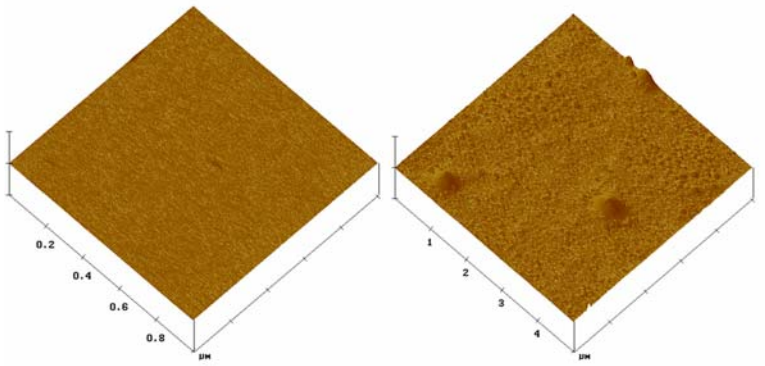

1 μm^2 Scanning 5 μm^2 Scanning

Figure 9. AFM Pictures of Silicon Wafers: (a) Control, (b) He 3 min. and (c) He/O_2 3 min. (He Flow Rate=12 lpm and O_2 Flow Rate = 0.3 lpm)

At scanning are 5 μm^2, the effect of flow rate on surface roughness of silicon wafer was significant in He/O_2 plasma. The surface roughness decreased initially and then increased as exposure time increases for both gas plasmas. In addition, at longer exposure times, RMS values exceeded that of untreated wafer. Through plasma treatments, the surface roughness of silicon wafer became smoother by etching effect initially, and then re-deposition might play a role in affecting surface roughness for longer exposure time.

3.5 Tensile Properties of Plasma Treated PET Films

The tensile strength and initial modulus of PET film increased after atmospheric pressure plasma treatment (Table 9) ($P < 0.05$). For He plasma treatment, the highest tensile strength and initial modulus were obtained at helium flow rate 8 lpm. However, the tensile strength and initial modulus increased with an increase of flow rate in He/O_2 plasma. The increases of tensile strength and initial modulus are greater with He plasma treatment than He/O_2 plasma along exposure time.

Generally, tensile strength of polymer material exposed on plasma is reduced due to ablation or etching effect of plasma treatments [2]. Although etching effect was observed in all plasma treated samples by AFM (Figure 8), there was no negative effect on the tensile strength. This is due to lower active particle densities in atmospheric pressure plasma than low-pressure plasma and helium is the most efficient inert gas for cross-linking on polymer surfaces compared with other gases [18].

Table 9. Tensile Strength of Plasma Treated PET Films
(He/O_2 plasma: He Flow Rate=12 lpm)

Gas	Exposure Time, min.	Flow, lpm	Tensile Strength, MPa			Initial Modulus, GPa		
			Mean	SD	Increase, %	Mean	SD	Increase, %
Control	-	-	152.1[a]	11.9	0.0	2.03[a]	0.07	0.0
He	3	4	169.6[b]	6.7	11.5	2.22[a,b]	0.13	7.5
		8	171.9[b]	1.5	13.0	2.31[b]	0.14	11.7
		12	168.8[b]	4.6	11.0	2.27[b]	0.15	9.4
He/O_2	3	0.1	170.5[b]	2.1	12.1	2.34[b]	0.11	13.2
		0.2	167.9[b]	1.2	10.4	2.22[b]	0.13	7.2
		0.3	164.3[b]	4.6	7.8	2.23[b]	0.06	7.9
He	1	12	165.2[b]	4.4	8.5	2.19[a,c]	0.08	5.7
	2	12	169.9[b]	5.1	11.7	2.24[a]	0.08	8.2
	3	12	168.8[b]	6.4	11.0	2.27[b]	0.15	9.4
	4	12	171.6[b]	2.3	12.8	2.26[b]	0.05	9.1
	5	12	170.9[b]	3.9	12.4	2.44[b,c]	0.04	17.7
He/O_2	1	0.3	165.1[a,b]	5.4	8.5	2.16[a,c]	0.04	4.3
	2	0.3	169.2[a,b]	6.9	11.2	2.19[a]	0.13	5.9
	3	0.3	164.3[b]	4.6	7.8	2.23[b]	0.06	7.9
	4	0.3	164.7[b]	5.3	8.3	2.31[b]	0.06	11.5
	5	0.3	168.8[a,b]	1.4	11.0	2.33[b,c]	0.07	12.6

[a,b,c] Means with different letters are statistically significantly different at $p < 0.05$.
*SD=Standard Deviation

4. Discussion

4.1 Etching/Re-deposition Behavior

In plasma-substrate interaction, etching and re-deposition are carried out concurrently. Etching can play a role in increasing not only weight loss (%) of substrate but also surface roughness, while re-deposition can lead to reduction of weight loss (%) and an increase of

smoothness on substrate surface. Etching effect on PET film was significant with an increase of flow rate for both gas plasmas (Figure 2 and Table 7). However, the competition between etching and re-deposition was shown apparently as plasma exposure time increased (Figure 3 and Table 7). For both gas plasmas, it was found that weight loss (%) and surface roughness of PET films increased initially and then decreased. The surface of plasma treated silicon wafers with PET films became smoother at 1 μm^2 AFM scanning area, however, 5 μm^2 AFM scans showed an increase of surface roughness at higher flow rate and longer exposure time for both gas plasmas (Table 8 and Figure 9). Thus, etching and re-deposition are related to surface morphology change on PET film and silicon wafer.

Surface chemical compositions on PET films and silicon wafers were affected by etching and re-deposition. Si_{2p3} (%) increment was found on the outer surface of PET films after plasma treatment (Table 3). In addition, (C_{1s}+Si_{2p3}) composition decreased at shorter exposure time, and then increased again at longer exposure time as shown in Figure 10. This result matches the weight loss (%) trend. Initially, etching effect is dominant over re-deposition at shorter exposure time, and then re-deposition becomes dominated over etching at longer exposure time. Also, it was found that re-deposition was significant on the surface of silicon wafer (Table 5). C_{1s}/Si_{2p3} atomic ratio increased with an increase of flow rate and exposure time for both gas plasmas. The results show that He/O_2 plasma renders higher re-deposition than He plasma due to the higher activity of oxygen.

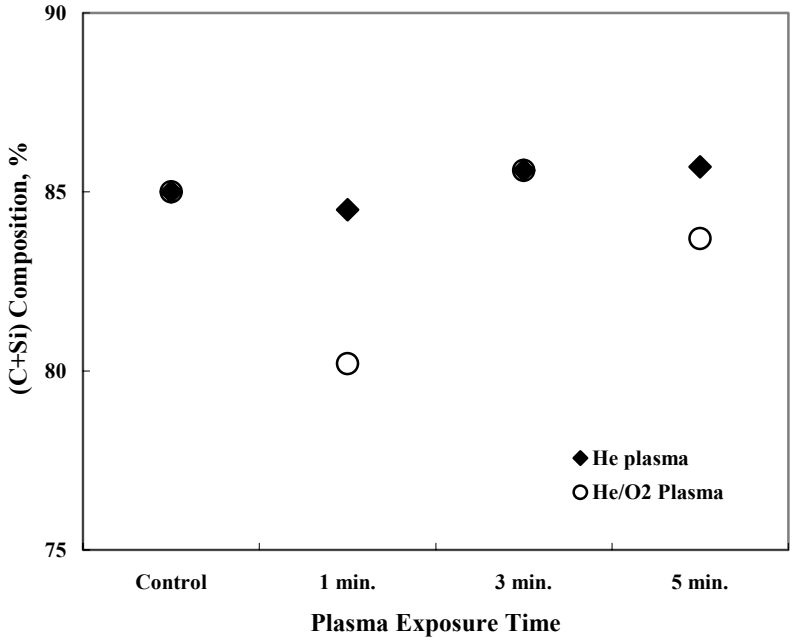

Figure 10. (C_{1s}+Si_{2p3}) Composition of Plasma Treated PET Film
(XPS Resolved Angle = 45º)

4.2 Functionalization by Chain Scission

Generation of new functional groups is obtained from chemical interactions between reactive particles (radicals and ions) in plasma and radical sites on polymer formed by chain scissions and dehydrogenation [3-6,22]. XPS deconvolution analysis (Table 4) showed the reduction of C-O and COO groups, which are weaker bonds in PET molecules. However, new functional groups (C-OH, CH=O and OCOO) increased after plasma treatment.

Potential chemical interaction positions in PET molecule are illustrated as follows:

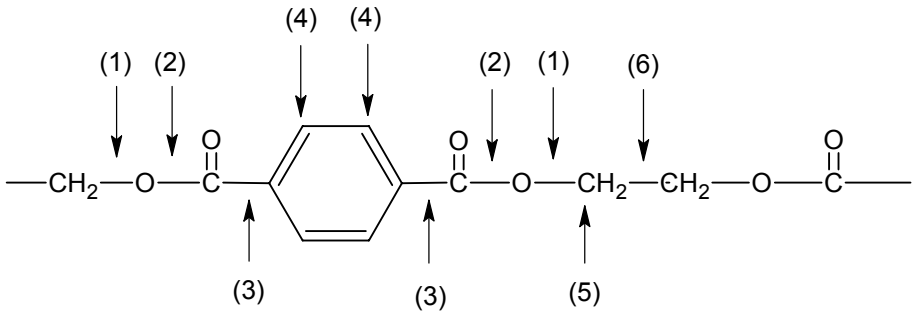

Ion bombardment can introduce not only chain scission at positions (1), (2), (3) and (6), but also dehydrogenation at positions (4) and (5), leading to formation of free radicals. These free radicals can interact with reactive particles in plasma, and generate new functional groups. The proposed mechanisms for new functional group formation on PET film are shown in Figure 11. CH=O and C-OH groups can be generated easily by interactions between free radicals in polymer and those (•H and •OH) in plasma. However, OCOO group formation may involve more complicated mechanisms. New functional groups are more hydrophilic, influencing surface wettability and weight change as storage time increased. Initially, after plasma treatment, hydrophilic functional groups increase surface wettability, and etching effect rendered the reduction of weight. However, plasma treated films started to gain weight (Table 2) after 1-day storage time, and weight of films exceeded untreated samples at 2-day storage time. This weight increment might be due to moisture retention by generating hydrogen bonds between new hydrophilic functional groups and moisture in air. In addition, weights of 2-day stored films decreased again after drying, but still heavier than those immediately after plasma treatment. Even drying cannot remove all moistures contained on film surface, this result indicates that the further reaction of the surface with moisture occurs in air during storage.

(a)

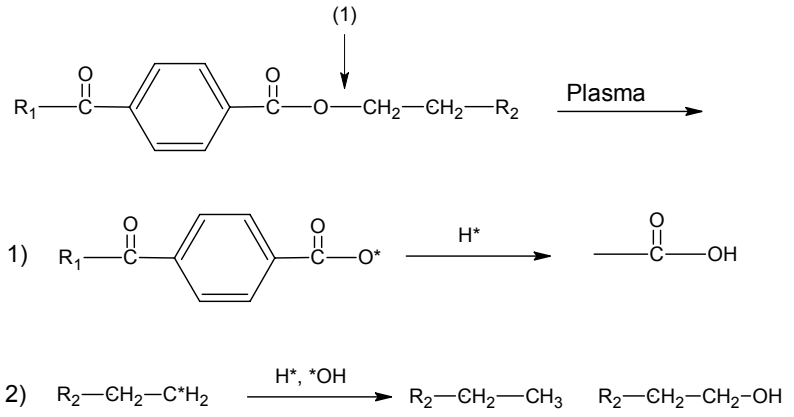

(b)

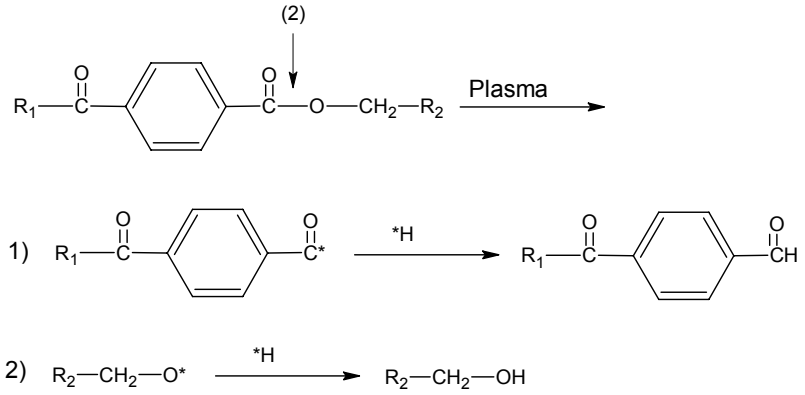

(c)

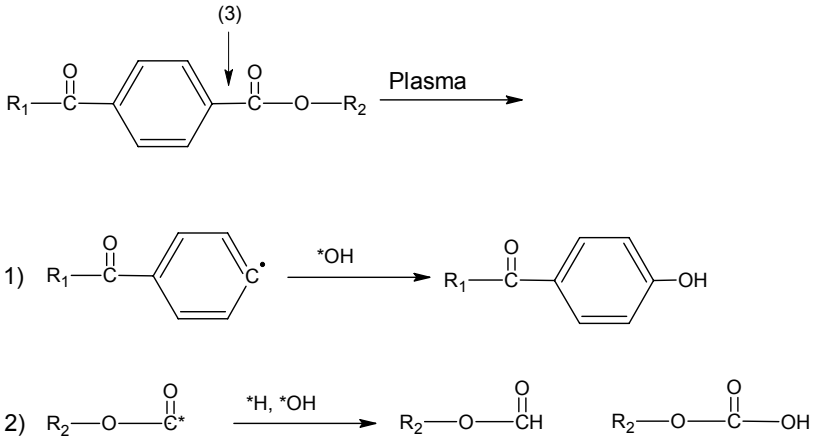

Figure 11. Chain Radical Formation and Functionalization in PET Molecules by Helium Containing Plasma Treatment [15,16,18]: (a) Position 1, (b) Position 2, (c) Position 3, (d) Position 4, (e) Position 5 and (f) Position 6 – Continued

(d)

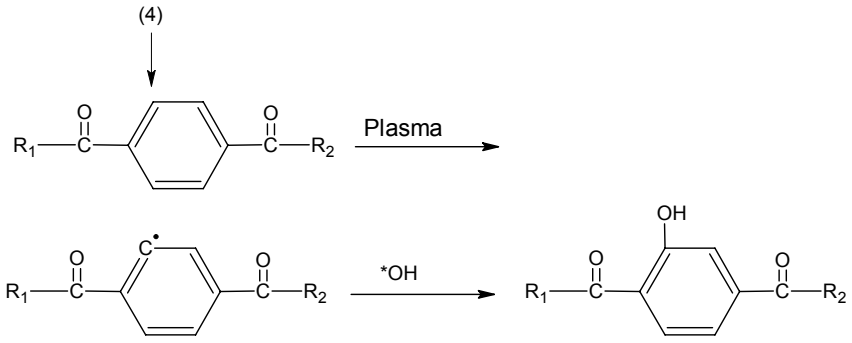

(e)

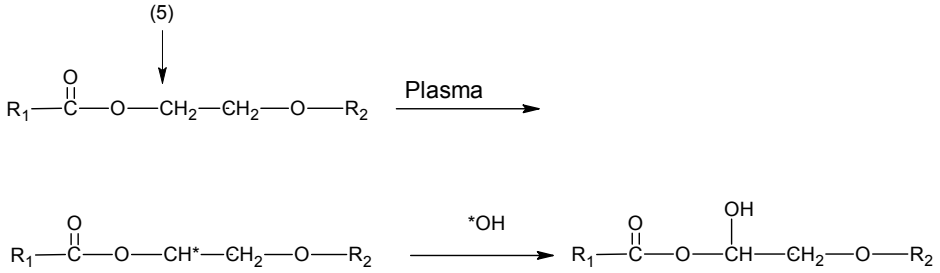

(f)

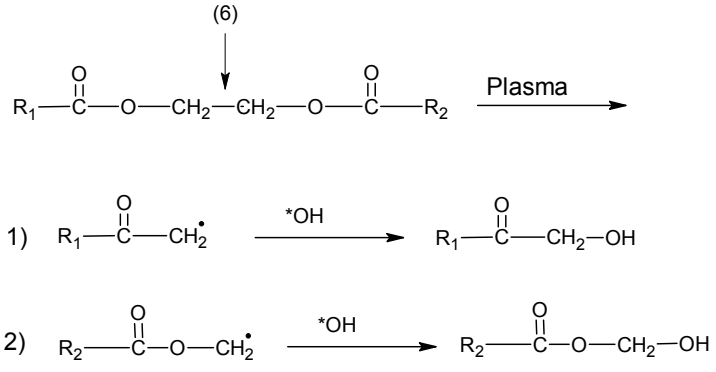

4.3 Cross-linking

It is known that helium can produce the largest amount of UV radiation leading to cross-linking of polymeric materials in plasma [16,18]. In this study, helium gas was used to initiate and generate the plasma at atmospheric pressure before another gas is introduced to the system.

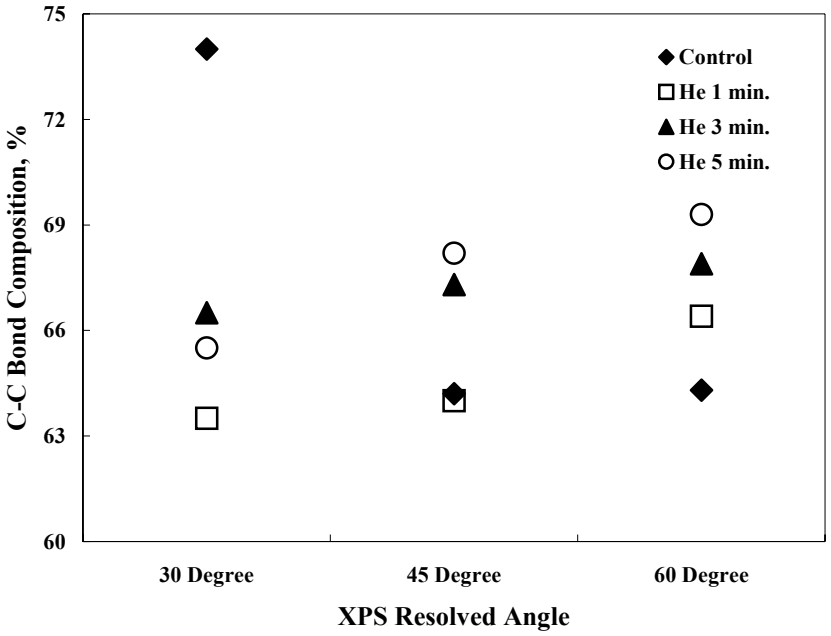

Figure 12. C-C Bond Compositions (%) of He Plasma Treated PET Films along XPS Resolved Angle

As shown in Figure 12, C-C bond compositions (%) of He plasma treated PET films increased with an increase of XPS resolved angle, while control sample showed a decrease of C-C bond. At outer surface of the film, it is known that functionalization is dominated over cross-linking in plasma [7,8]. However, photo-initiated reactions can be carried out without

any chemical reactions in subsurface. The UV-radiation in plasma can penetrate much deeper into the substrate, and the photons can generate the radicals, which can form cross-linking. Increment of C-C bond in subsurface is strongly related to cross-linking formation, shown in both gas plasmas (Table 4). He plasma treatment provided higher portion of C-C group than He/O_2 plasma, because He plasma has higher helium content leading to higher possibility of cross-linking formation. The possible cross-linking reactions in subsurface would occurred at position 4 and 5 (Figure 13) as follows:

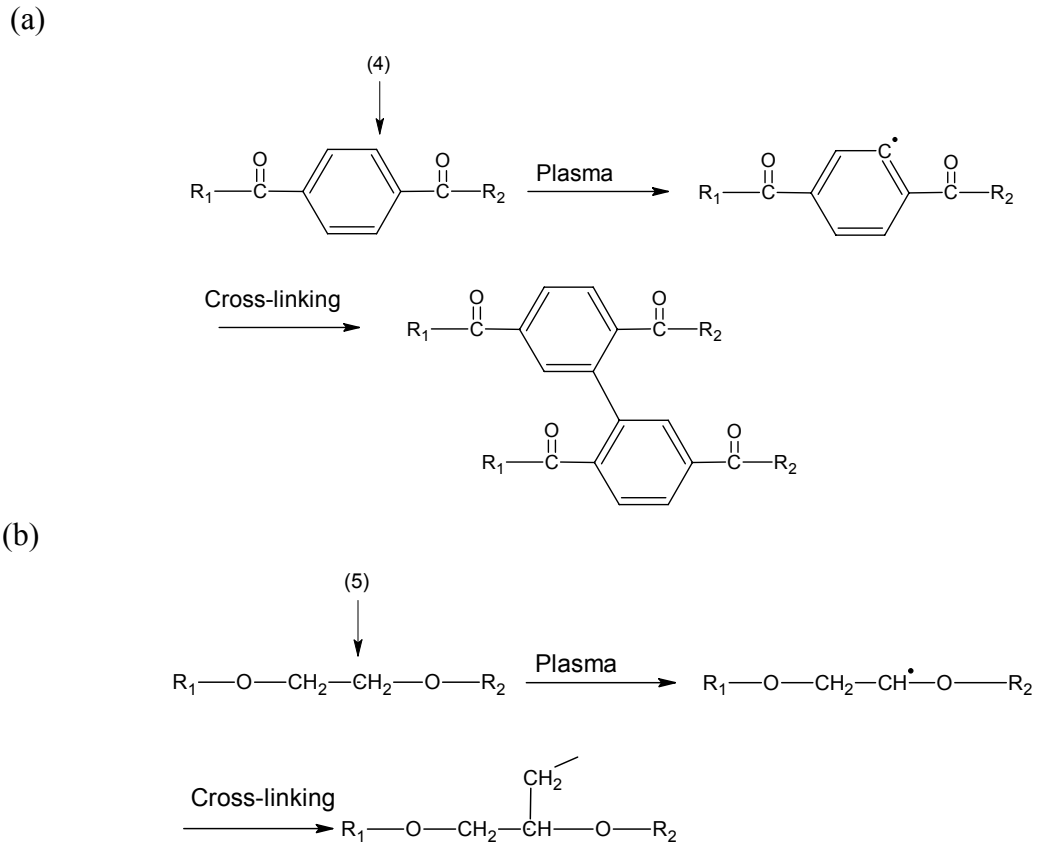

Figure 13. Possible Cross-linking Mechanism in Subsurface of PET Molecules by He Containing Plasma [16,18]: (a) Recombination between Benzene Rings and (b) Combination with Other Carbon chains

In addition, cross-linking formation can affect tensile properties of PET films. In this study, it was found that the tensile strength and initial modulus increase after plasma treatments. It is believed that cross-linking occurs in subsurface of PET film due to helium gas in atmospheric pressure plasma. Previous studies [23,24] showed the similar results of tensile strength enhancement by helium containing plasmas.

4.4 Ageing Behavior of Wettability

Surface wettability changed as a function of storage time and environments. The film surface becomes stabilized through storage by migration of oxidized molecules and diffusion of oxidized functional groups into polymer bulk [20,21]. Thus, the hydrophilic surface becomes hydrophobic after storage. XPS results showed the reduction of oxygen and an increase of carbon on outer surface of plasma treated films after 40-day storage (Table 6), and oxygen content and O/C ratio in subsurface were higher than outer surface of 40-day stored PET films.

The results show that helium gas plasma led to higher cross-linking formation (Table 4), and that ageing of wettability was slower in He plasma than He/O_2 plasma (Figure 5). Previous study [25] showed that the decay of wettability was dependent on degree of cross-linking, and that the rate of ageing could be much slower for highly cross-linked polymers, resulting in reduced mobility of polymer chain.

5. Conclusion

PET films and silicon wafers were treated together by He and He/O_2 plasma under atmospheric pressure for different gas flow and exposure time. The etching effect is

dominant initially and that re-deposition becomes dominated as exposure time increases, indicating the existence of competition between etching and re-deposition.

XPS results of plasma treated PET films showed that surface functionalization was altered by plasma treatment. The functionalization on PET film surface is related to chain scission and chemical interactions between plasma particles and free radicals on PET film. The generations of new functional groups (C-OH, CH=O and OCOO) confirmed the chain scission due to ion bombardment. In addition, it was found that surface wettability of PET film increased after plasma treatment, resulted from the hydrophilicity of new functional groups. XPS angle resolved analysis illustrated that He/O_2 plasma could render deeper surface oxidation due to higher oxygen activity. Surface oxidation led to a weight increment as storage time increases, indicating adsorption of moisture in air.

Contact angle measurement showed that hydrophobic recovery of PET film occurred as storage time increased. XPS results proved that the decay of wettability is due to a reduction of hydrophilic groups on the surface of PET film. He plasma treated films have lower hydrophobic recovery rate than He/O_2 plasma. It is suggested that migration of oxidized molecules is limited due to degree of cross-linking formation. XPS resolved angle analysis revealed that C-C bond content was higher in He plasma than He/O_2 plasma. Tensile property measurement showed that tensile strength and initial modulus were higher in He plasma, indicating higher cross-linking formation.

Acknowledgement

This study is supported by National Textile Center and College of Textile at North Carolina State University.

6. References

(1) B. Beake, J. Ling and G. Leggett. Scanning Force Microscopy Investigation of Poly(ethylene terephthalate) Modified by Argon Plasma Treatment. *Journal of Materials Chemistry*, 8(8): 1735-1742, 1998

(2) T. Yasuda, M. Gazicki and H. Yasuda. Effects of Glow Discharges on Fibers and Fabrics. *Journal of Applied Polymer Science- Applied Polymer Symposia*, 38: 201-214, 1984

(3) T. Ward, H. Jung, O. Hinojosa and R. Benerito. Characterization and Use of Radio Frequency Plasma-Activated Natural Polymers. *Journal of Applied Polymer Science*, 23: 1987-2003, 1979

(4) P. Gröning, O. Küttel, M. Collaud-Coen, G. Dietler and L. Schlapbach. Interaction of Low-energy ions (< 10eV) with Polymethylemethacrylate during Plasma Treatment. *Applied Surface Science*, 89: 83-91, 1995

(5) N. Inagaki, S. Tasaka and H. Kawai. Surface Modification of Aromatic Polyamide Film by Oxygen Plasma. *Journal of Polymer Science Part A-Polymer Chemistry*, 33: 2001-2011, 1995

(6) S. Wu, J. Xing, C. Zheng, G. Xu, G. Zheng and J. Xu. Plasma Modification of Aromatic Polyamide Reverse Osmosis Composite Membrane Surface. *Journal of Applied Polymer Science*, 64: 1923-1926, 1997

(7) A. Hollander, R. Wilken and J. Behnisch. Subsurface Chemistry in the Plasma Treatment of Polymers. *Surface and Coatings Technology*, 116-119: 788-791, 1999

(8) T. Tamai, N. Ichinose, S. Kawanishi and K. Mizuno. Photochemical Oxygenation and Cross-Linking of Poly(4-trimethylsilymethylstyrene) Thin Film by UV Irradiation. *Macromolecules*, 33: 2881-2886, 2000

(9) M. Shenton, G. Steven, N. Wright and X. Duan. Chemical-Surface Modification of Polymers Using Atmospheric Pressure Nonequilibrium Plasmas and Comparisons with Vacuum Plasmas. *Journal of Polymer Science Part A-Polymer Chemistry*, 40: 95-109, 2002

(10) M. Shenton, M. Lovell-Hoare and G. Steven. Adhesion Enhancement of Polymer Surfaces by Atmospheric Plasma Treatment. *Journal of Physics D-Applied Physics*, 34: 2754-2760, 2001

(11) M. Shenton and G. Steven. Surface Modification of Polymer Surface: Atmospsheric Plasma versus Vacuum Plasma Treatments. *Journal of Physics D-Applied Physics*, 34: 2761-2768, 2001

(12) R. Gardri, J. Roth, T. Monti, K. Kelly-Wintenberg, P. Tsai, D. Helfritch, P. Feldman, D. Sherman, F. Karakaya and Z. Chen. Sterilization and Plasma Processing of Room Temperature Surfaces with a One Atmosphere Uniform Glow Discharge Plasma (OAUGDP). *Surface and Coatings Technology*, 131: 528-542, 2000

(13) E. Selli, G. Mazzone, C. Oliva, F. Martini, C. Riccardi, R. Barni, B. Marcandalli and M. Massafra. Characterisation of Poly(ethylene terephthalate) and Cotton Fibres after Cold SF_6 Plasma Treatment. *Journal of Materials Chemistry*, 11: 1985-1991, 2001

(14) B. Gupta, J. Hilborn, C. Hollenstein, J. Plummer, R. Houriet and N. Xanthopoulos. Surface Modification of Polyester Films by RF Plasma. *Journal of Applied Polymer Science*, 78: 1083-1091, 2000

(15) S. Weidner, G. Kühn, R. Decker, D. Roessner and J. Friedrich. Influence of Plasma Treatment on the Molar Mass of Poly(ethylene terephthalate) Investigated by Different Chromatographic and Spectroscopic Methods. *Journal of Polymer Science Part A-Polymer Chemistry*, 36: 1639-1648, 1998

(16) M. Gheorghiu, F. Arefi, J. Amouroux, G. Placinta, G. Popa and M. Tatoulian. Surface Cross Linking and Functionalization of Poly(ethylene terephthalate) in a Helium Discharge. *Plasma Sources Science and Technology*, 6: 8-19, 1997

(17) D. Clark and A. Dilks. ESCA Applied to Polymers. XXIII. RF Glow Discharge Modification of Polymers in Pure Oxygen and Helium-Oxygen Mixture. *Journal of Polymer Science Part A-Polymer Chemistry*, 17: 957-976, 1979

(18) G. Placinta, F. Arefi-khonsari, M. Gheorghiu, J. Amouroux and G. Popa. Surface Properties and the Stability of Poly(ethylene Terephthalate) Films Treated in Plasmas in Helium-Oxygen Mixture. *Journal of Applied Polymer Science*, 66: 1367-1375, 1997

(19) Y. Hwang, S**.** Matthews, Y**.** Park, M**.** McCord and M**.** Bourham**.** Surface Modification of Organic Polymer Films Treated in Atmospheric Plasmas**.** *202nd The Electrochemical Society Meeting*, Salt Lake City, Utah, USA**,** October, 2002

(20) R. Foerch, G. Kill and M. Walzak. Plasma Surface Modification of Polypropylene: Short-Term vs. Long-Term Plasma Treatment. *Journal of Adhesion Science and Technology*, 7: 1077-1089, 1993

(21) A. Mas, H. Jaaba, F. Schue, A. Belu, C. Kassis, R. Linton and J. Desimone. Poly(hydroxylbutyrate-co-9% Hydroxyvalerate) Film Surface Modification by Ar, O_2, H_2O/O_2, H_2O, and H_2O_2 Plasma Treatment. *Journal of Macromolecular Science-Pure and Applied Chemistry*, 34: 67-79, 1997

(22) N. Inagaki, S. Tasaka, K. Narushima and K. Teranishi. Surface Modification of Poly(tetrafluoroethylene) with Pulsed Hydrogen Plasma. *Journal of Applied Polymer Science*, 83: 340-348, 2002

(23) S. Dahl, D. Rats, J. Stebut, L. Martinu and J. Klemberg-Sapieha. Micromechanical Characterisation of Plasma Treated Polymer Surfaces. *Thin Solid Film*, 335-356: 290-294, 1999

(24) Y. Hwang, Y. Qiu, C. Zhang, B. Jarrard, R. Stedeford, J. Tsai, Y. Park and M. McCord. The Effects of Atmospheric Pressure Helium Plasma Treatment on Adhesion and Mechanical Properties of Aramid Fibers. *Journal of Adhesion Science and Technology*, 2003, In Press

(25) H. Yasuda, A. Sharma and T. Yasuda. Effect of Orientation and Mobility of Polymer Molecules at Surfaces on Contact Angle and Its Hysteresis. *Journal of Polymer Science-Polymer Physics Edition 19*, 1285-1291, 1981